オーロラサブストーム

～何が説明されるべきか

（旧題：オーロラブレイクアップについて）

門倉 昭（極地研）

Classical Morphology

Akasofu, S.-I., The development of the auroral substorm, *Planet. Space Sci.*, *12*, 273-282, 1964.

(d) The front of the bulge reaches its northernmost point and within the bulge there are active bands. At the western edge of the bulge, the folds of the arcs called the Westward Travelling Surge

(e) During the recovery phase, the northernmost active band starts to return southward. The size of the bulge is reduced, the speed of

(f) During the later stage of the recovery phase, there appear quiet arcs slowly moving equatorward.

(a) During the quiet phase, there are several quiet and homogeneous arcs that are approximately parallel to the geomagnetic latitude circles there.

Within the bulge, "break-up" occurs such that a quiet curtain-like form appears to be disrupted and scattered all over the sky.

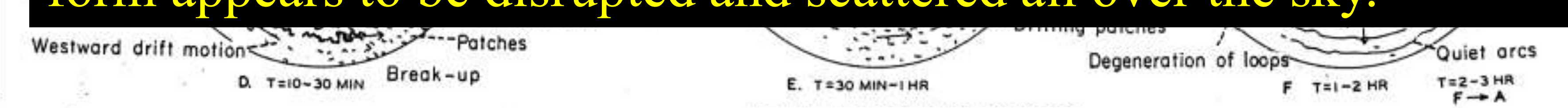

Expansive Phase (T=10~30 min)

Recovery Phase (T=30~60 min)

Recovery Phase (T=1~2 hour)

Classical Morphology に対する追加、修正

- Diffuse Aurora の発見 （ISIS-2衛星, Lui and Anger, *Planet. Space Sci., 21*, 799-809, 1973)

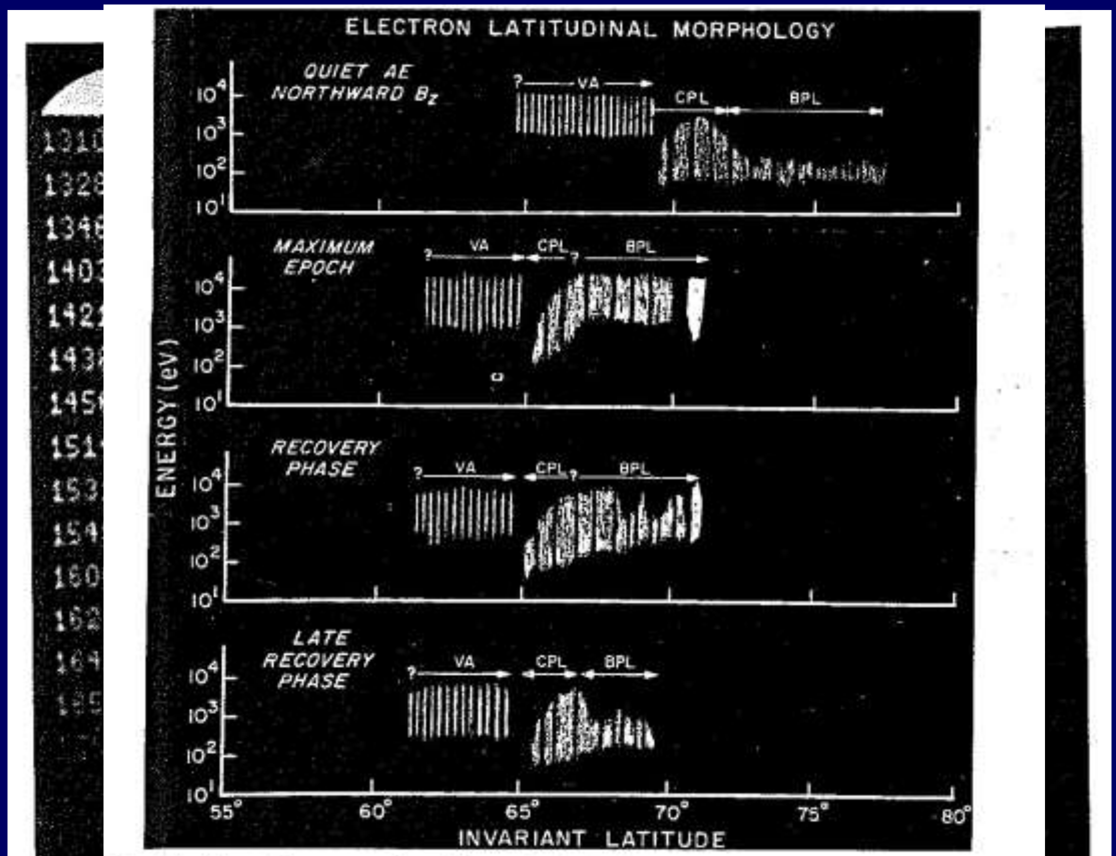

Fig. 18. Schematic representation of electron latitudinal morphology for various phases of a substorm.

These two characteristics of the precipitating electrons are categorized by *Winningham et al*. [1975] as the CPS (central plasma sheet) and BPS (boundary plasma sheet), respectively.

Classical Morphology に対する追加、修正

- Proton Aurora Substorm（*Montbriand* (1971), *Fukunishi* (1975))

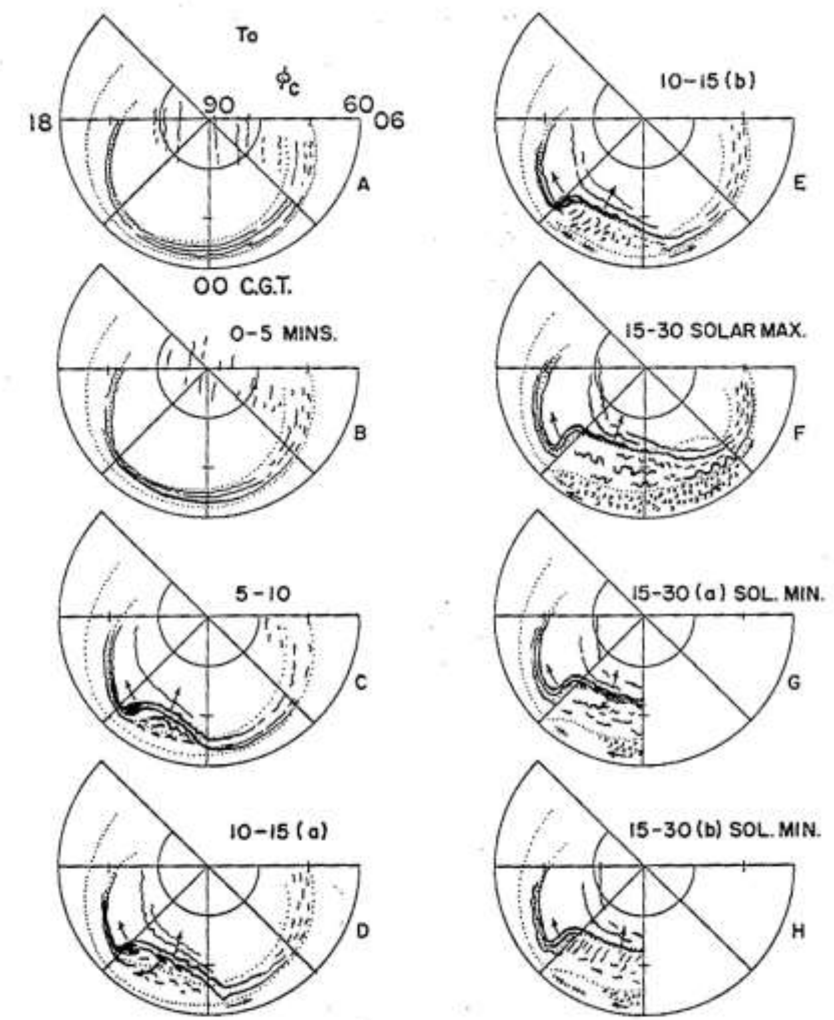

Fig. 4. The expensive phase of the intense auroral and proton auroral substorm.

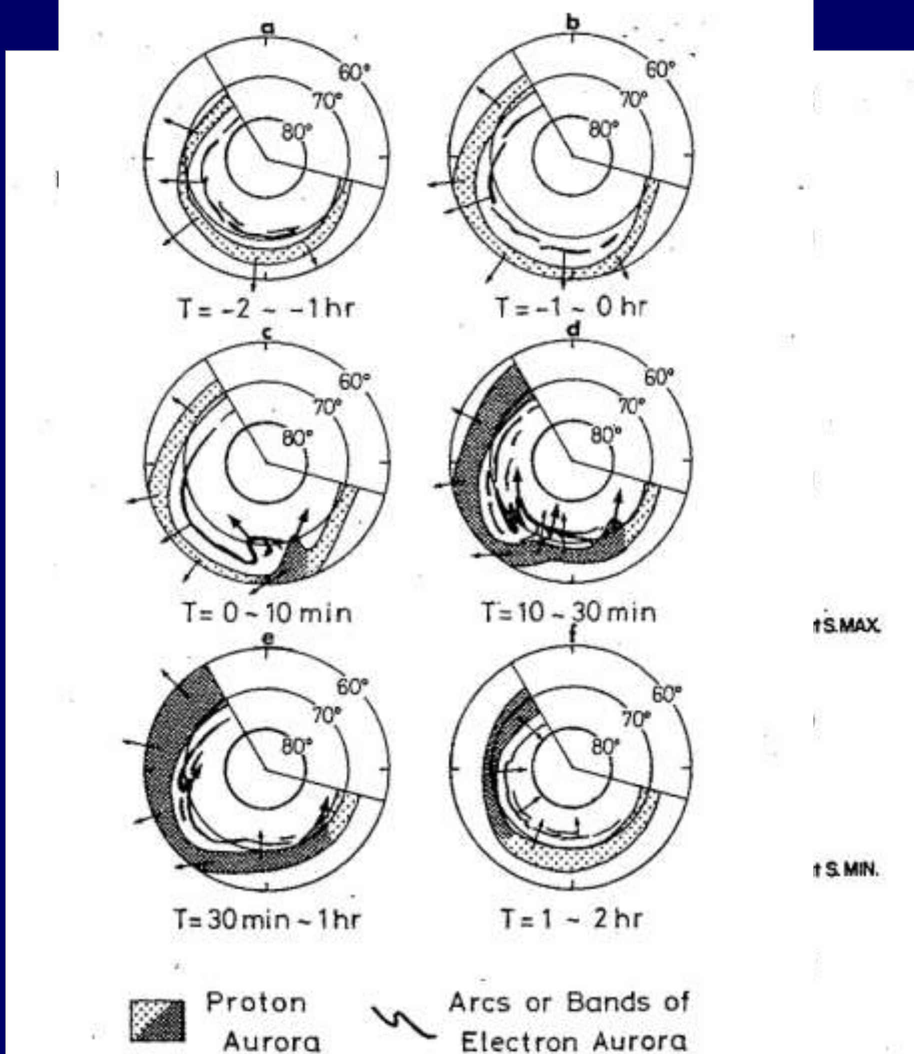

Fig. 23. Schematic diagrams showing the worldwide development f proton and electron auroral substorms; T = 0 is the onset time of ıe expansion phase. The notation is the same as that in Figure 21.

ɔstorm.

Classical Morphology に対する追加、修正

- Proton Aurora Substorm（*Oguti* (1973))

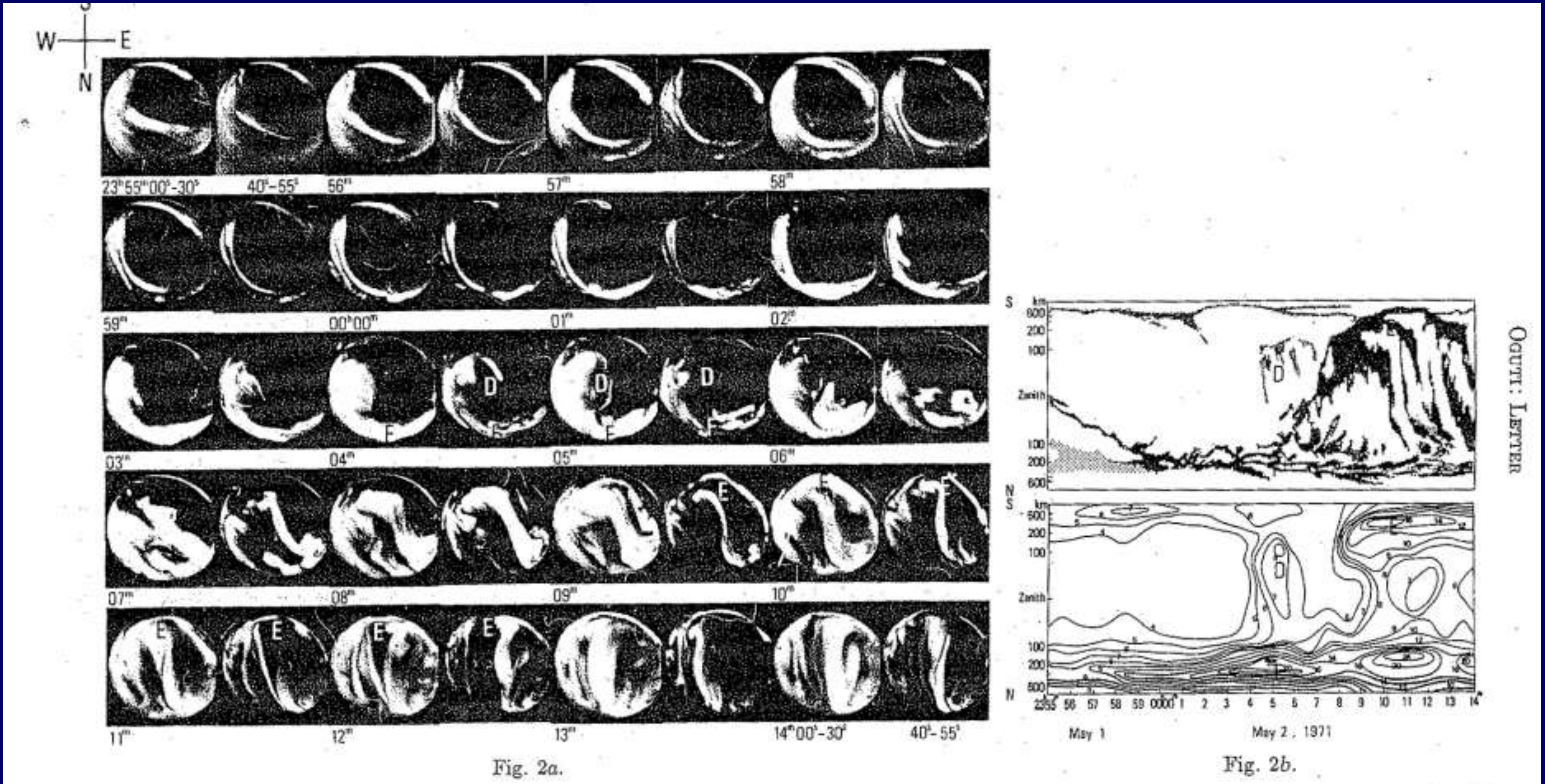

Fig. 2. Development of the electron aurora and hydrogen emission during the auroral breakup of May 1–2, 1971. (*a*) All-sky camera photographs. (*b*) Meridian-time display of the electron aurora (top), and meridian-time display of the hydrogen emission (bottom).

➢ Proton Aurora Substorm（*Takahashi & Fukunishi* (2001))

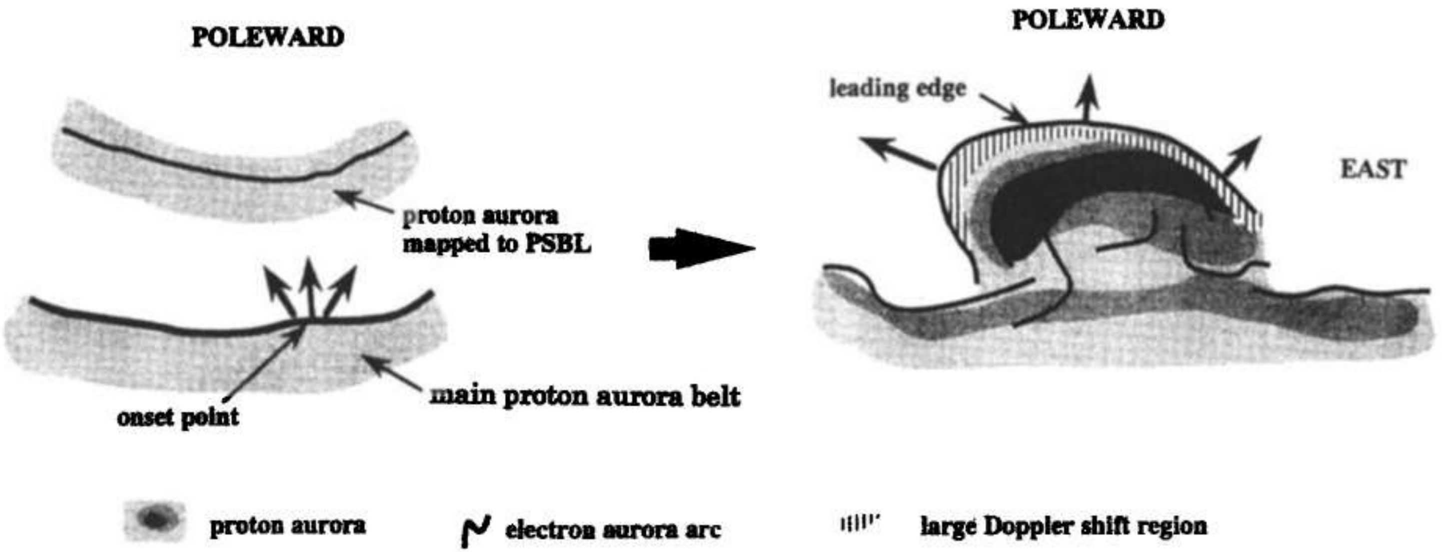

Figure 8. Schematic features of the development of proton and electron auroras during the auroral breakup event: (left) the prebreakup phase and (right) the expansion phase. PSBL, plasma sheet boundary layer.

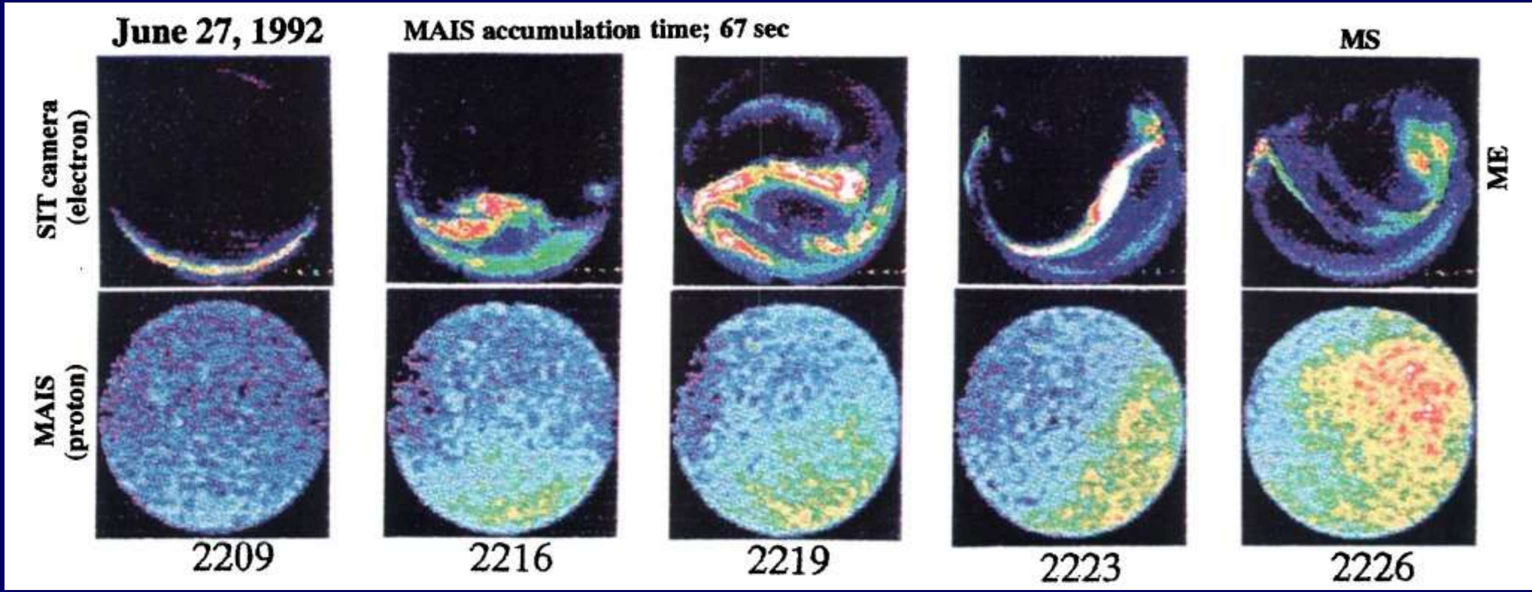

- Proton Aurora Substorm（*Takahashi & Fukunishi* (2001))

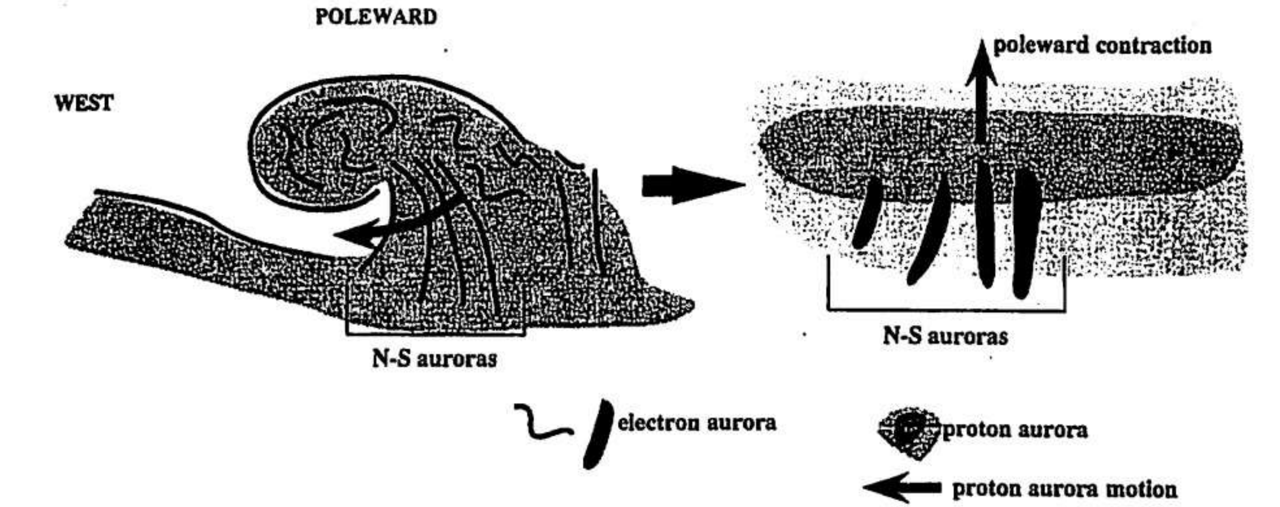

Figure 9. Schematic summary of the development of proton and electron auroras during the auroral breakup event with N-S auroras.

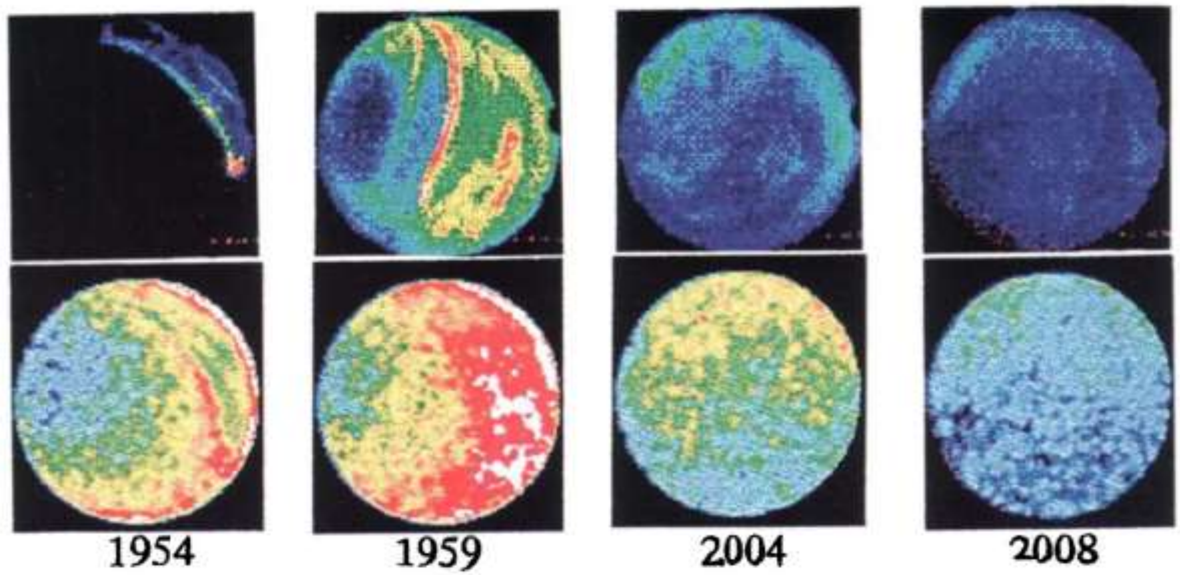

Plate 6. Same as Plate 3, simultaneous image pairs of proton and electron auroras picked up from Plates 4 and 5.

Classical Morphology に対する追加、修正

- Proton Aurora Substorm（IMAGE衛星、*Mende et al.* (2001))

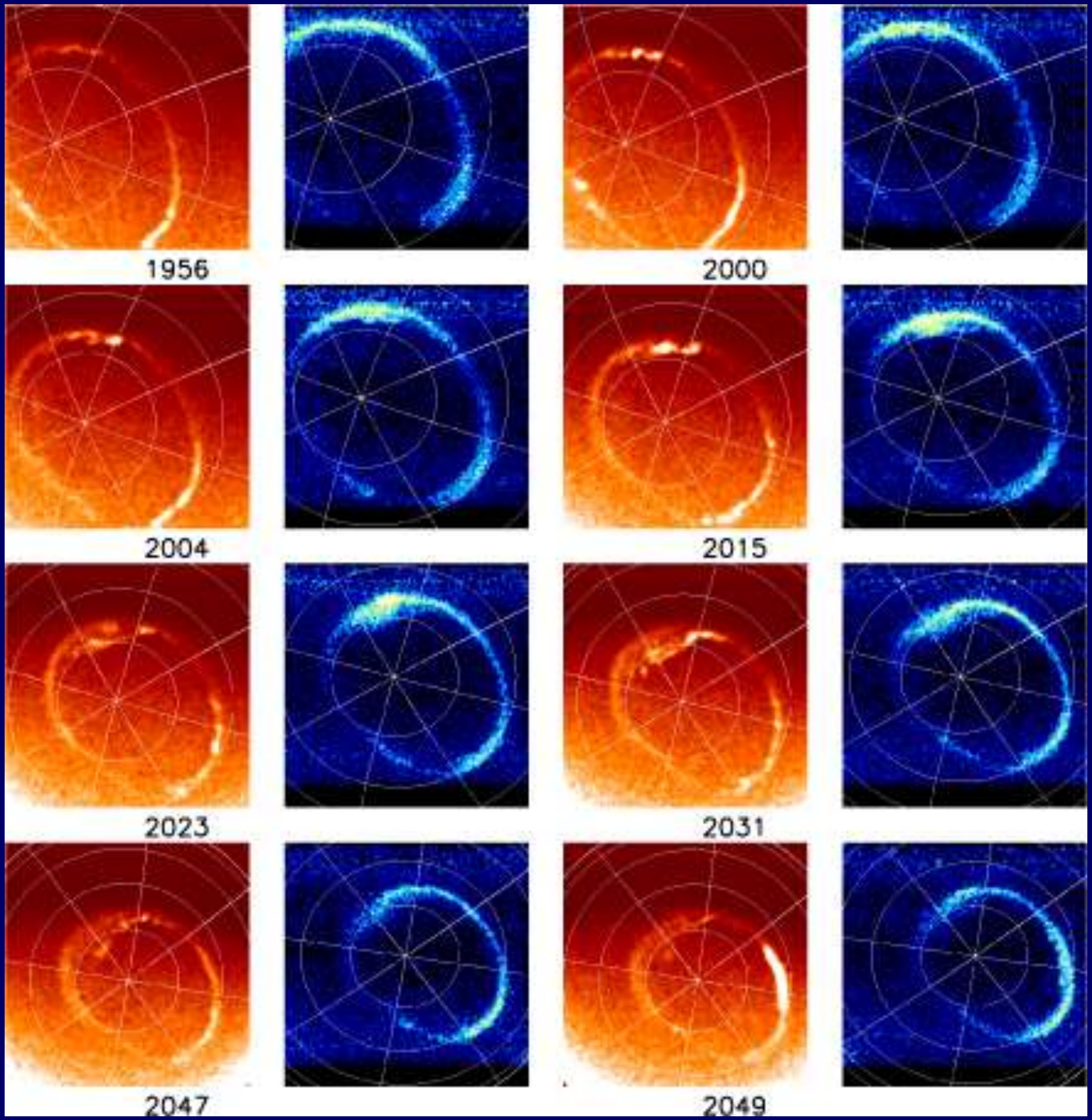

Classical Morphology に対する追加、修正

- Growth Phase

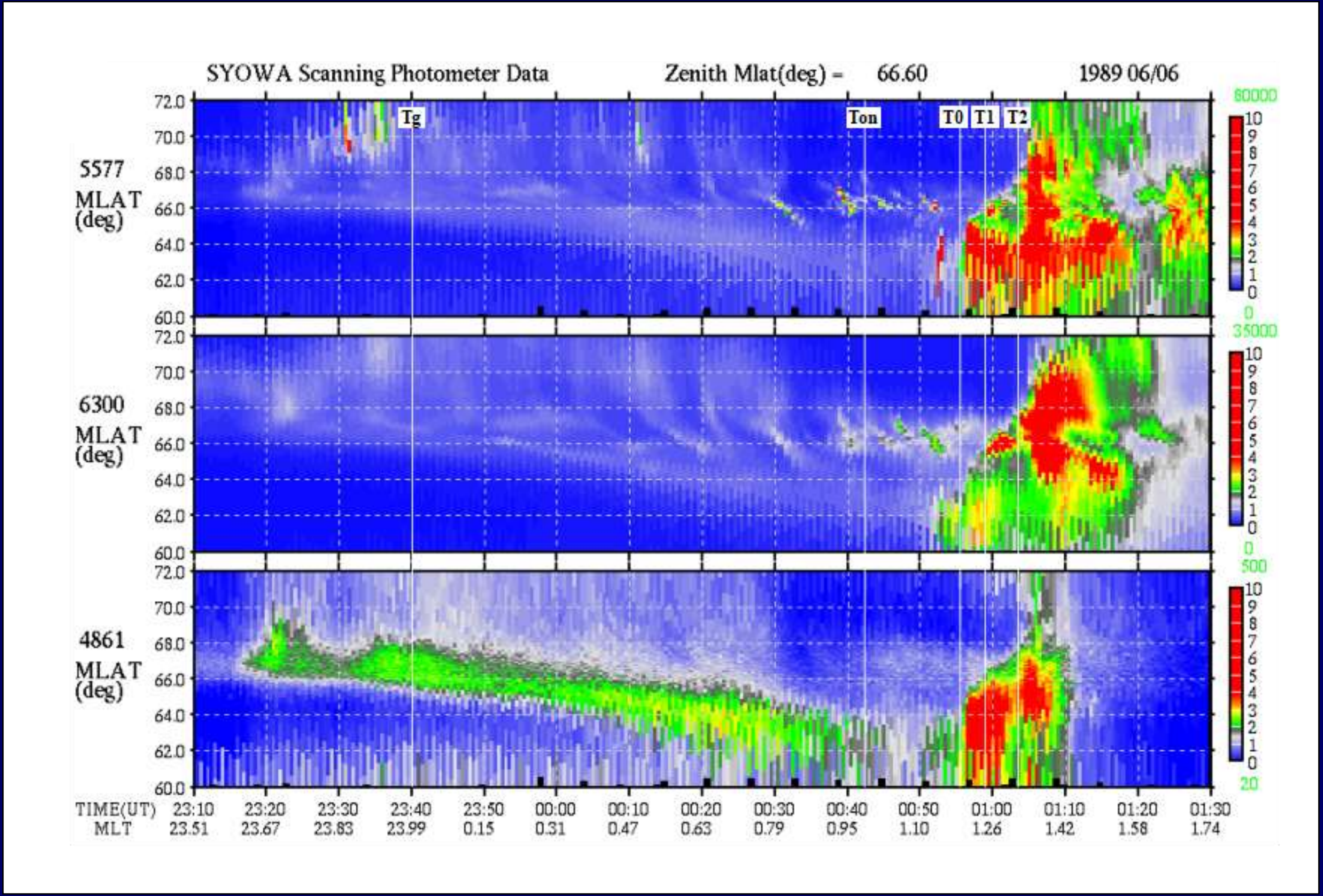

Classical Morphology に対する追加、修正

- Growth Phase *Brittnacher et al.* (1999) (POLAR UVI)

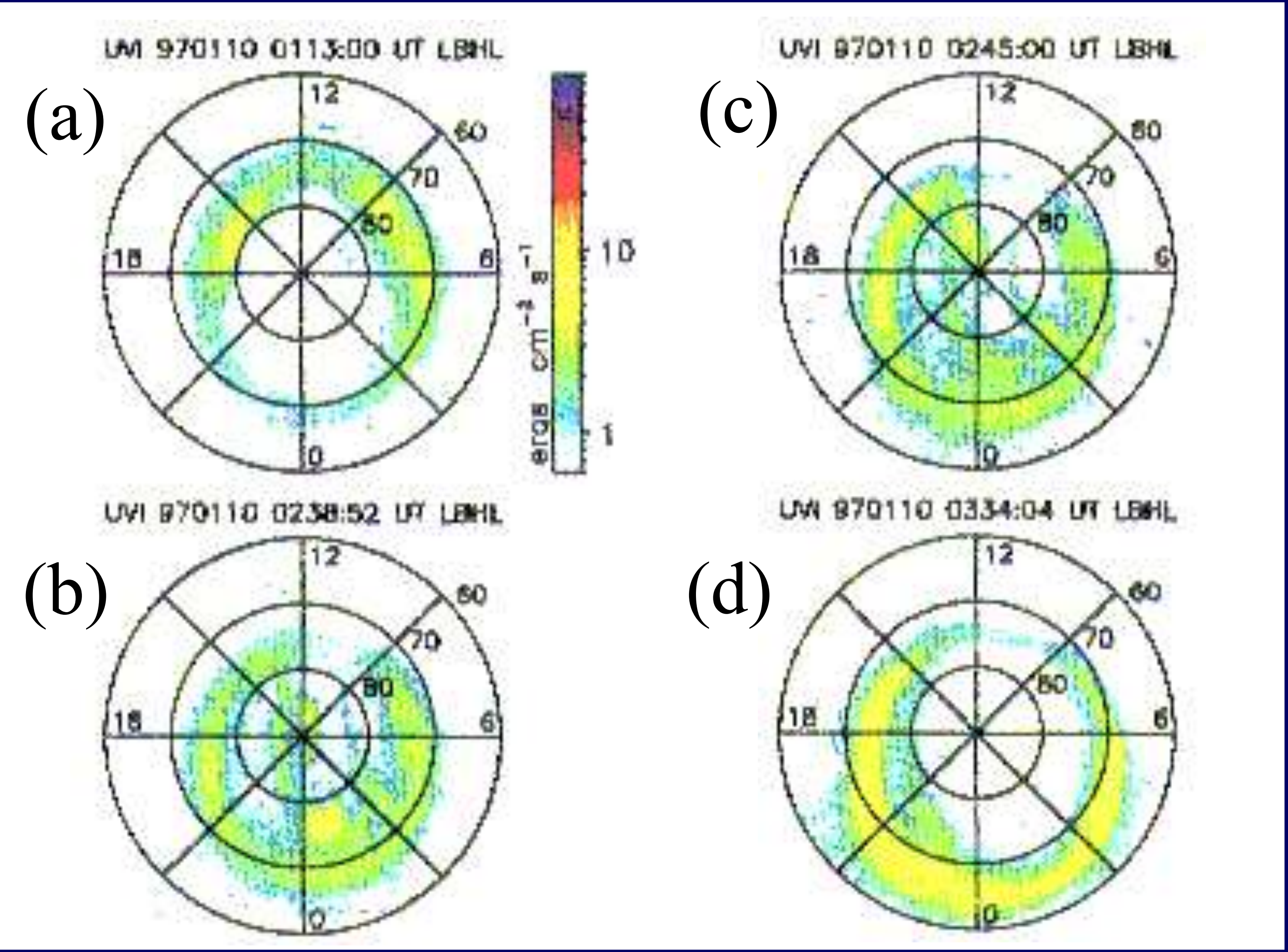

Classical Morphology に対する追加、修正

- Premidnight preference & localization of onset region
- Double oval configuration during the recovery phase

POLAR UVI (1997)

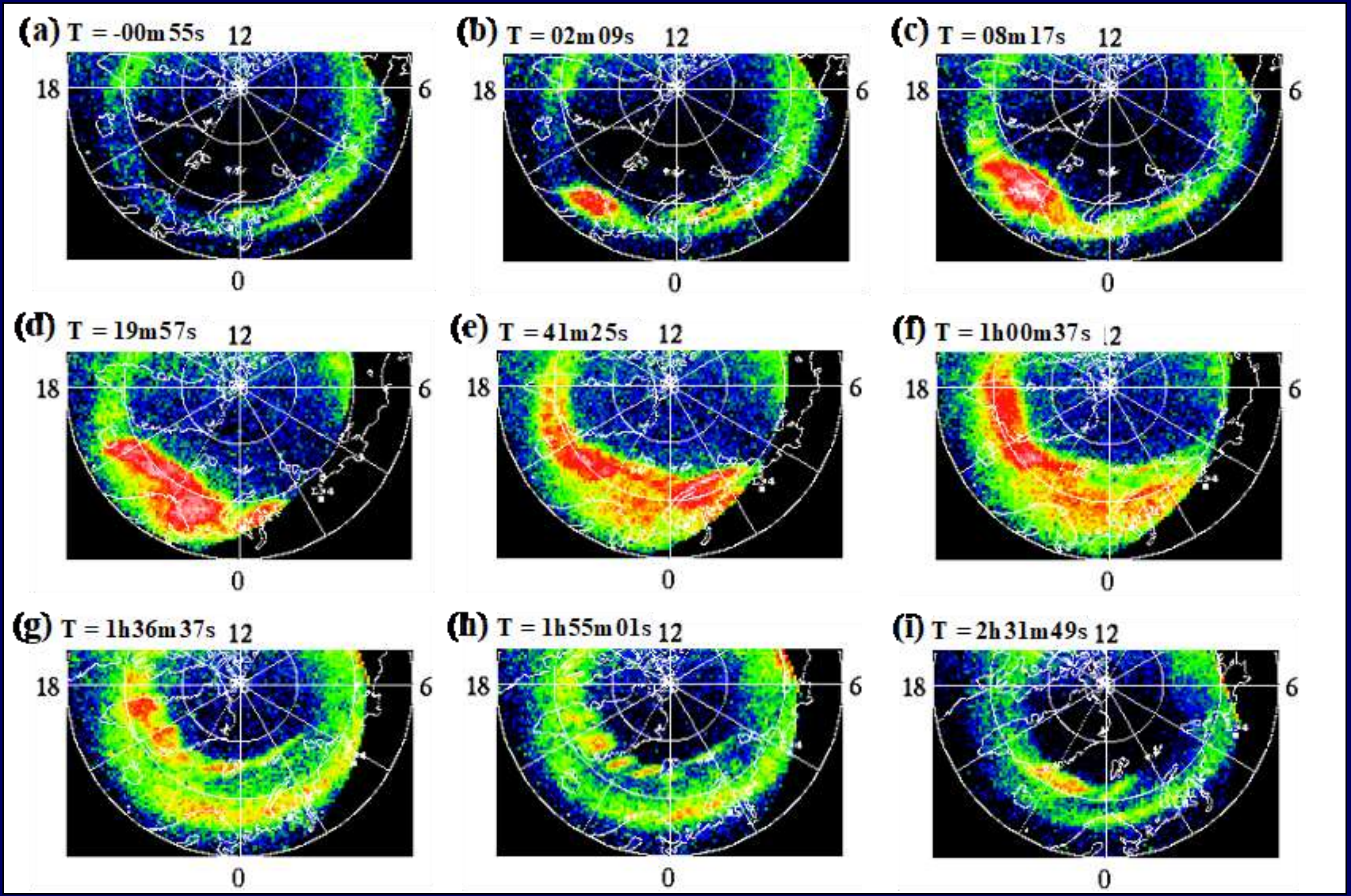

Classical Morphology に対する追加、修正

- Premidnight preference & localization of onset region

Elphinstone et al. (1995) for VIKING 80 events
Average location : 22.9±1.2 hr MLT and 65.9±3.5 deg CGMLAT
Spatial extent : about 1 hr MLT

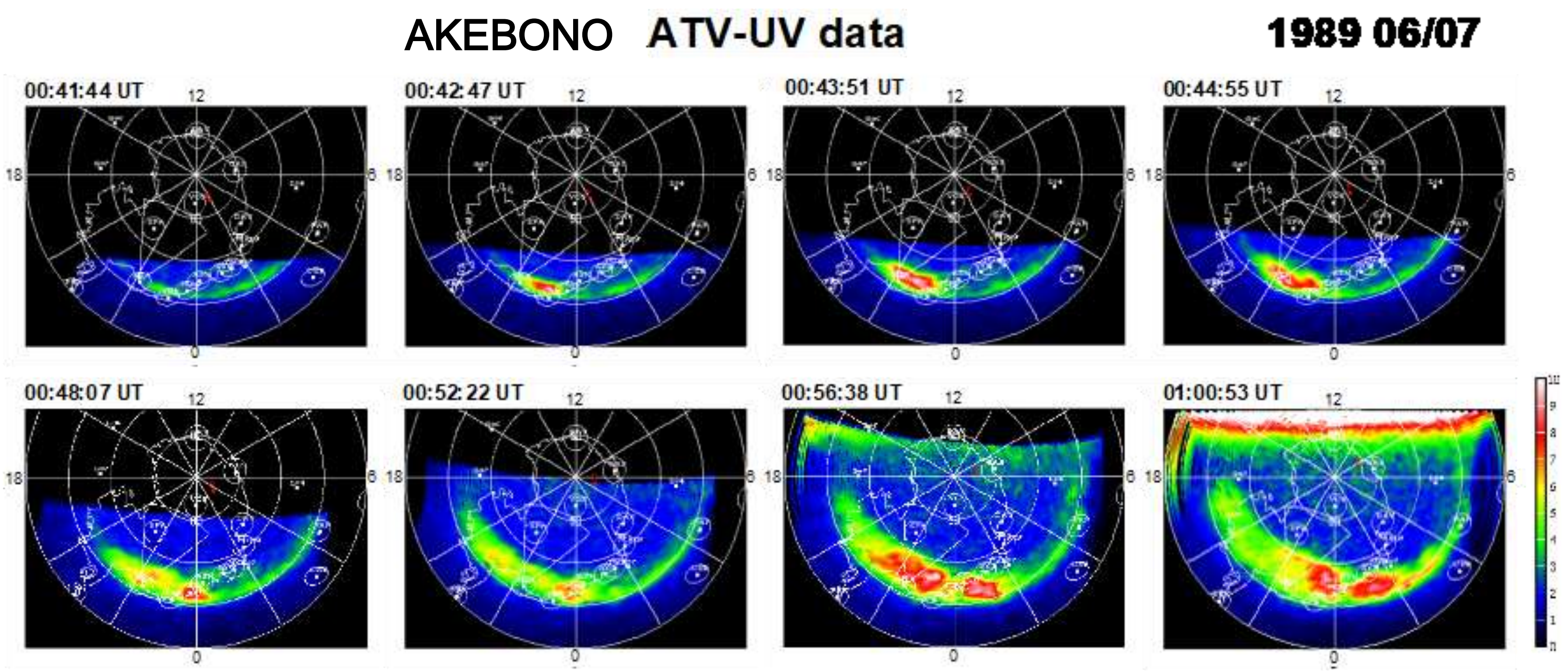

Kadokura et al. (2002)

Classical Morphology に対する追加、修正

- Premidnight preference of onset region

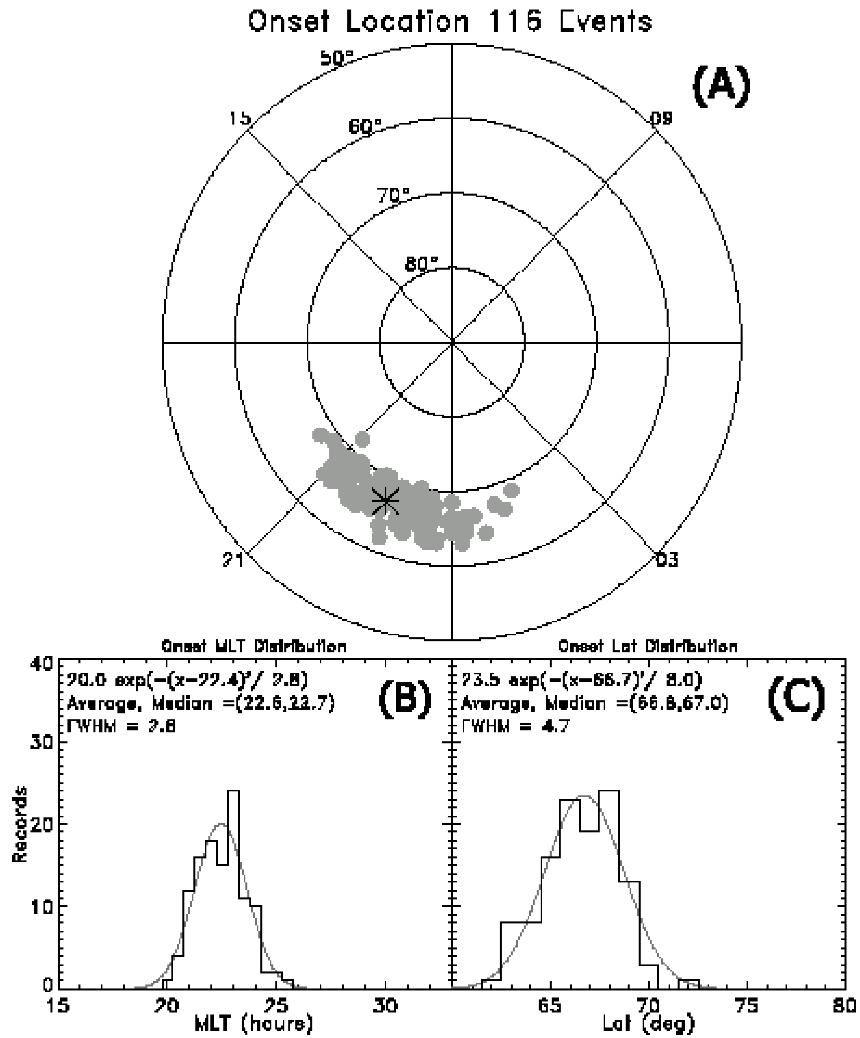

Figure 6. (a) The distribution of onset locations in MLT/ILat. with the average marked as an asterisk. (b and c) The distribution as histograms in MLT and ILat, respectively, of the onset locations. Gaussian curves are fitted to the data, with the equation, average, median, and full-width at half-maximum included.

POLAR
VIS Earth camera

Gjerloev et al.
(JGR, 112, 2007)

Premidnight preference & localization of onset region

AKEBONO ATV-UV

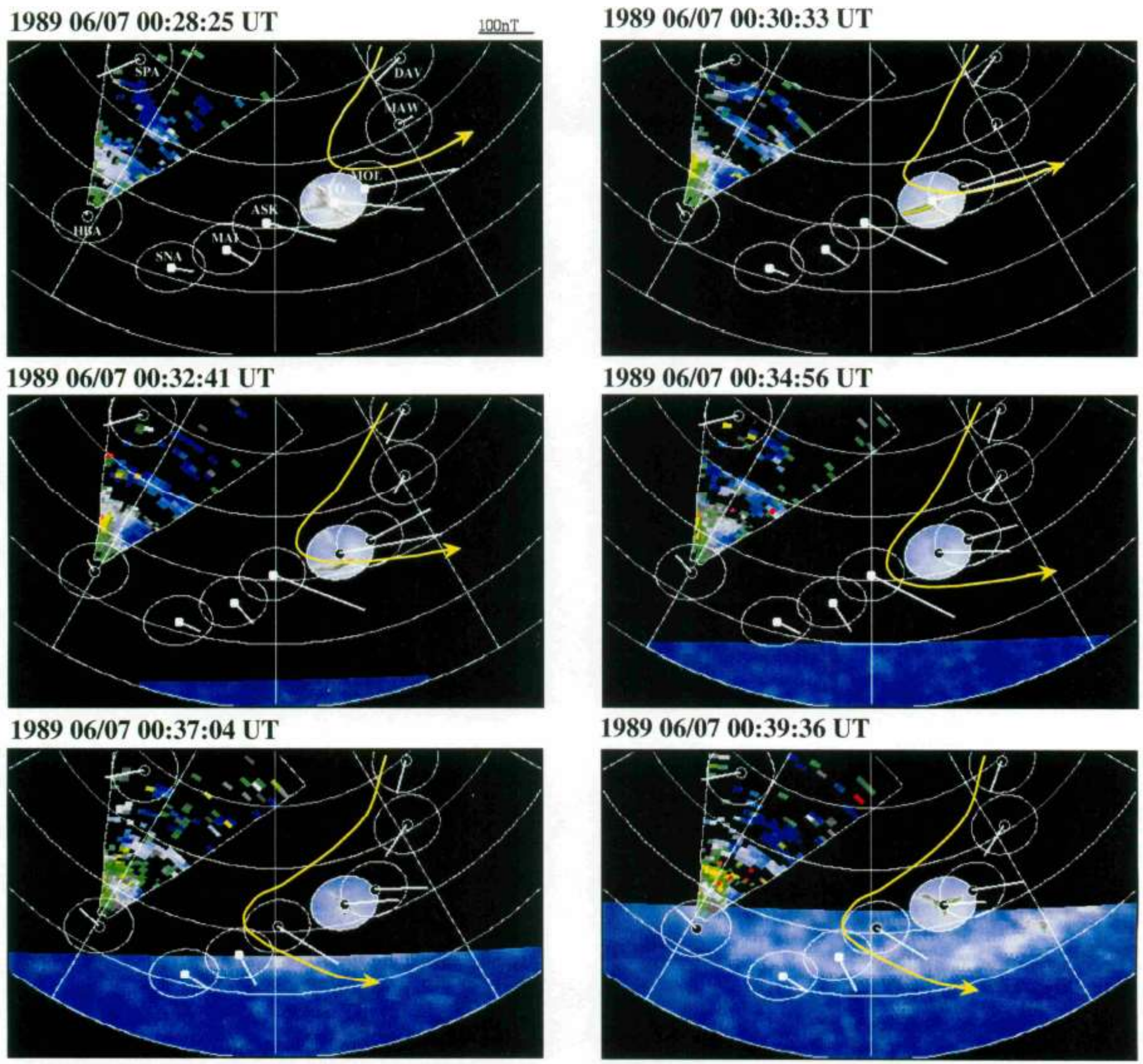

Premidnight preference & localization of onset region

AKEBONO ATV-UV

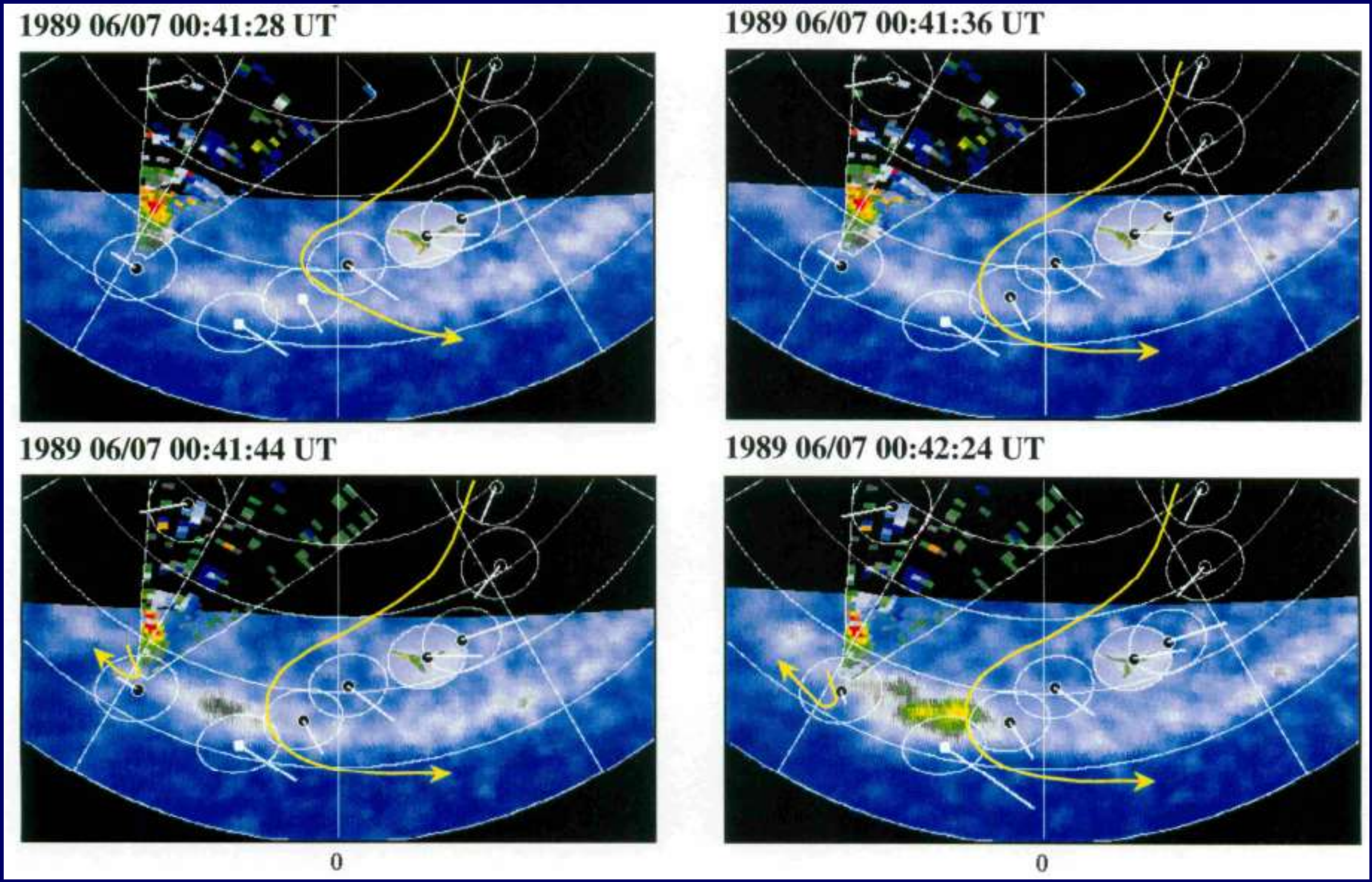

Onset location & Convection

AKEBONO ATV-UV

1989 06/07 00:39:36 UT

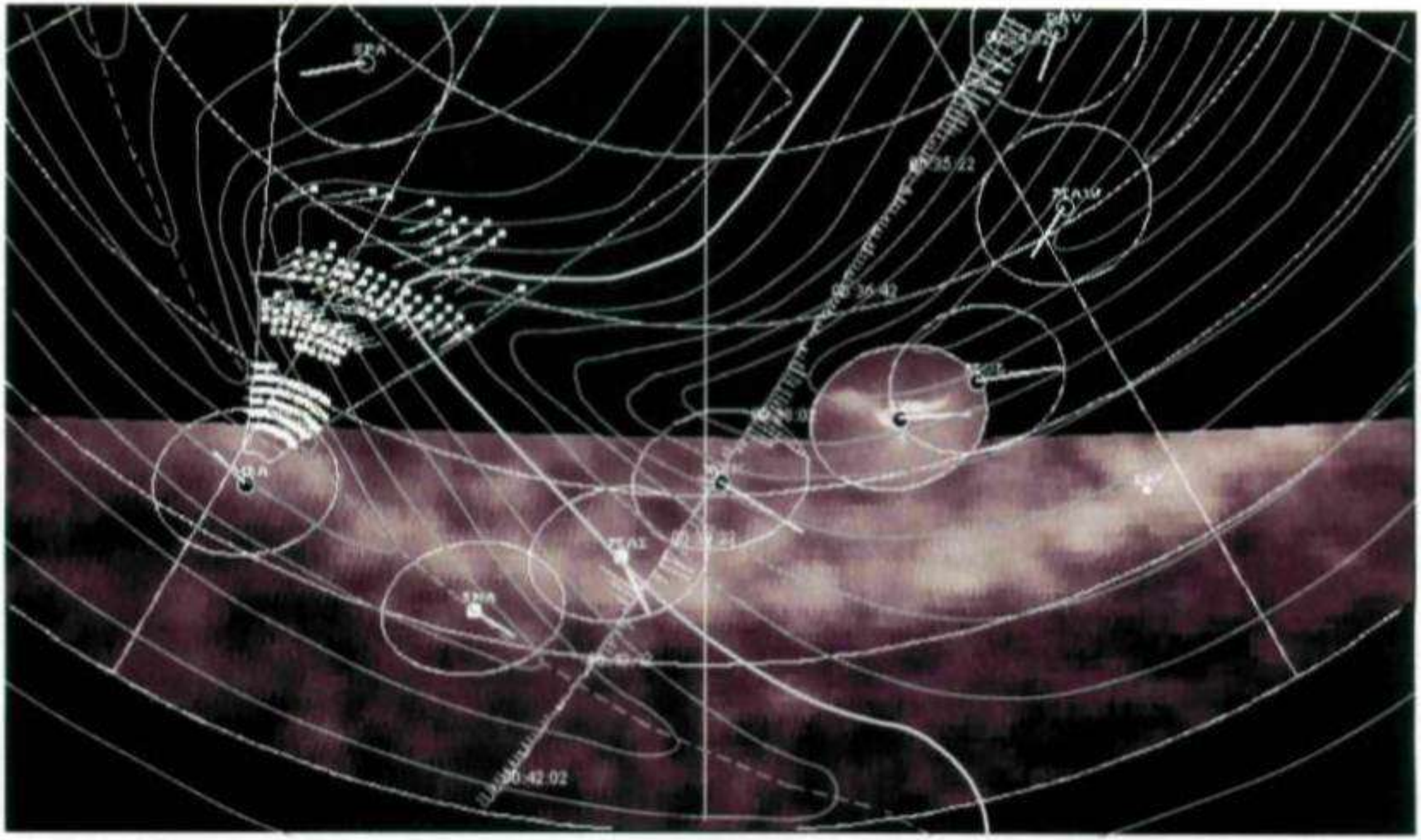

thin gray lines : Heppner and Maynard (1987) Convection model BC
(northern hemisphere +Y IMF, southern -Y IMF) (3+ ≤ Kp ≤ 4-)

Onset location & Convection

AKEBONO ATV-UV

1989 06/07 00:42:24 UT

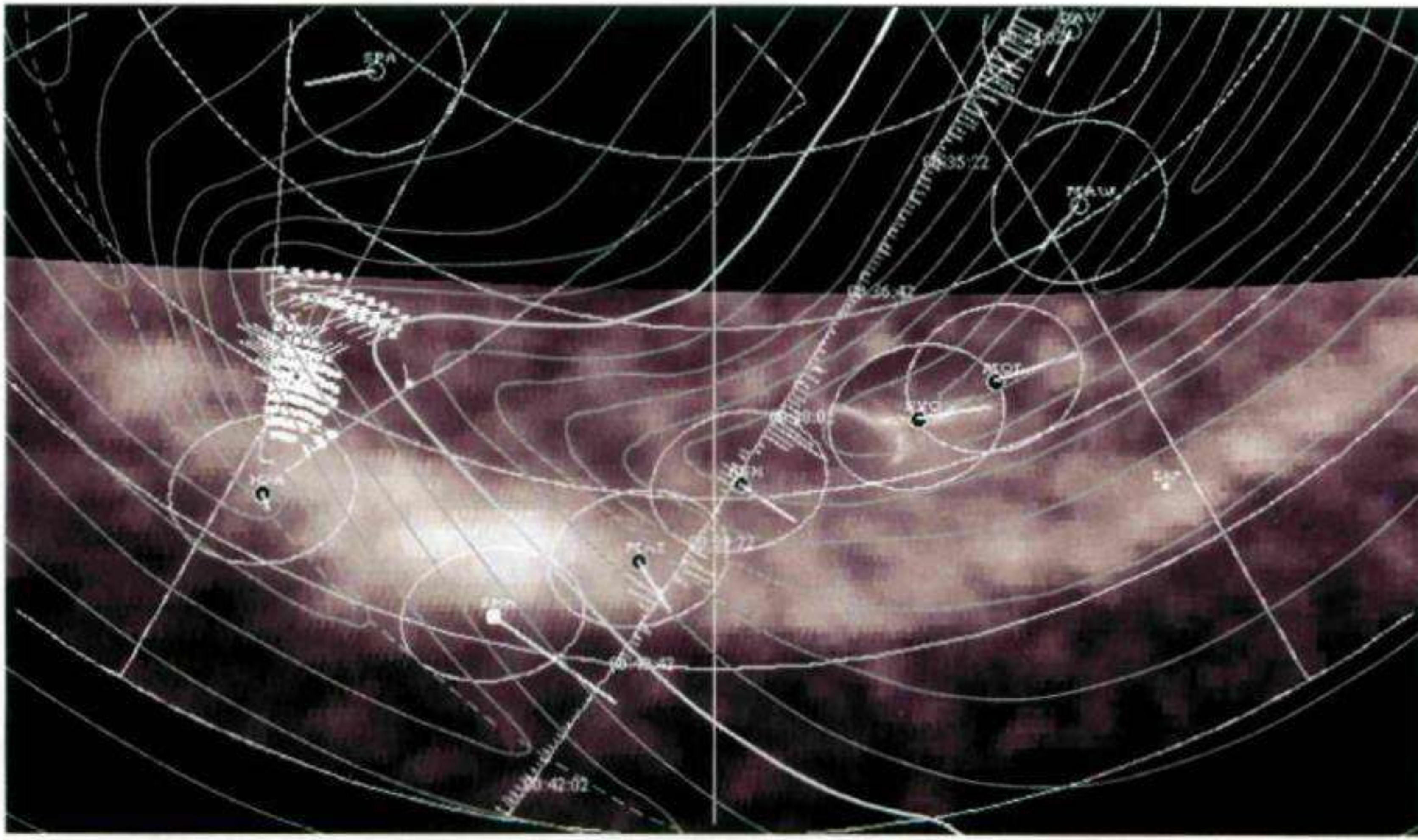

thin gray lines : Heppner and Maynard (1987) Convection model BC
(northern hemisphere +Y IMF, southern -Y IMF) (3+ ≤ Kp ≤ 4-)

Relationship between onset location and convection

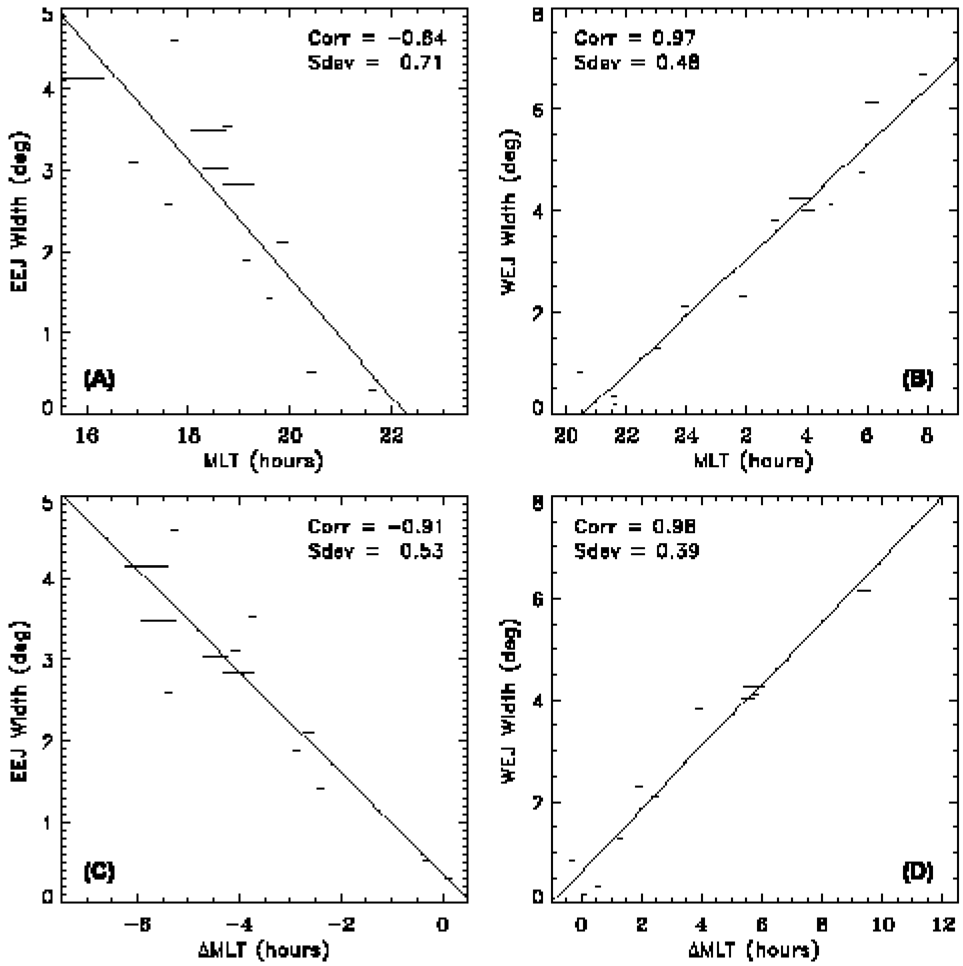

Figure 4. Latitudinal width of the auroral electrojets during the growth phase of classical bulge-type auroral substorms. Top panels (A and B) show the widths as a function of MLT while the bottom panels (C and D) show the widths as a function of the MLT distance to the future optical onset location. Zero MLT indicates the location of the future substorm onset. Corr and Sdev indicate the linear Pearson correlation coefficient and the standard deviation, respectively.

DE-1 & DE-2

Gjerloev et al. (GRL, 30, 2003)

Onset location & Onset Arc

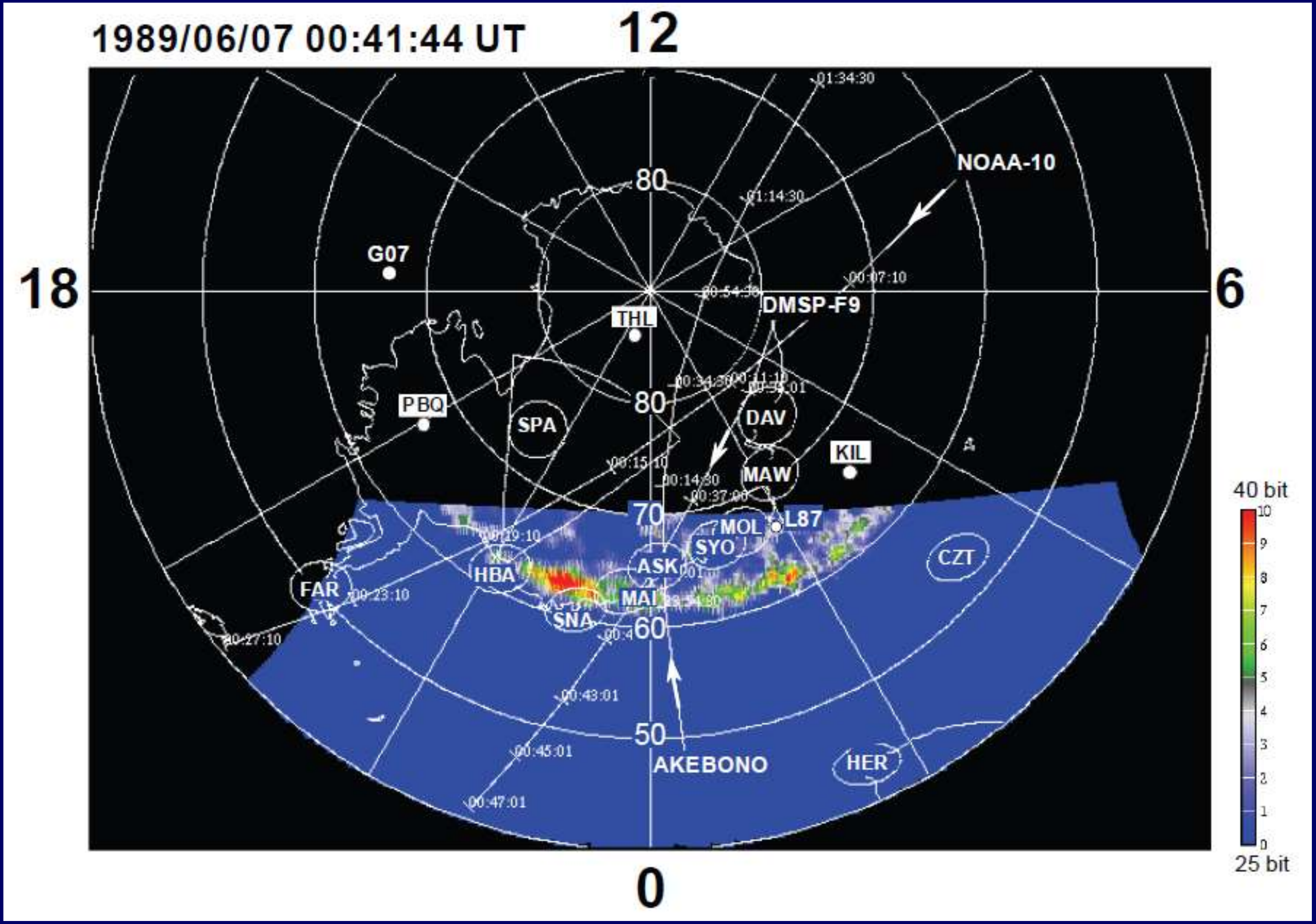

Kadokura et al. (2002)

Onset location & Onset Arc

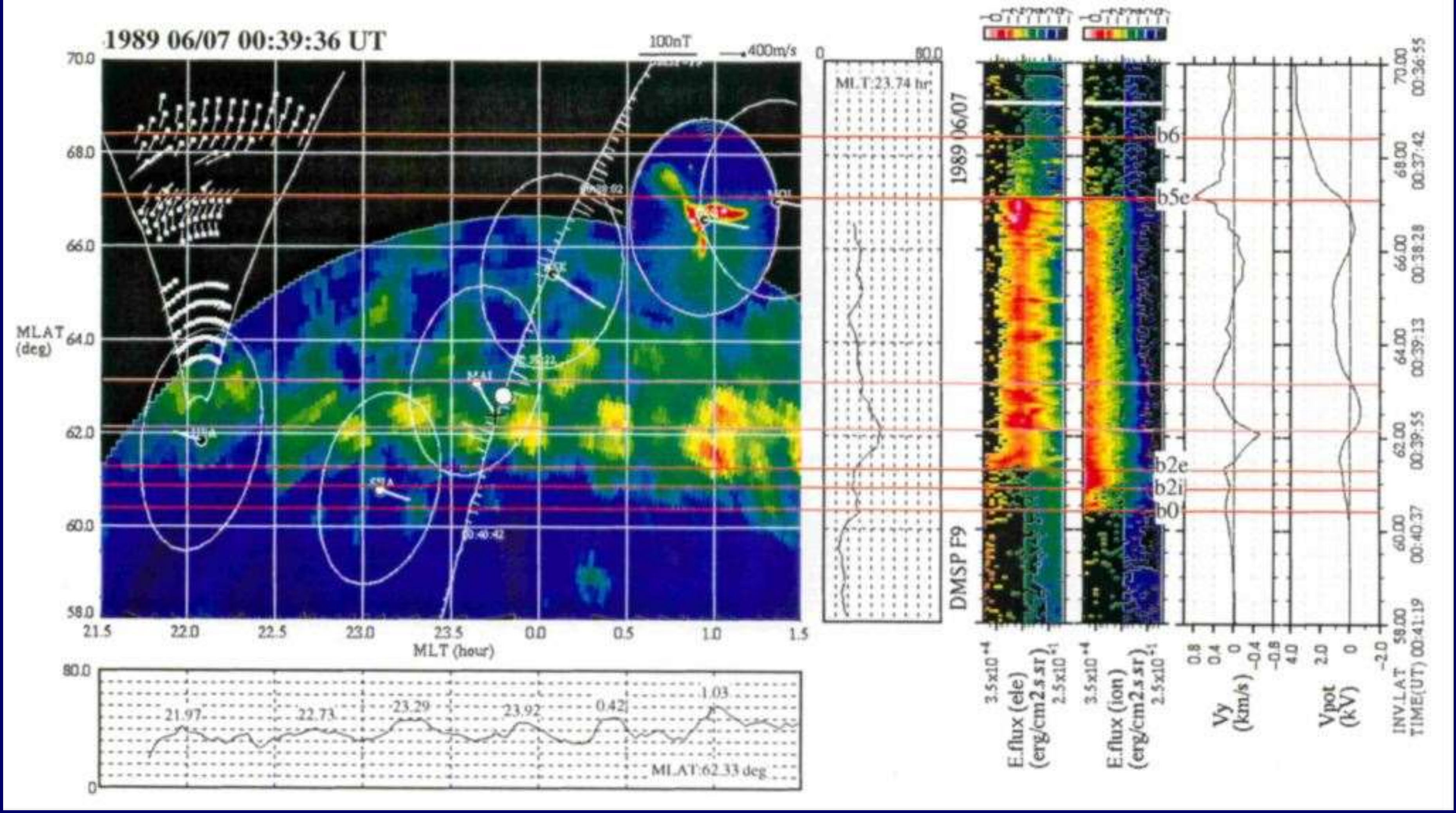

Onset location & Onset Arc

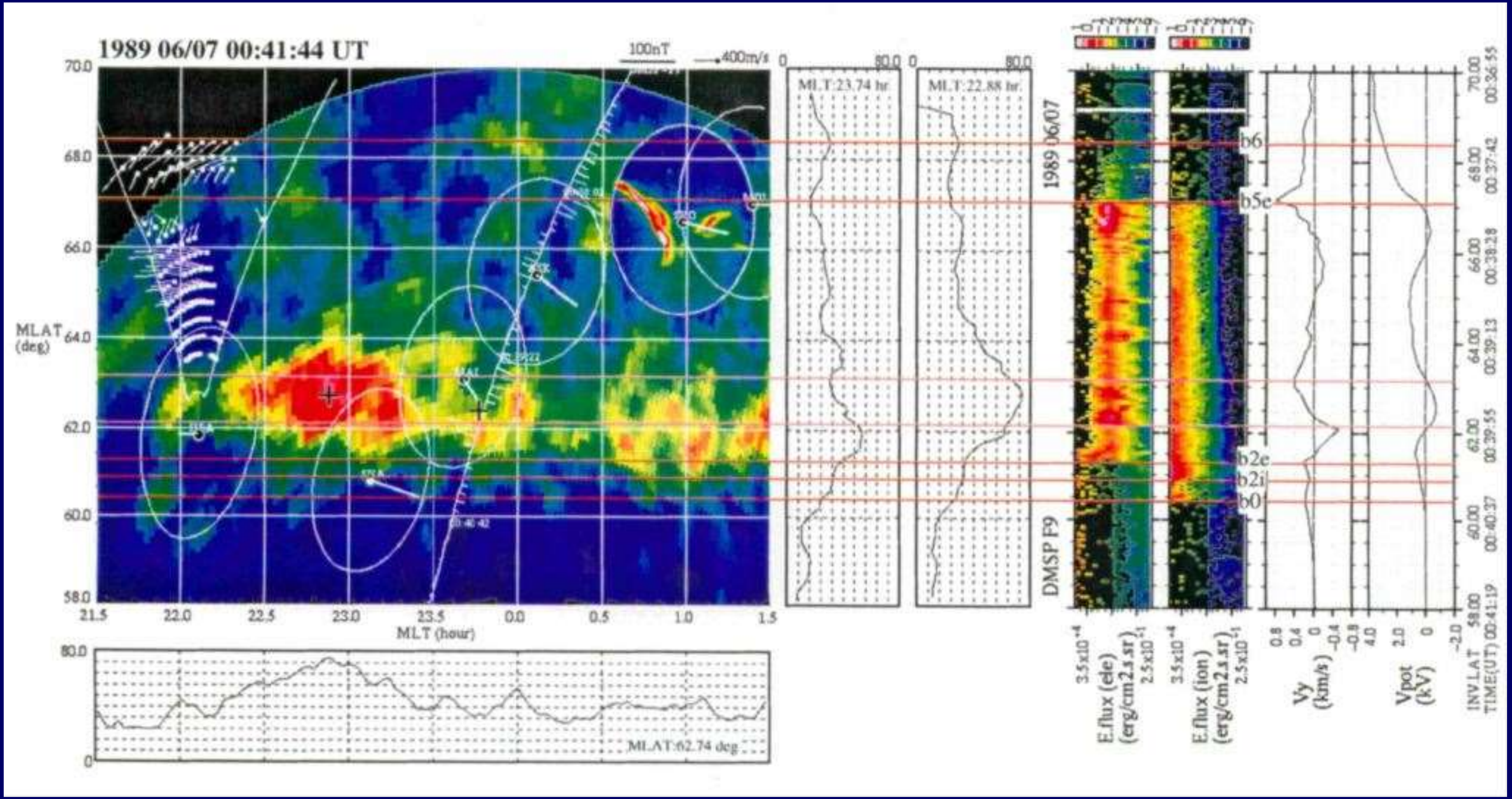

Onset location & Onset Arc

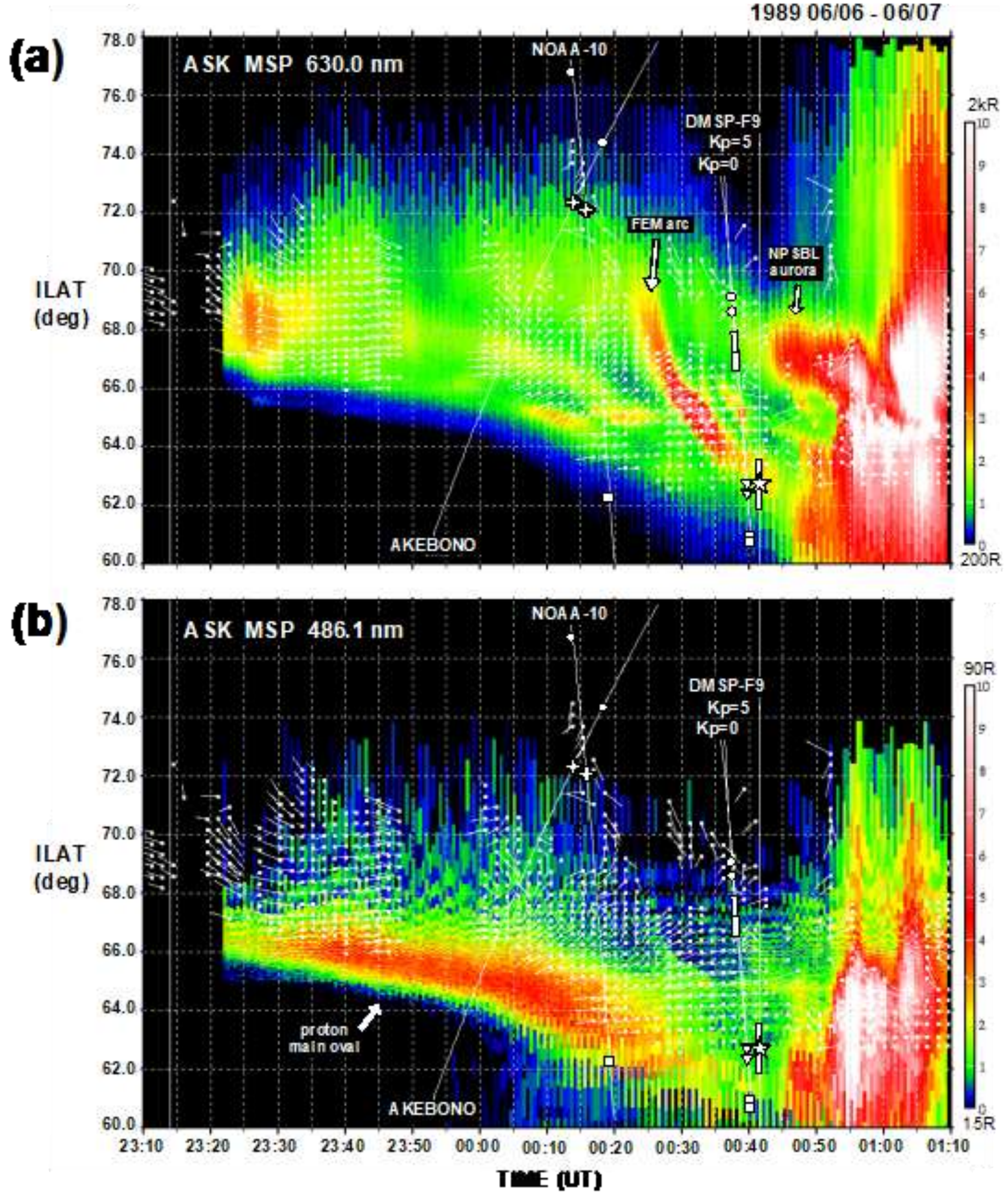

Kadokura et al. (2002)

Onset location & Onset Arc

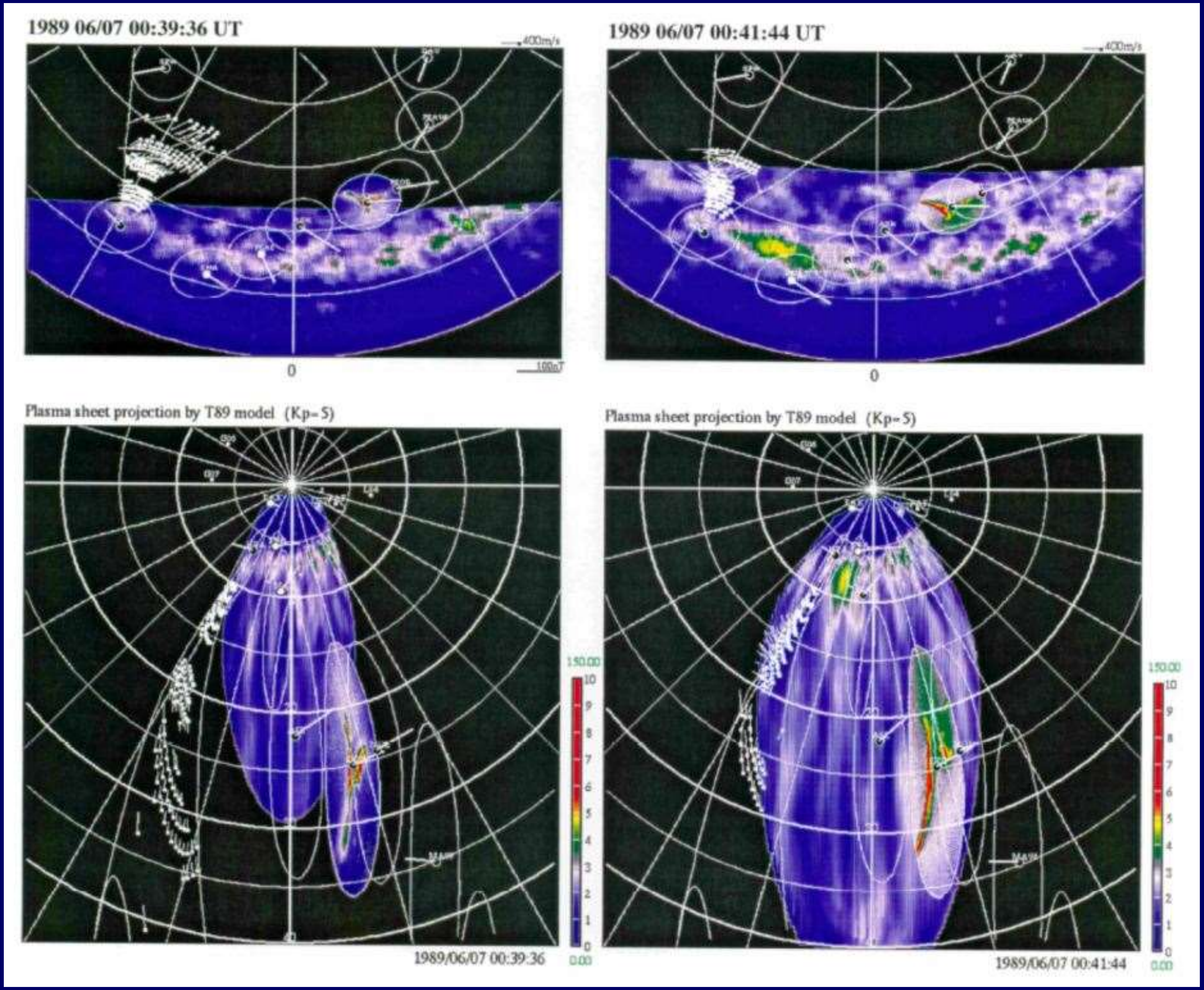

Onset location & Onset Arc

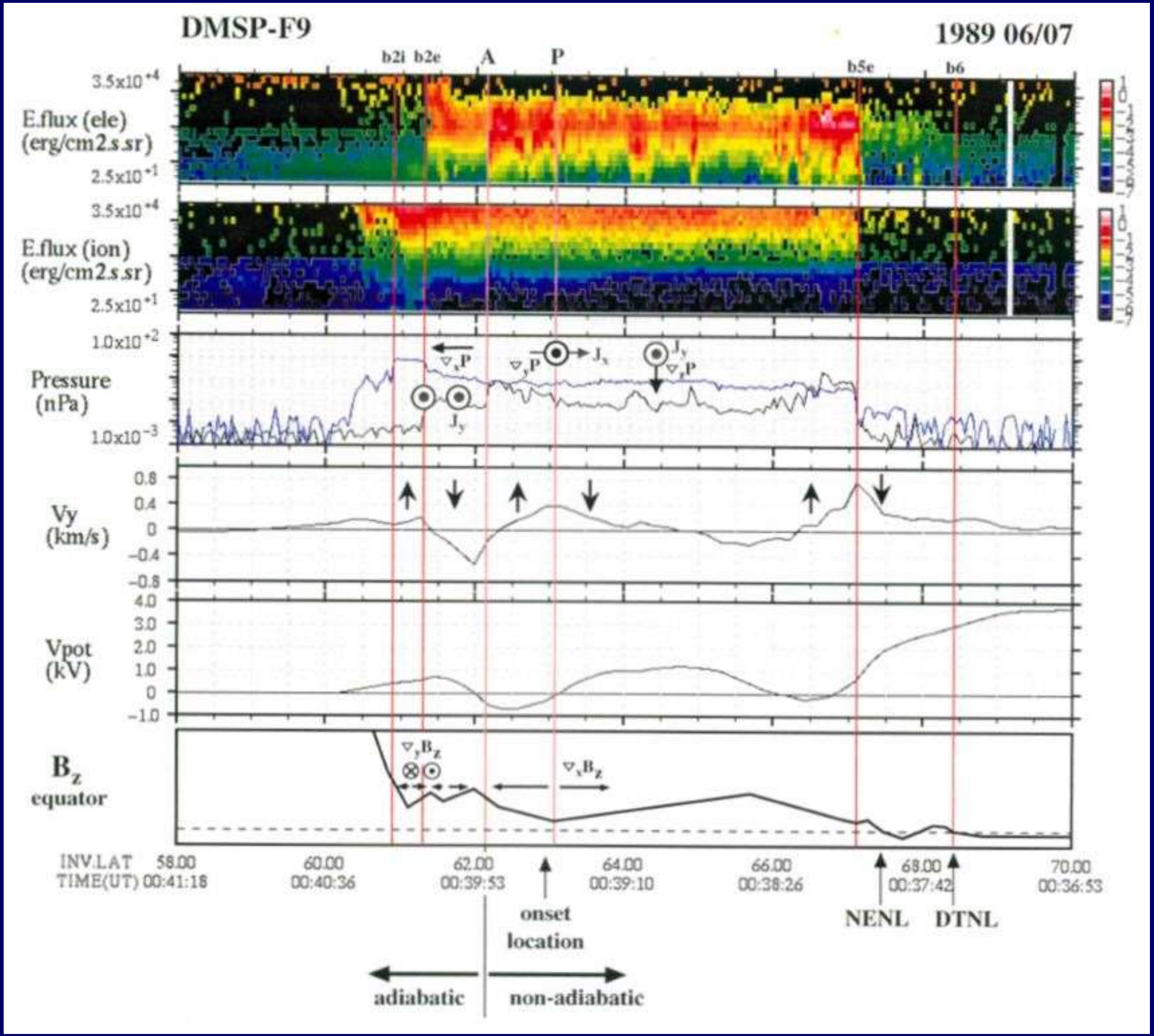

Growth Phase

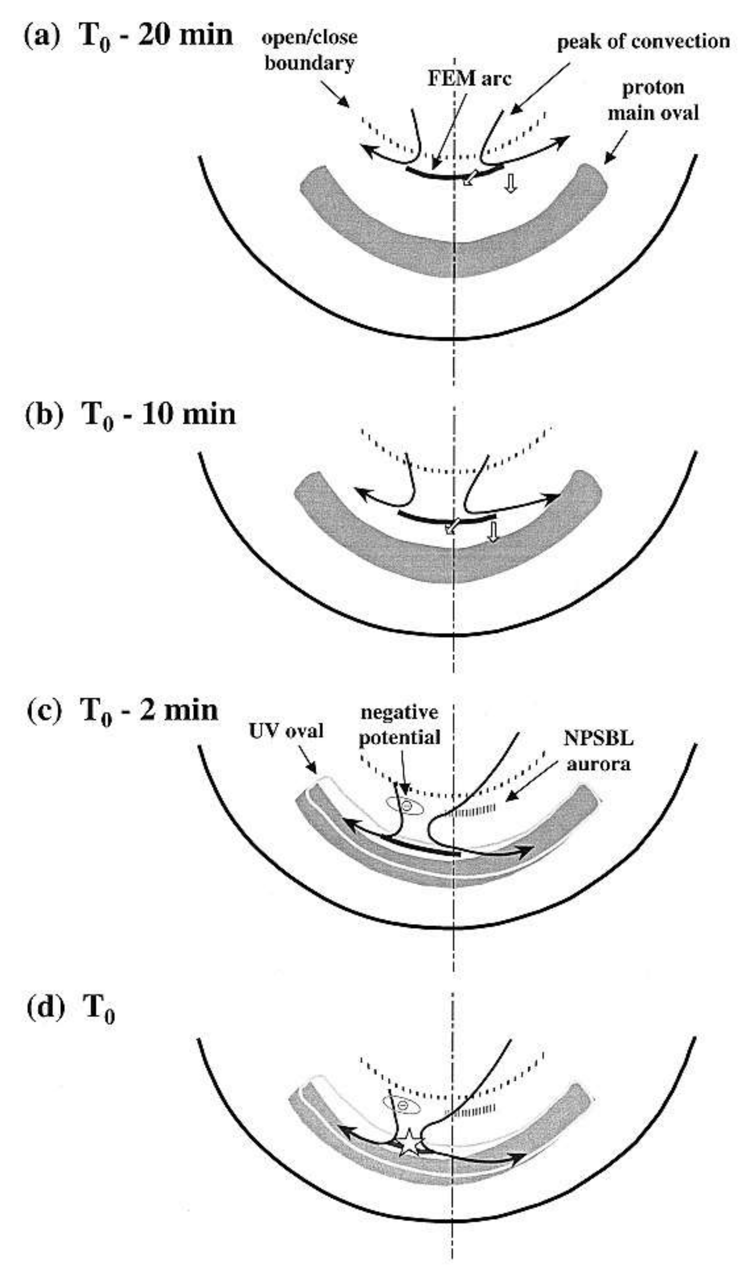

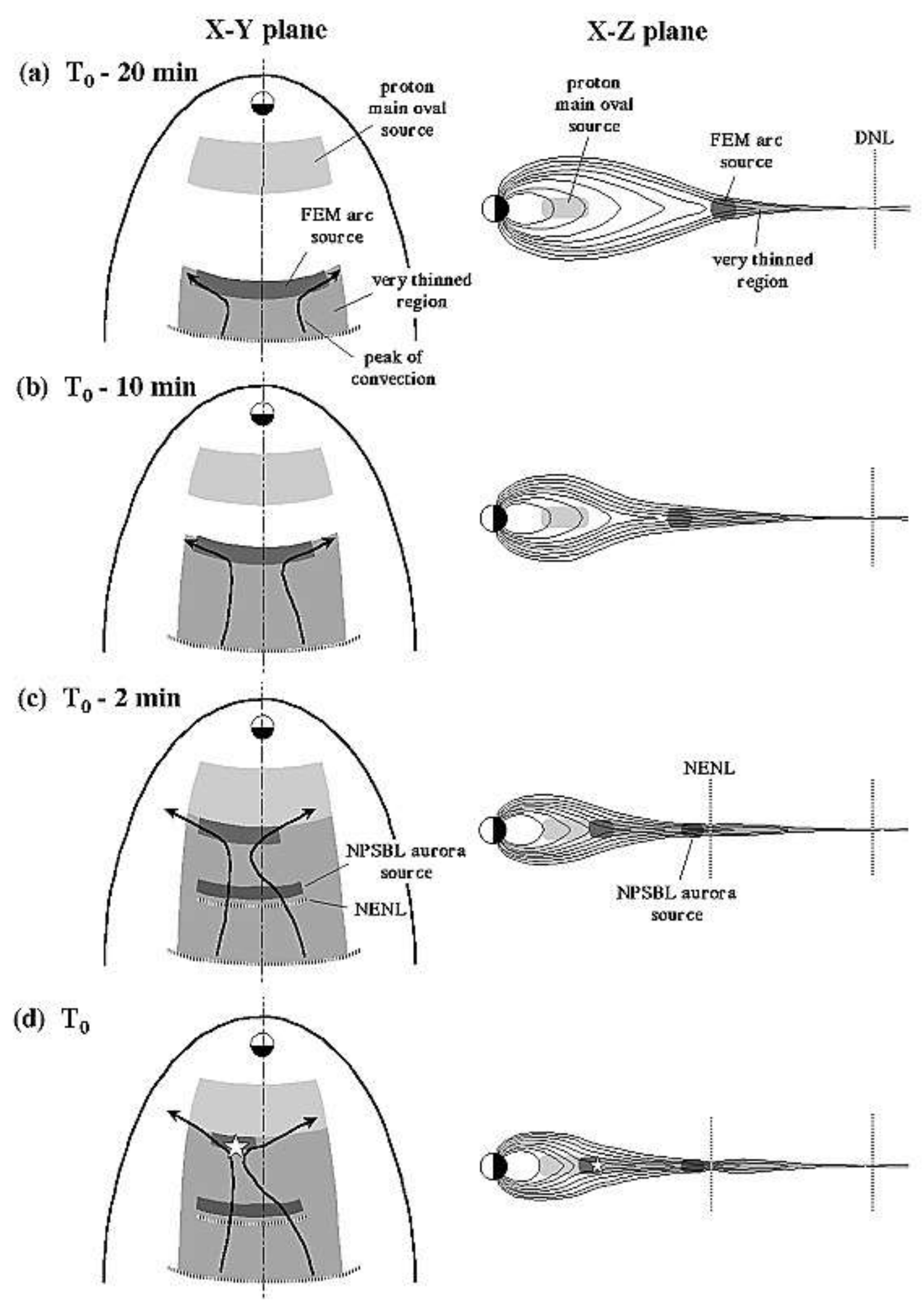

Onset location & Onset Arc

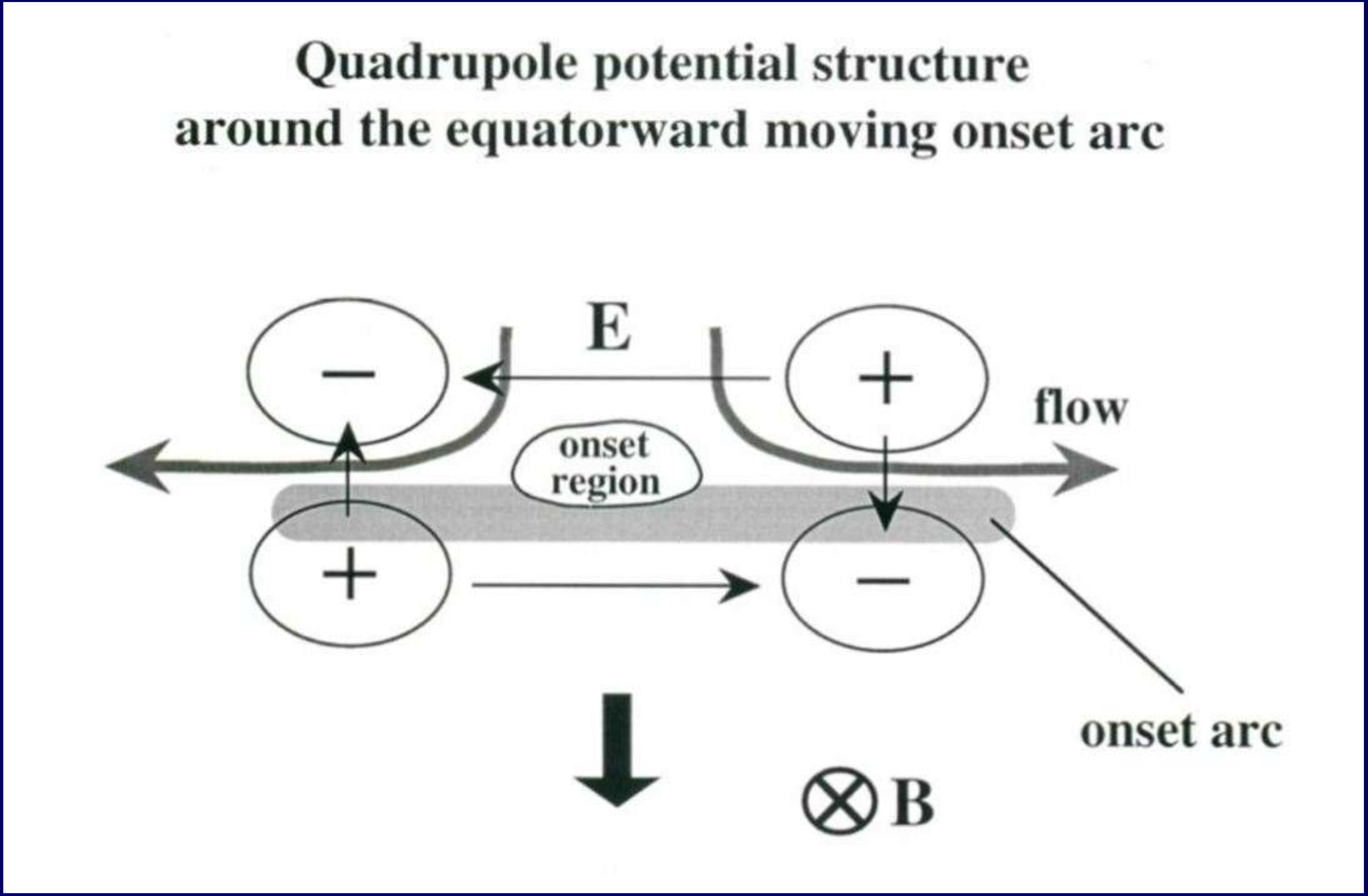

Possible Configuration in Magnetosphere

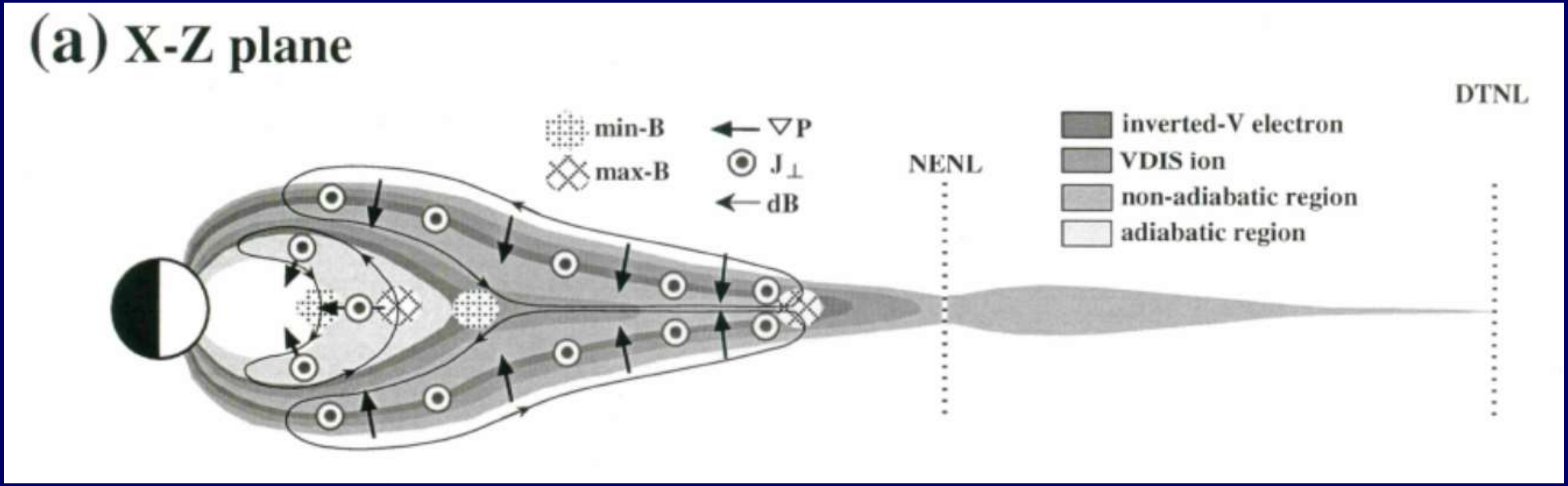

Possible Configuration in Magnetosphere

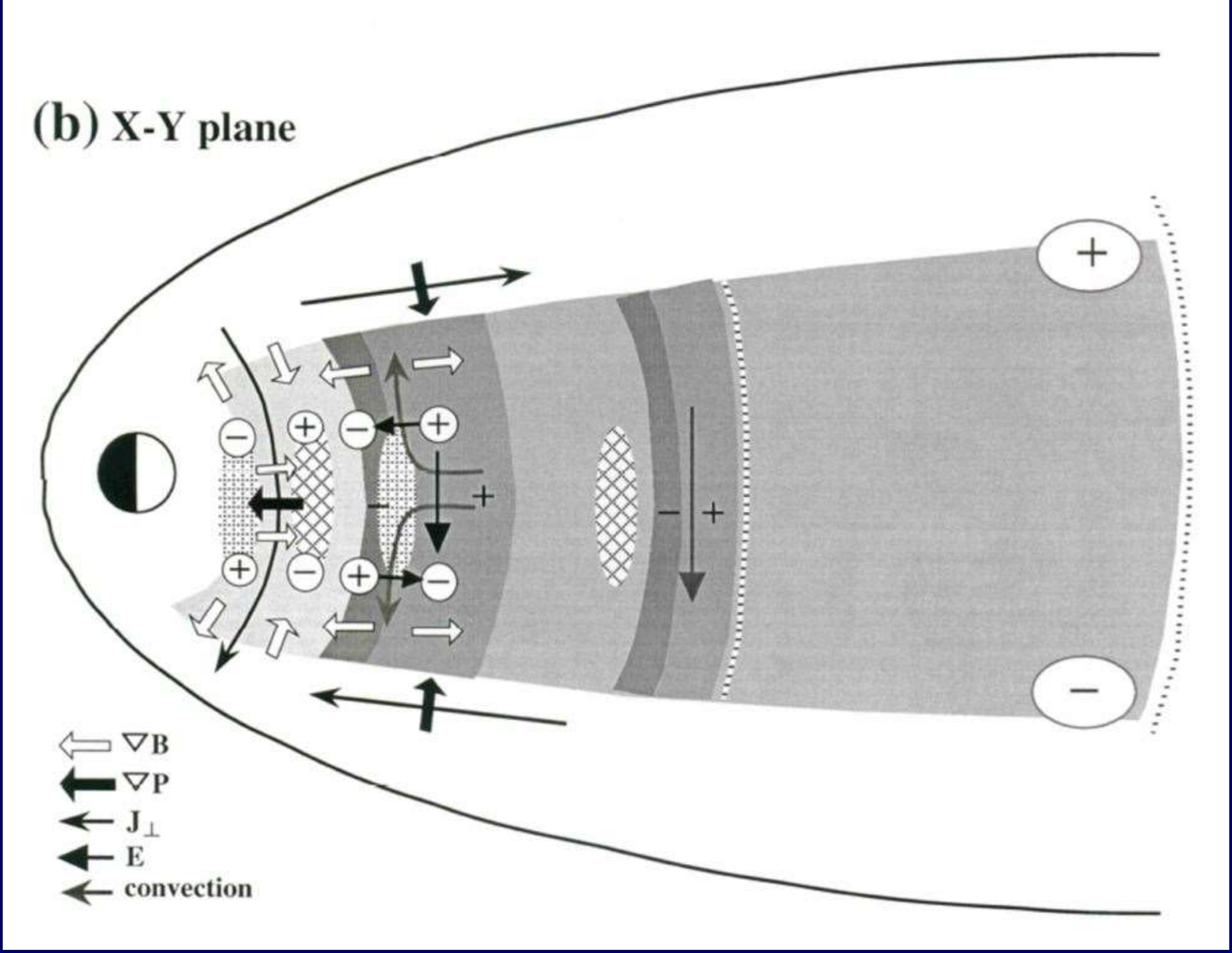

[Source mechanism for the onset arc]

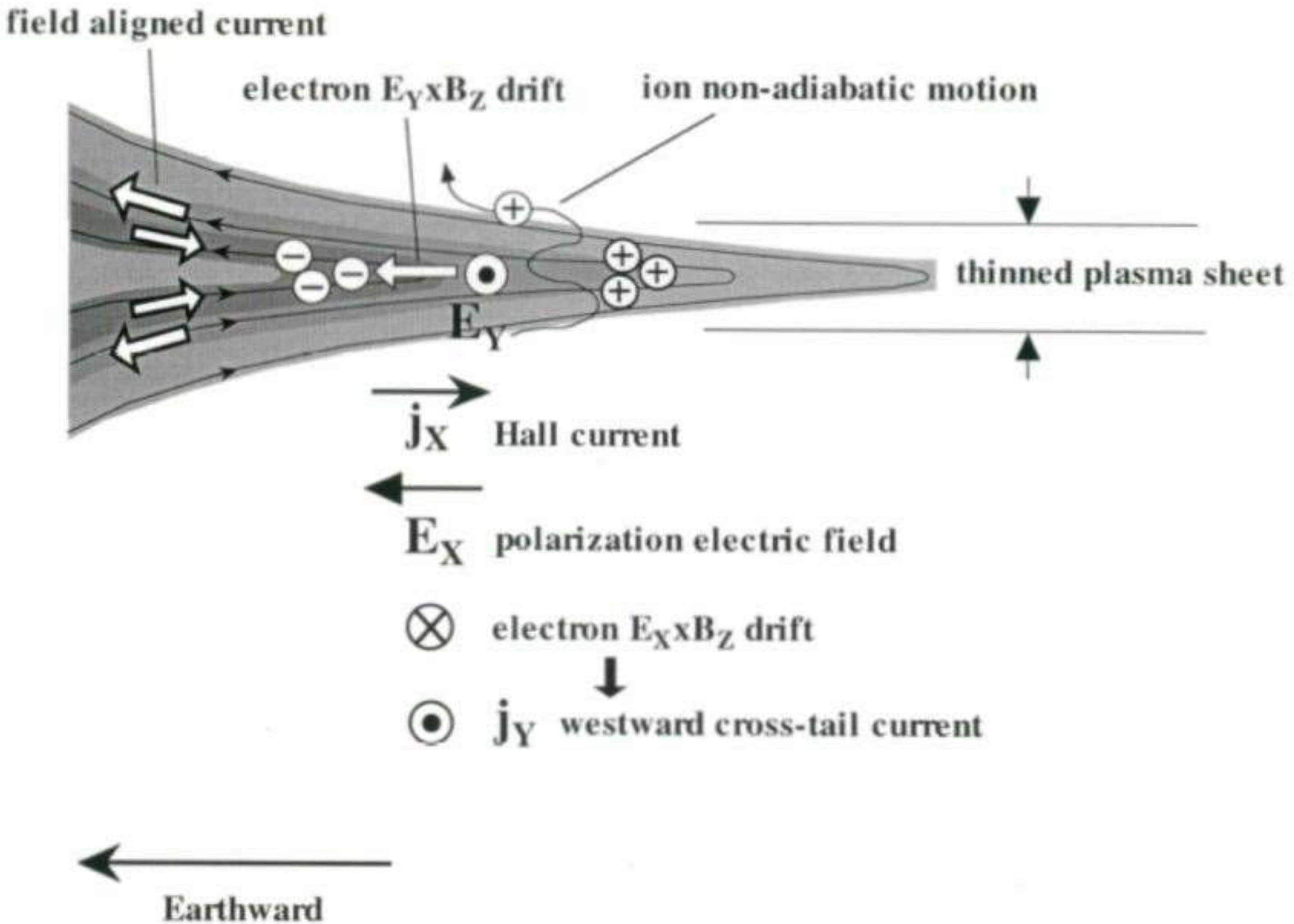

Localization & Explosive Growth

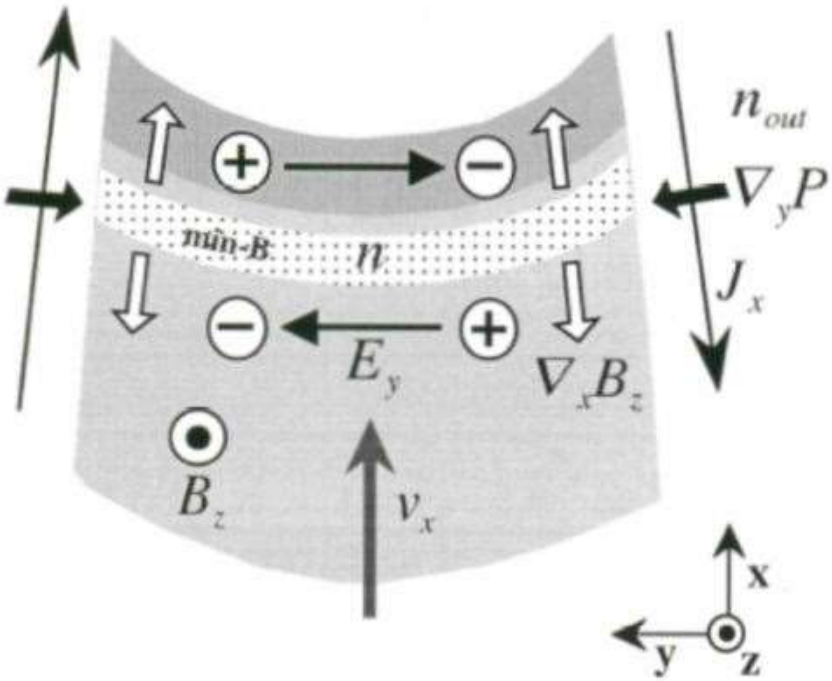

$$\frac{\partial n}{\partial t} + \nabla \bullet (n v_x) = 0$$

$$v_x = \frac{E_y}{B_z}$$

$$\frac{\partial n}{\partial t} + \frac{n}{B_z}\frac{\partial E_y}{\partial x} = 0$$

$$n = n_0 \exp\left(-\frac{\frac{\partial E_y}{\partial x}}{B_z} t\right)$$

$E_x = 20$ mV/m, $dx = 100$ km, B=36711 nT : at DMSP-F9

$E_x = 0.33$ mV/m, $dx = 0.95$ Re, B_z=10 nT : at equatorial plane

$$\tau = \frac{B_z}{\frac{\partial E_y}{\partial x}}$$

$\tau = 184$ sec

Localization & Explosive Growth

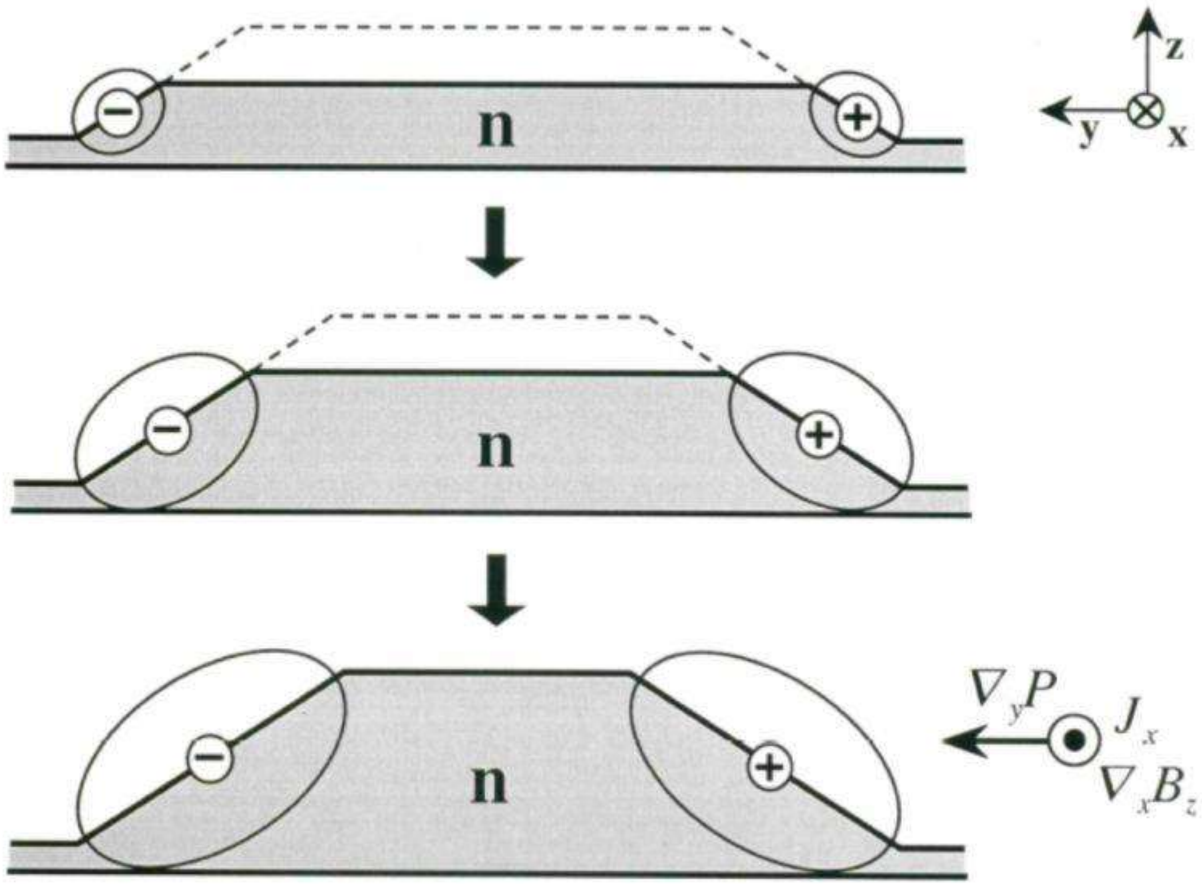

Precursor phenomena & Explosiveness

- Auroral fading
  (e.g. *Kauristie et al.* (1997))
- AAF (Azimuthally spaced Auroral Forms)
  (*Elphinstone et al.*, 1995)
- Enhancement of equivalent current
  (e.g. *Kawasaki and Rostoker*, 1979)

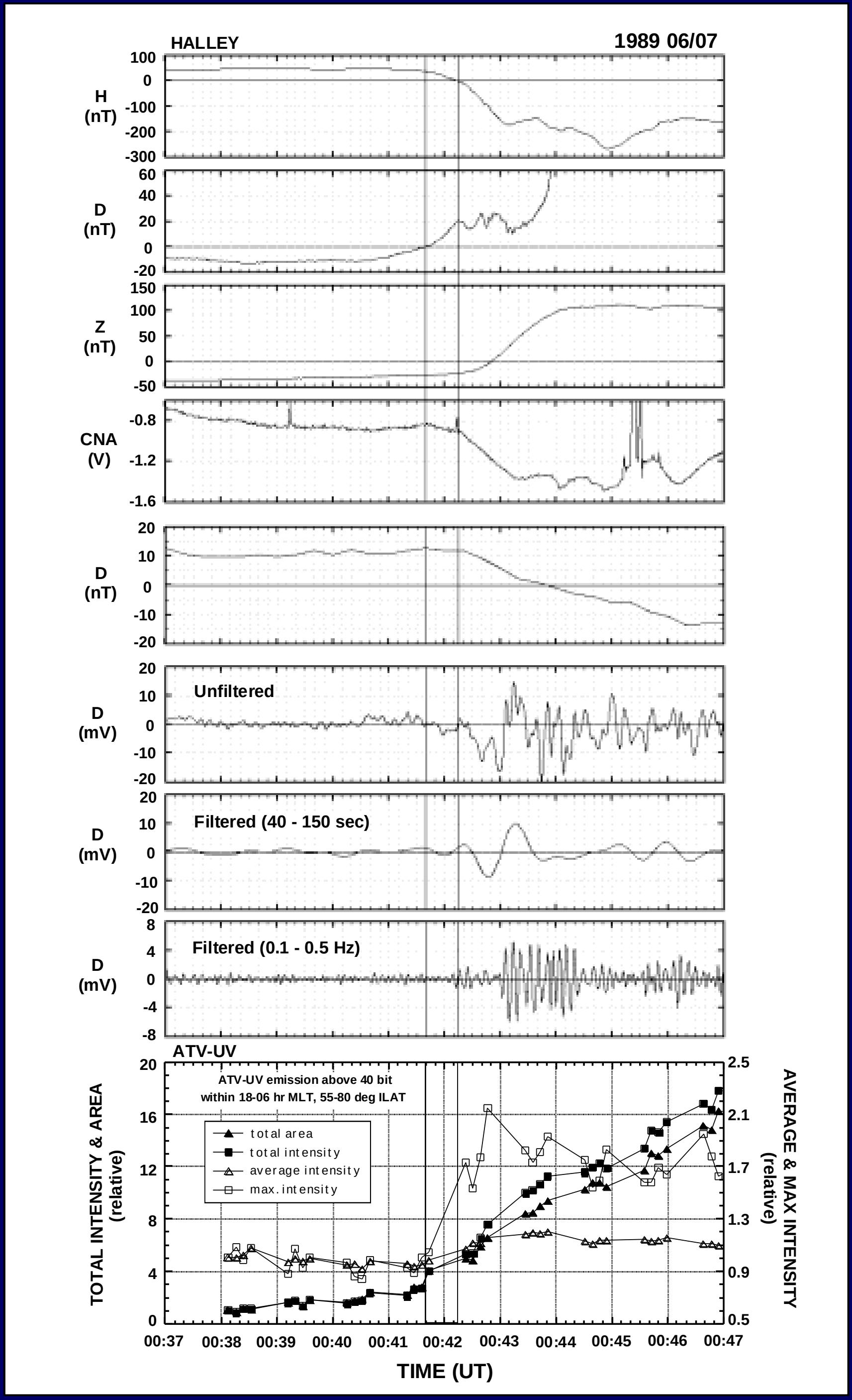

Kadokura et al. (2002)

Explosive Growth

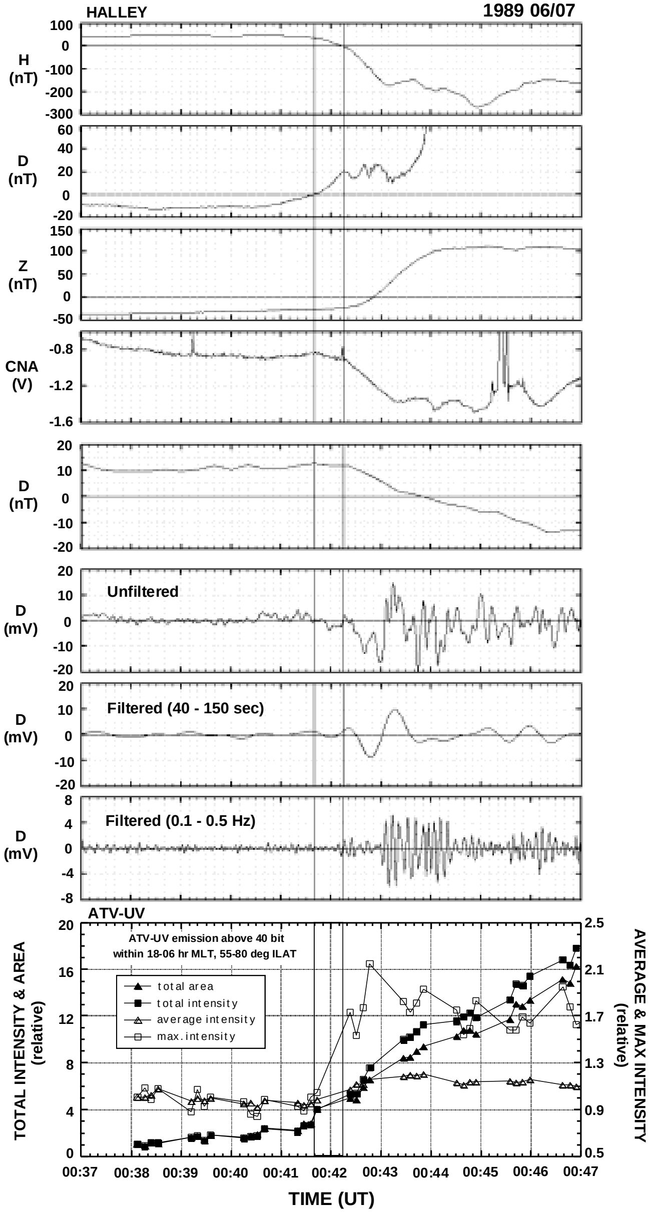

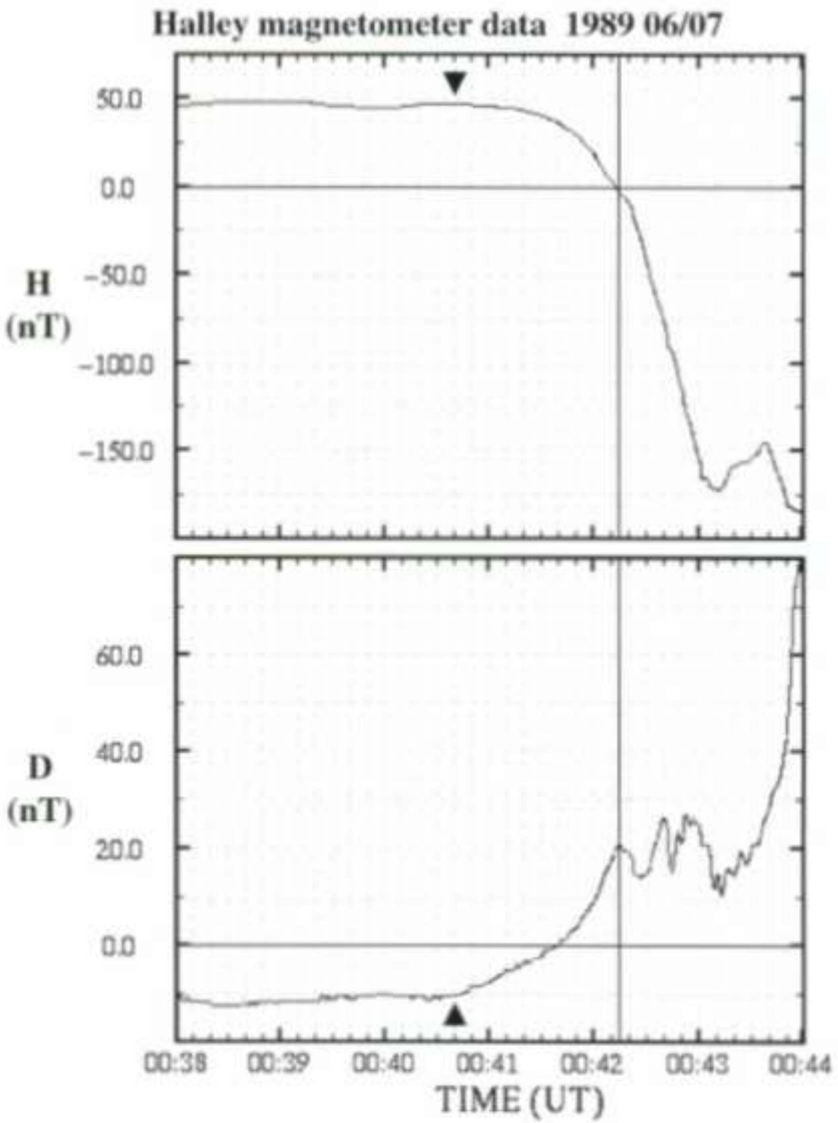

Precursor phenomena

Henderson, 2009

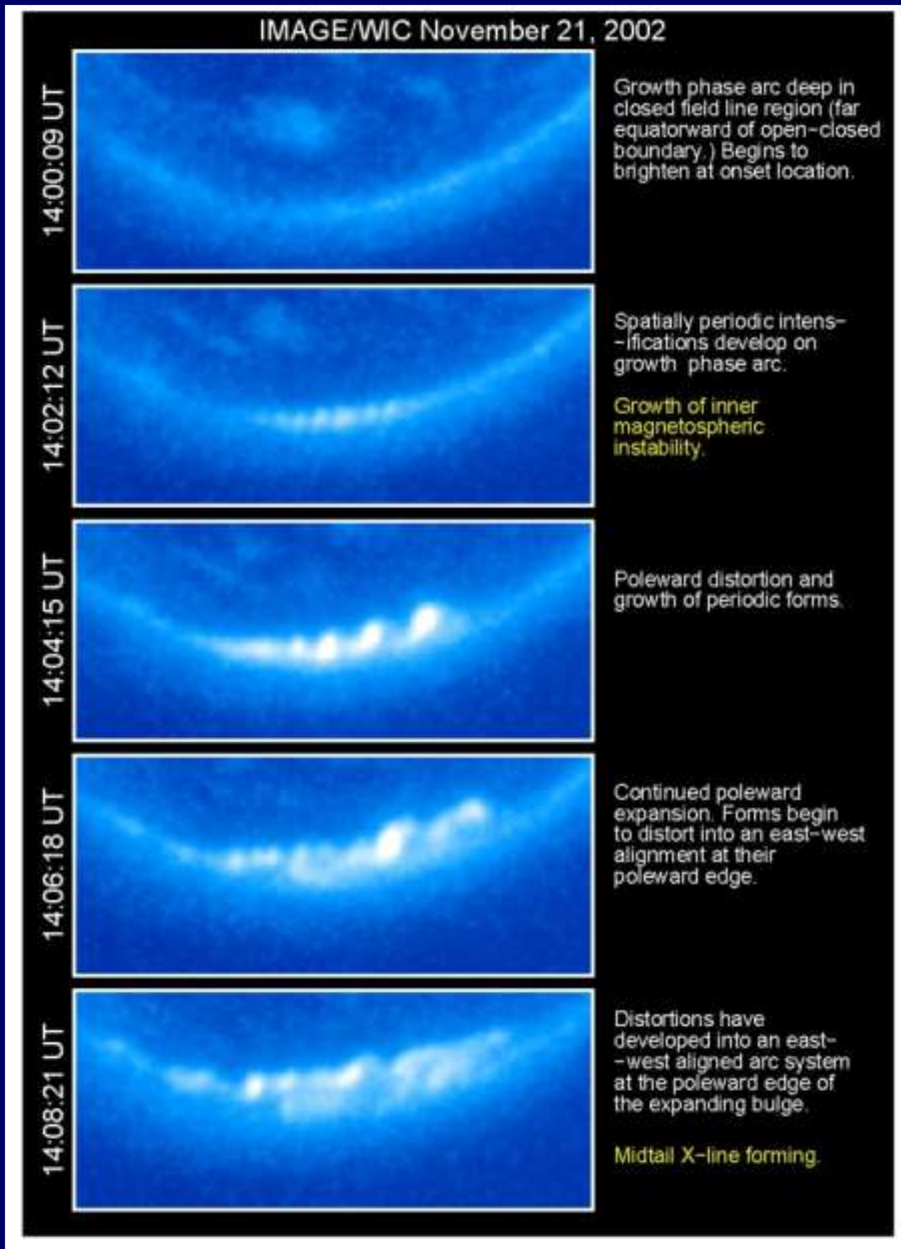

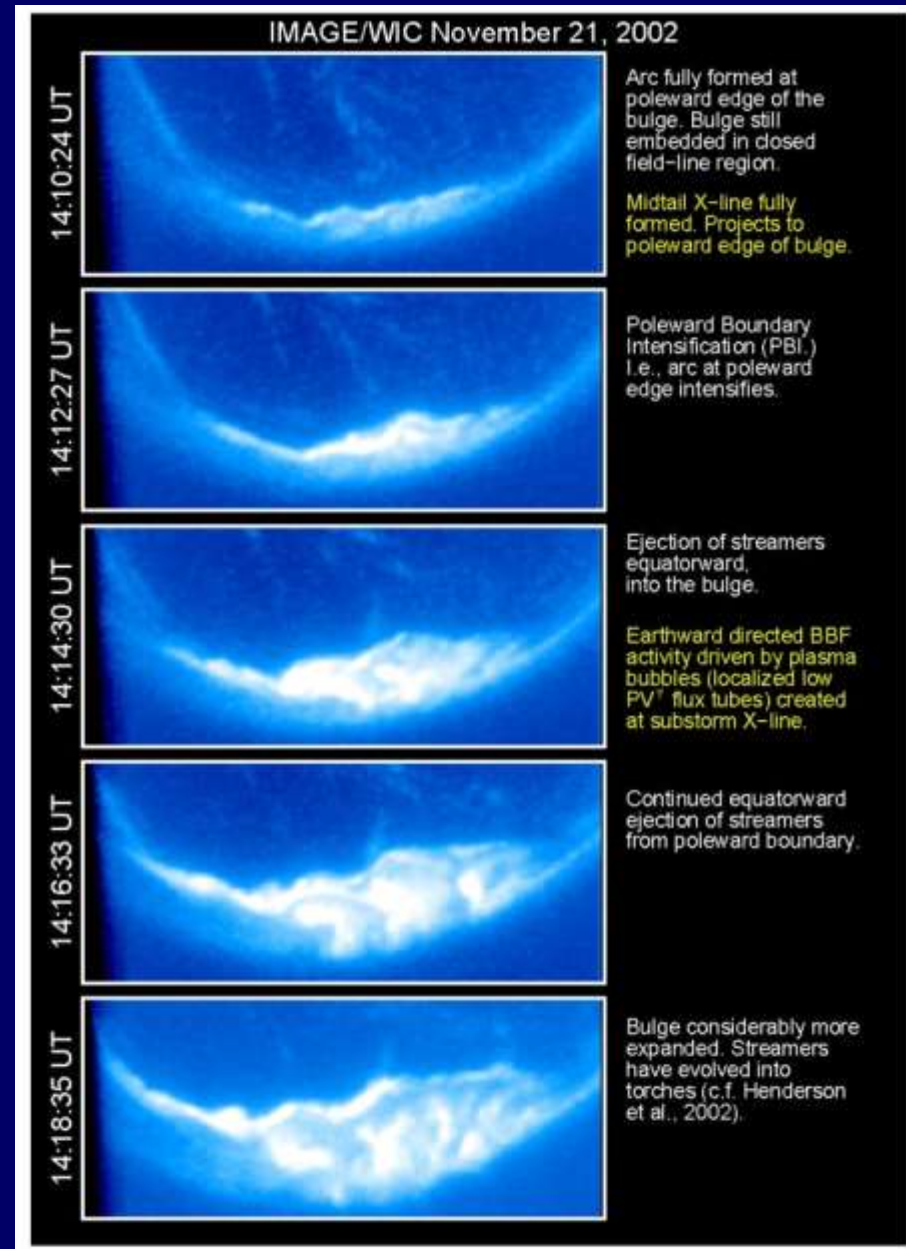

Phenomena at the beginning

Sakaguchi, et al., 2009

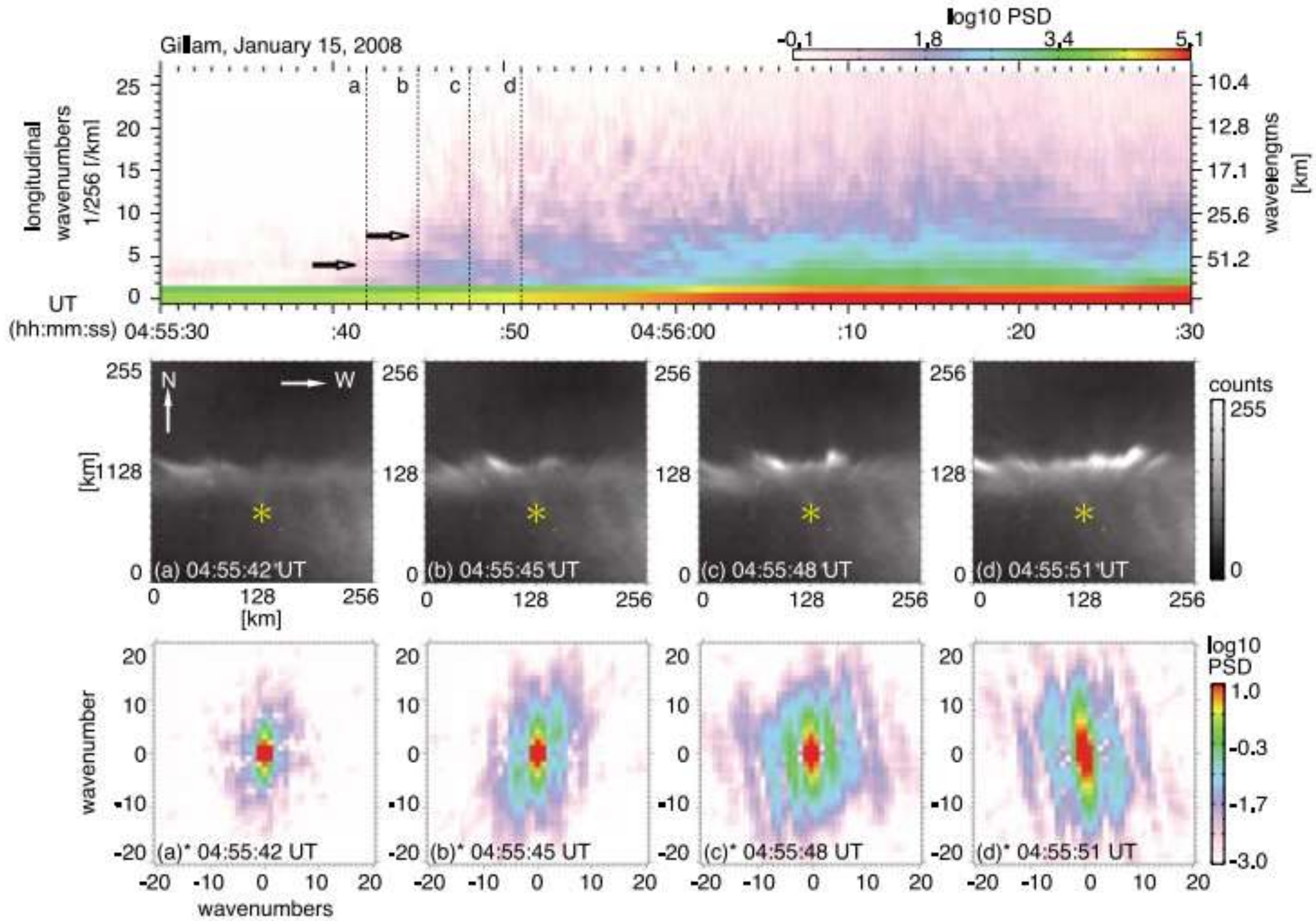

Figure 2. Brightening auroral images and wavenumber spectra at the beginning of a substorm on January 15, 2008. (top) Dynamic spectra of wavenumeber/wavelength (left/right axis) in the east-west direction at 04:55:30–04:56:30 UT, (middle) white-light auroral images every 3 s, and (bottom) power spectral densities in wavenumber domain of Figure 2 (middle) obtained by Fourier translation. A yellow asterisk in Figure 2 (middle) indicates the location of the magnetic zenith.

Phenomena at the beginning

Sakaguchi, et al., 2009

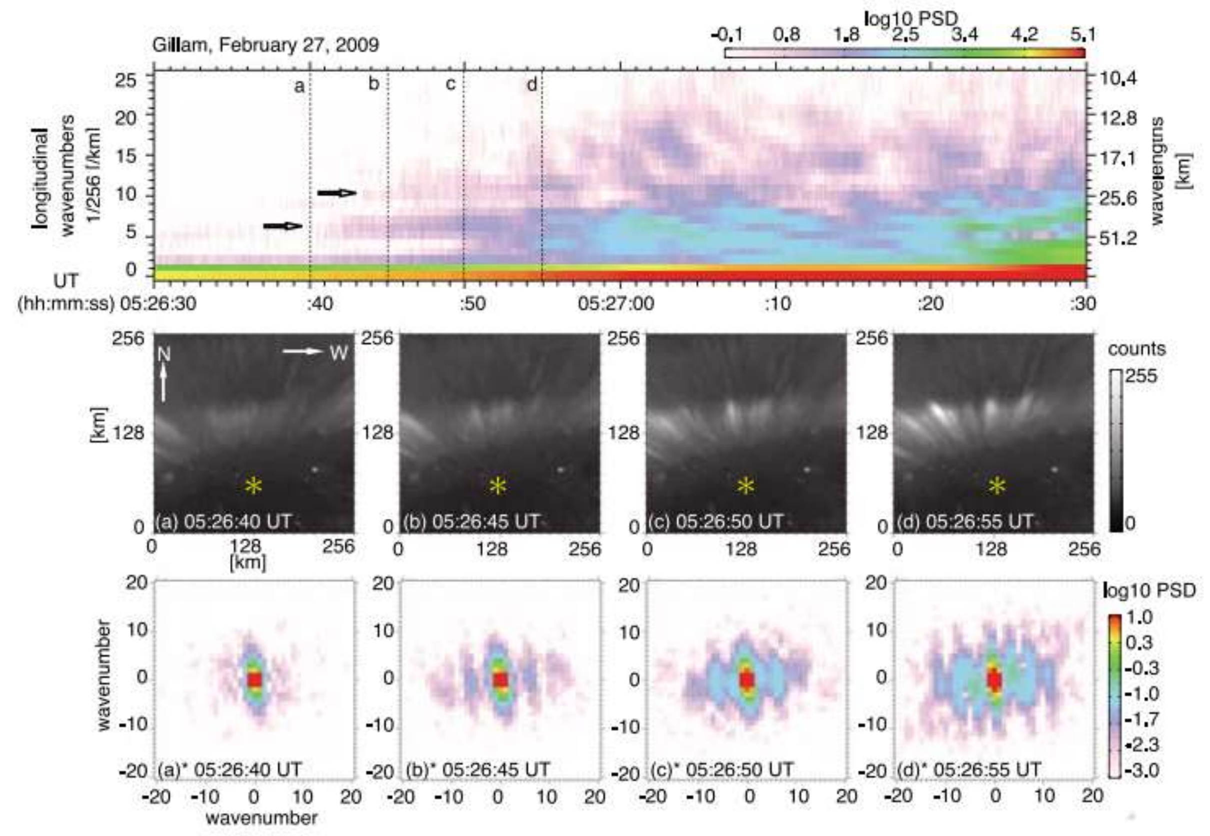

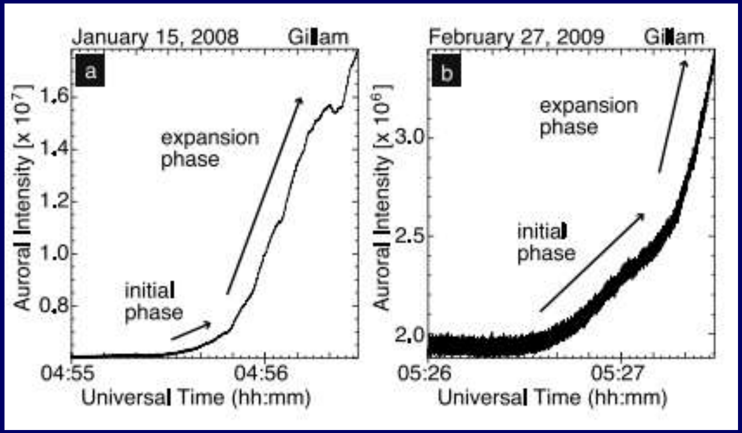

Precursor phenomena　Auroral Beads

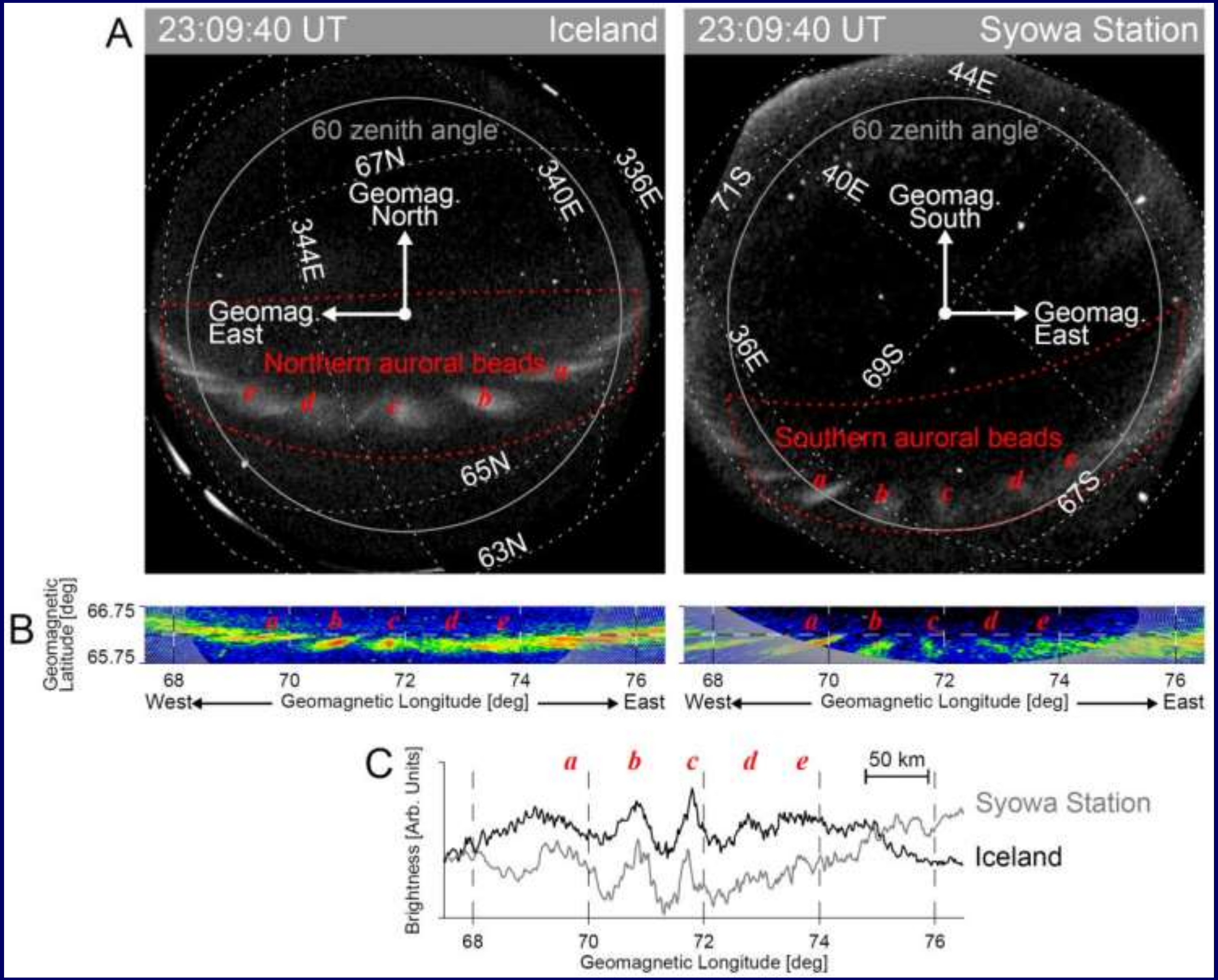

Motoba et al.,GRL, 2012

Precursor phenomena　　Auroral Beads

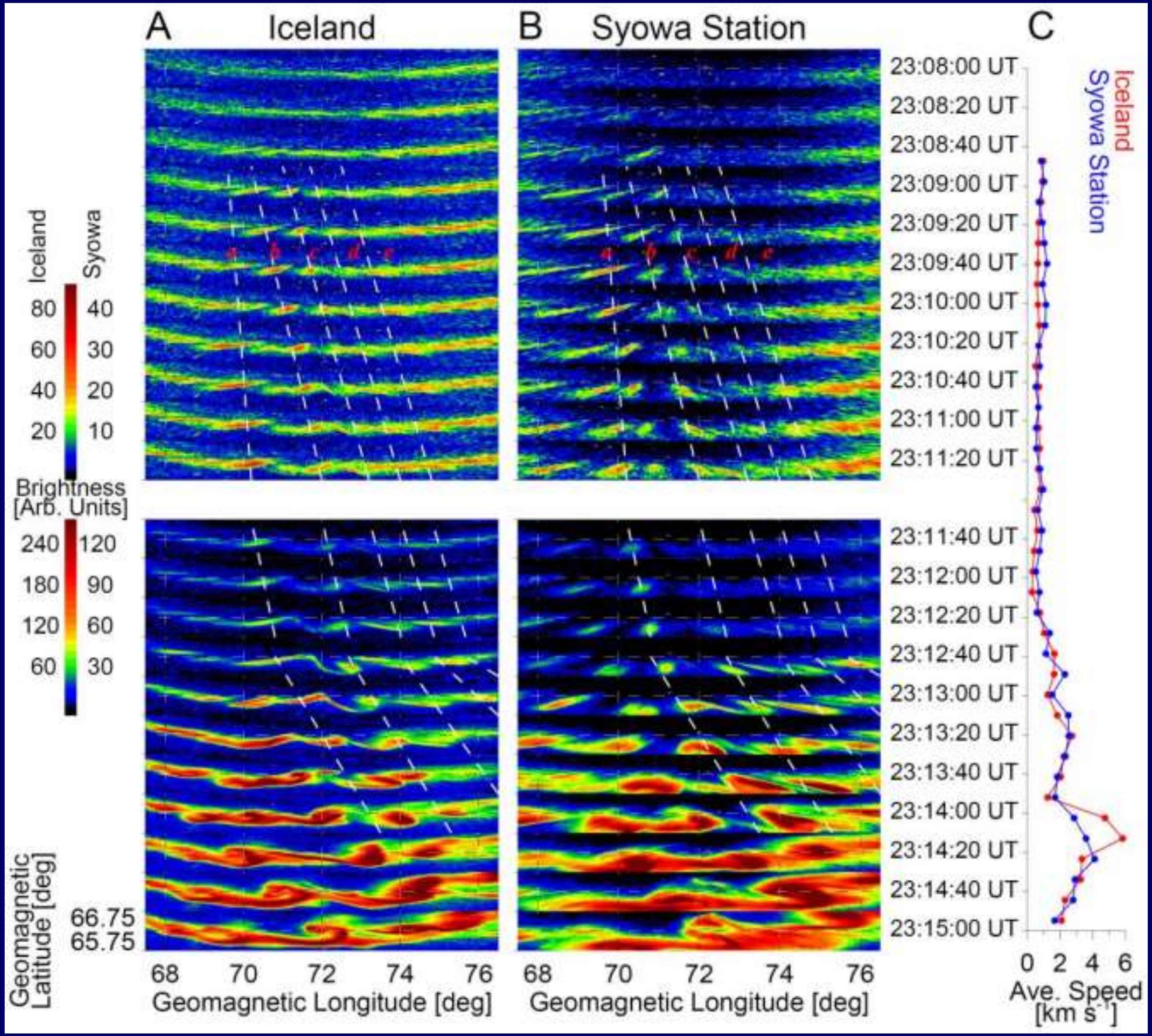

Motoba et al.,GRL, 2012

Classical Morphology に対する追加、修正

- Stepwise evolution during the expansion phase

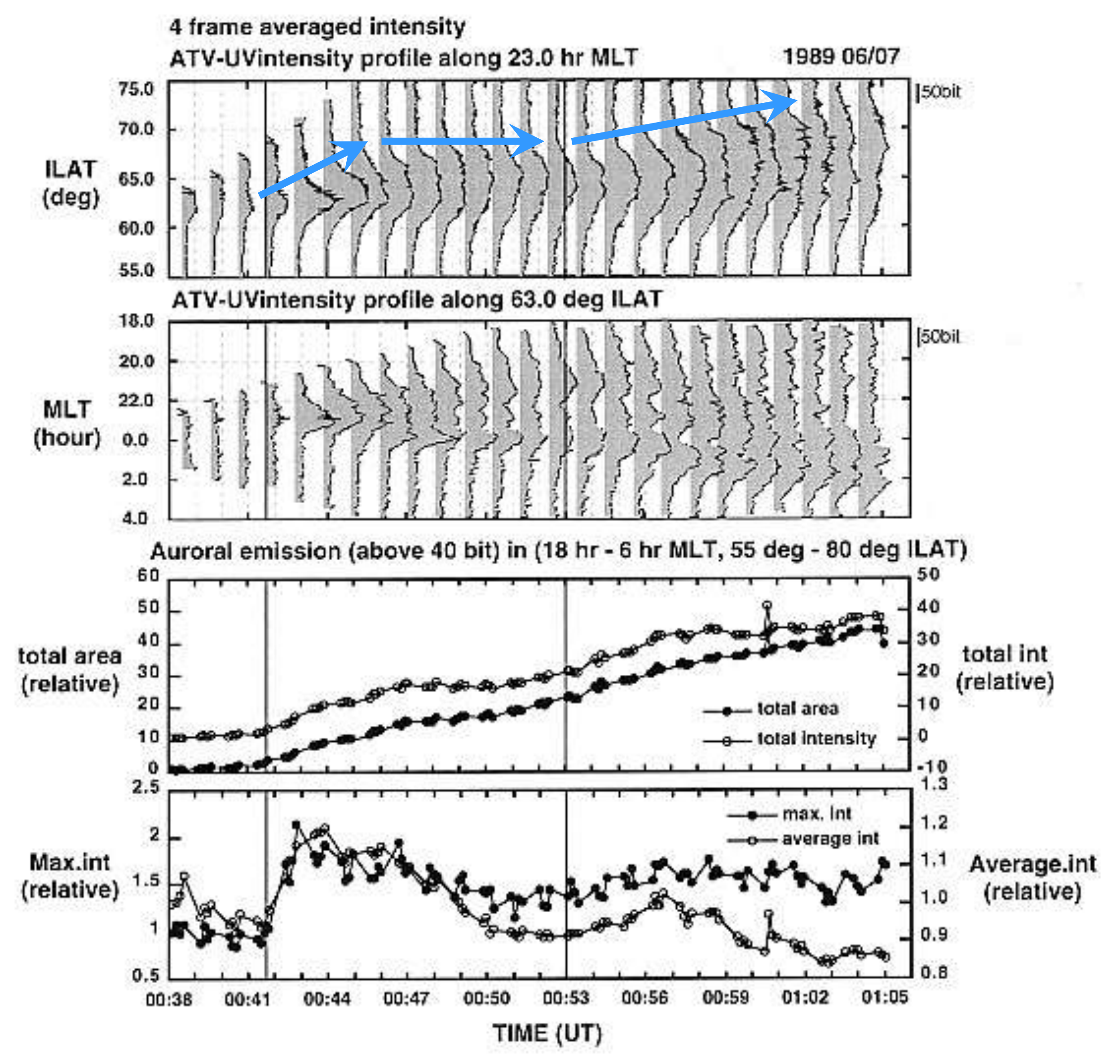

Stage-1: Rapid poleward expansion

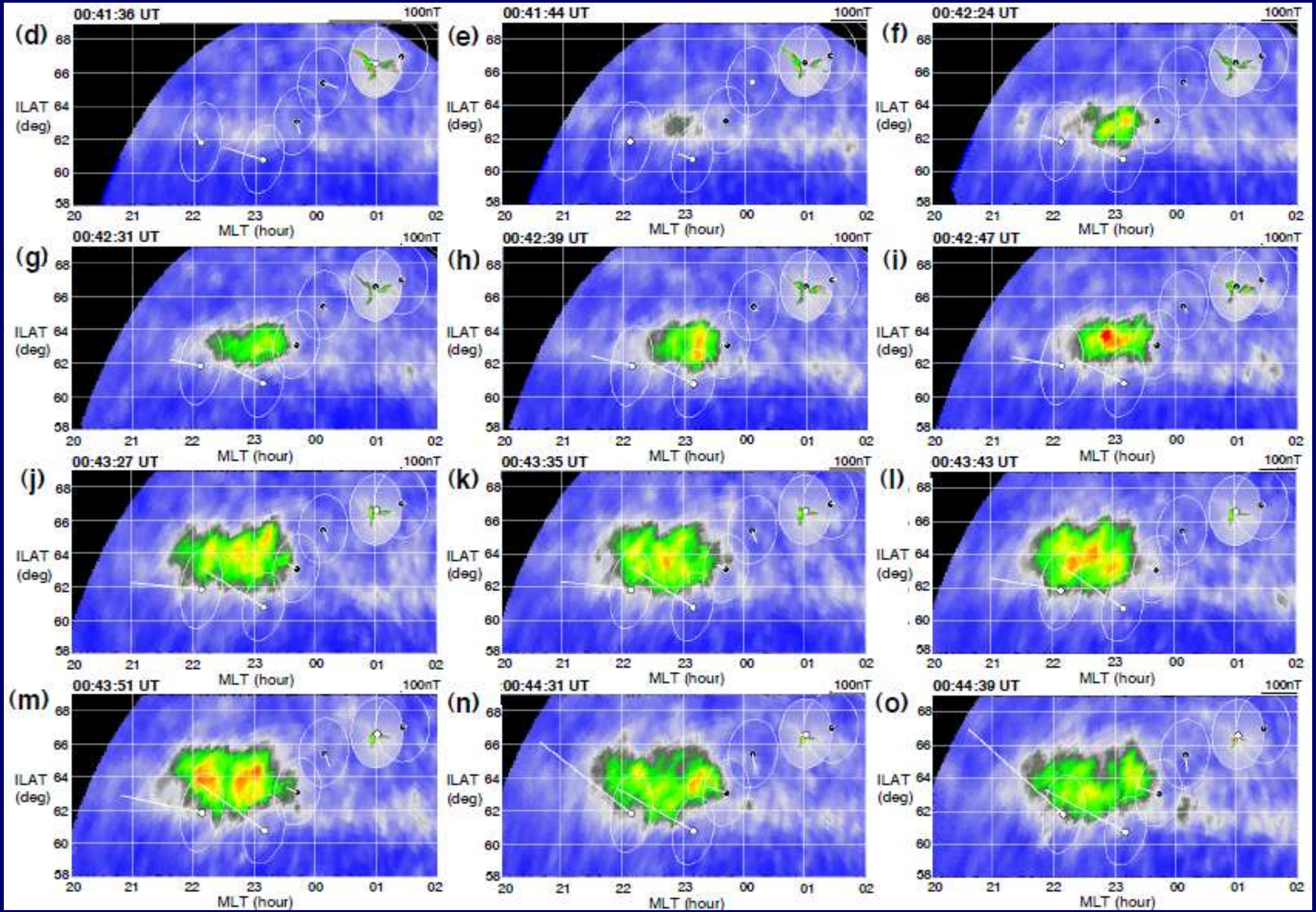

Breakup region ≠ Negative potential center

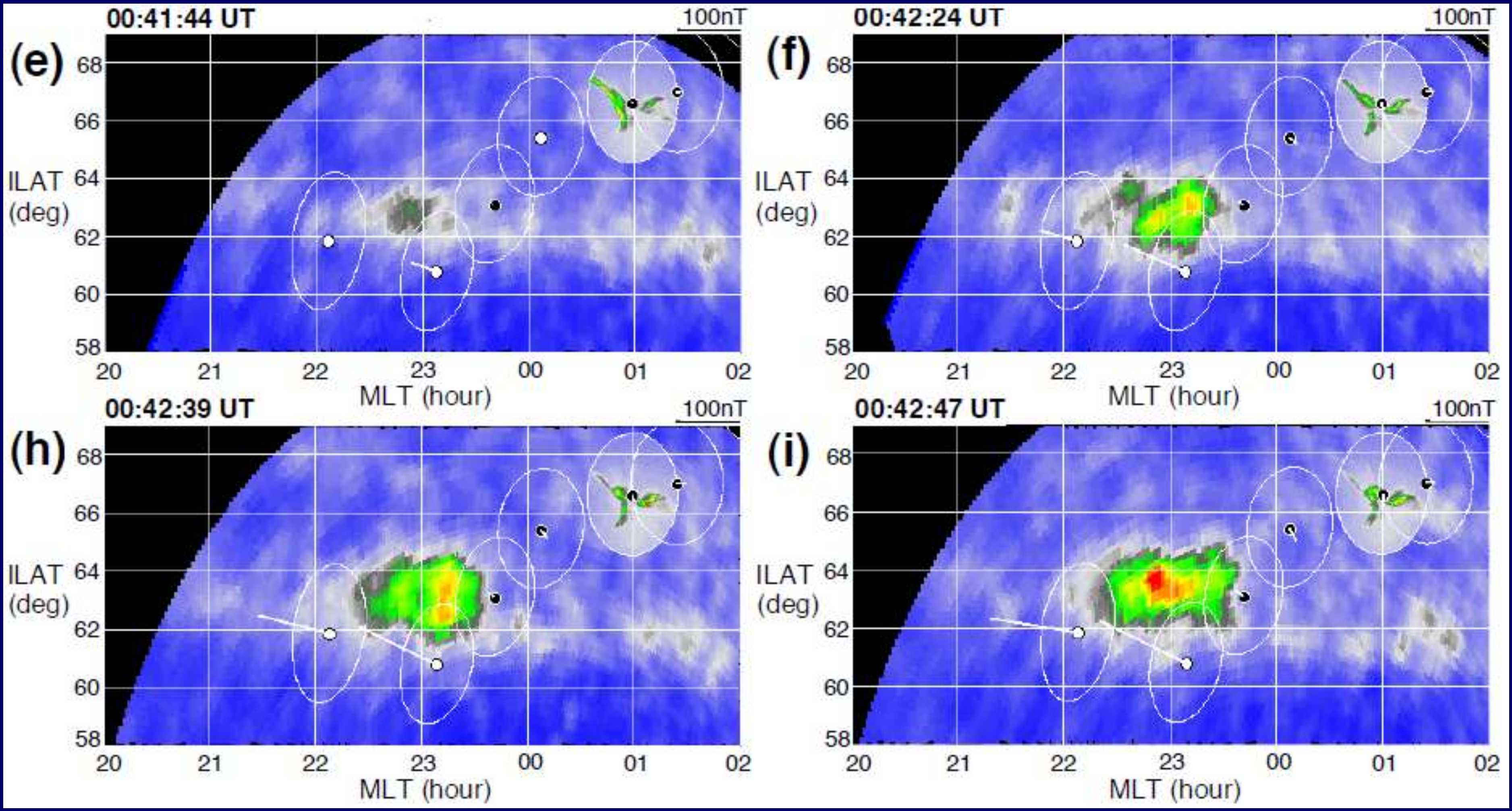

Stage-1: Pure Pi2 wave form

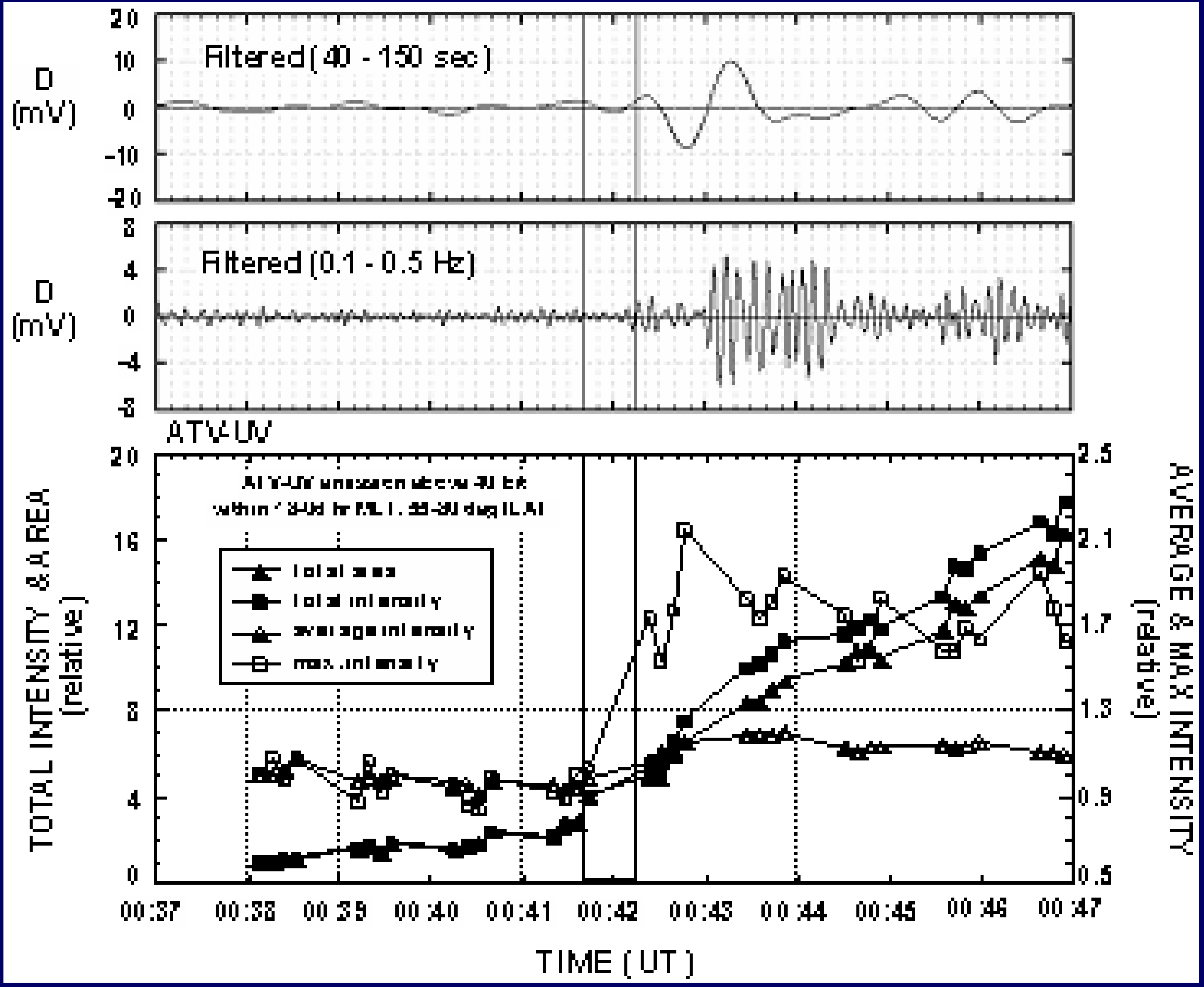

Onset Phenomena: Pi2, Pi1B

Magne-H

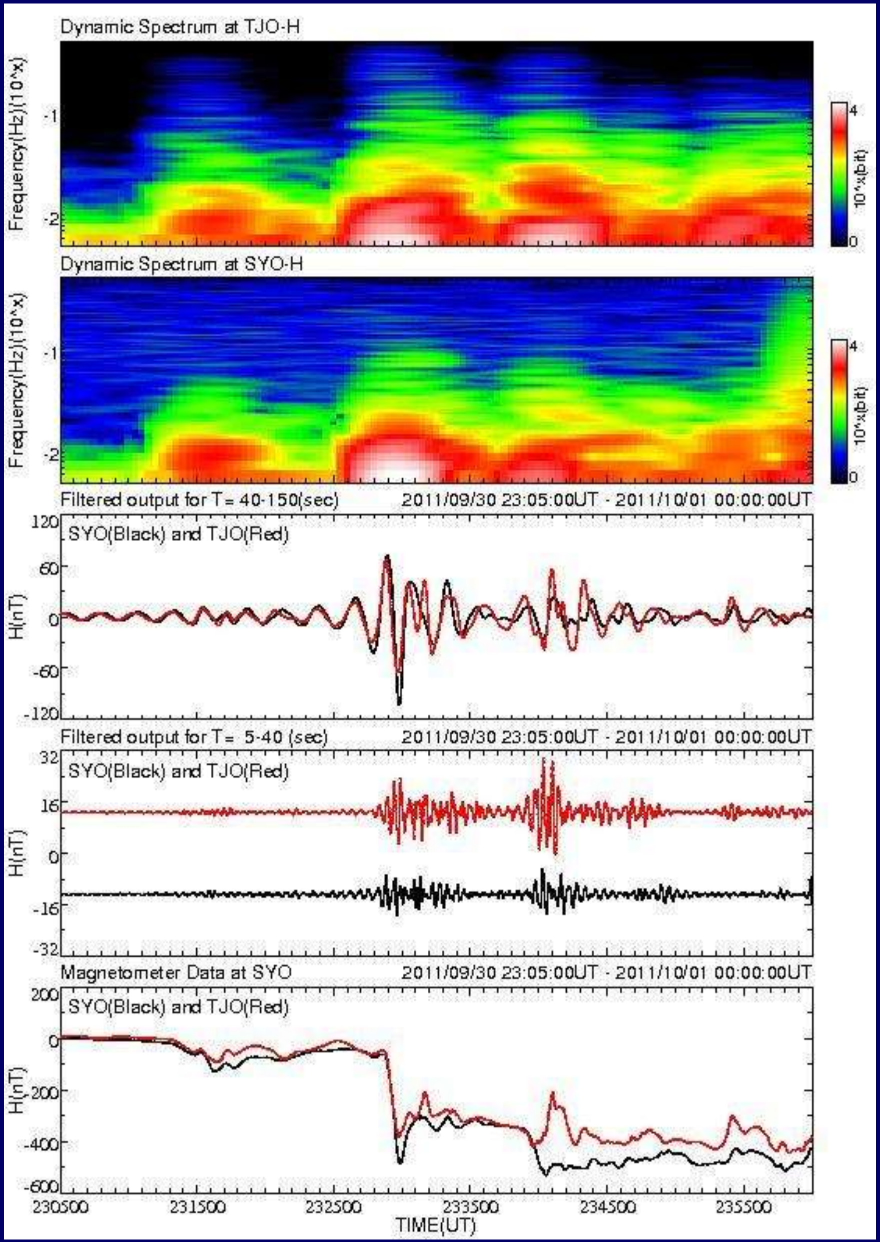

Aurora

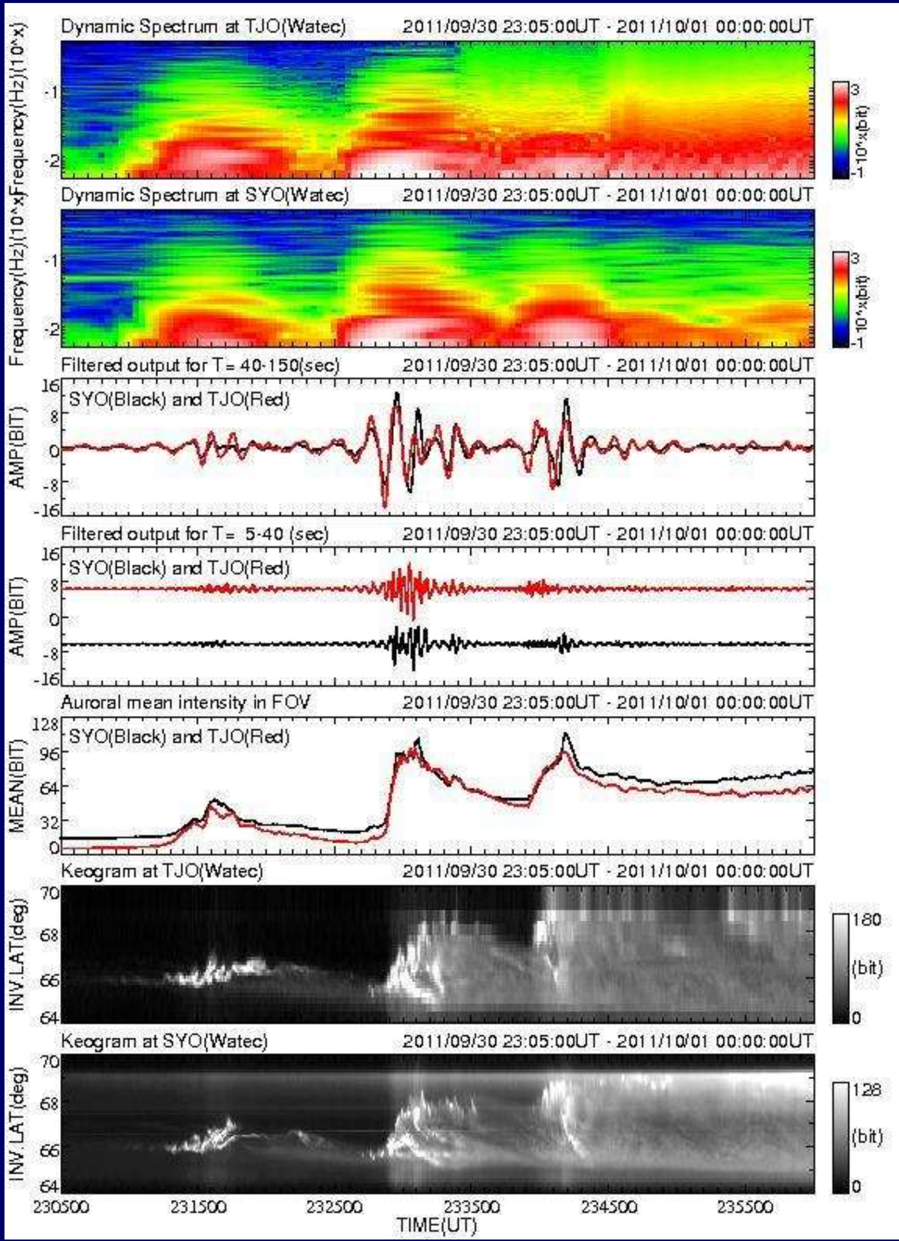

Onset Phenomena: Pi2, Pi1B

TJO

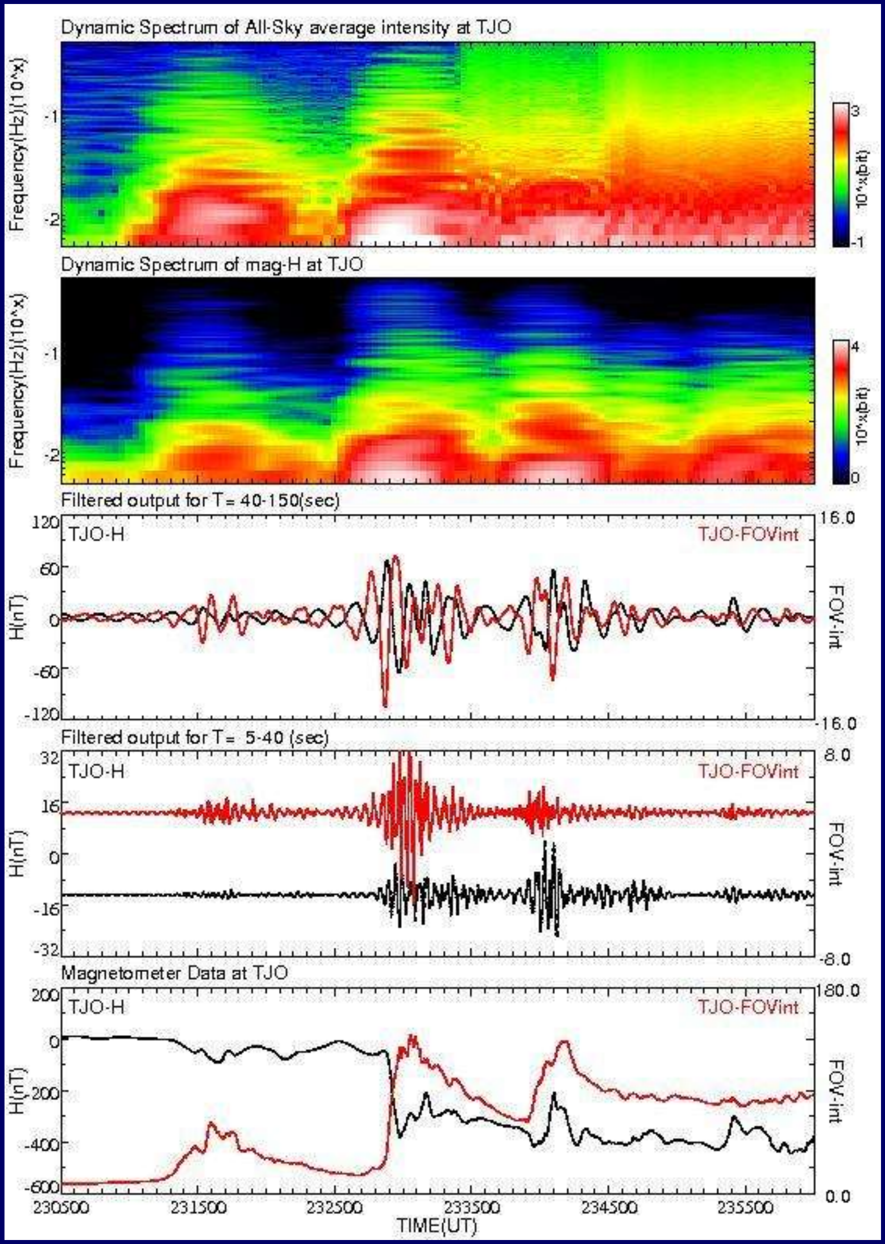

SYO

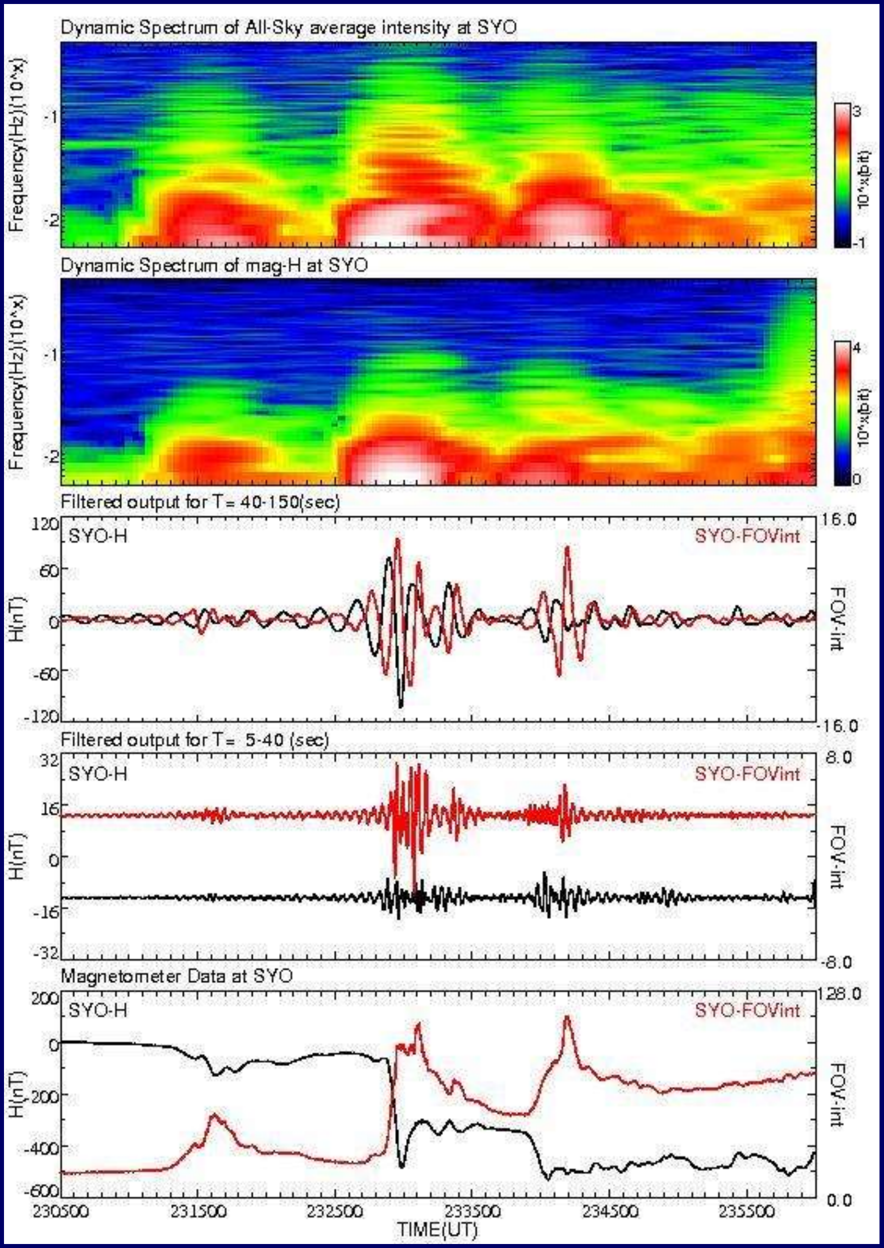

Stage-3

Re-activation of the further expansion

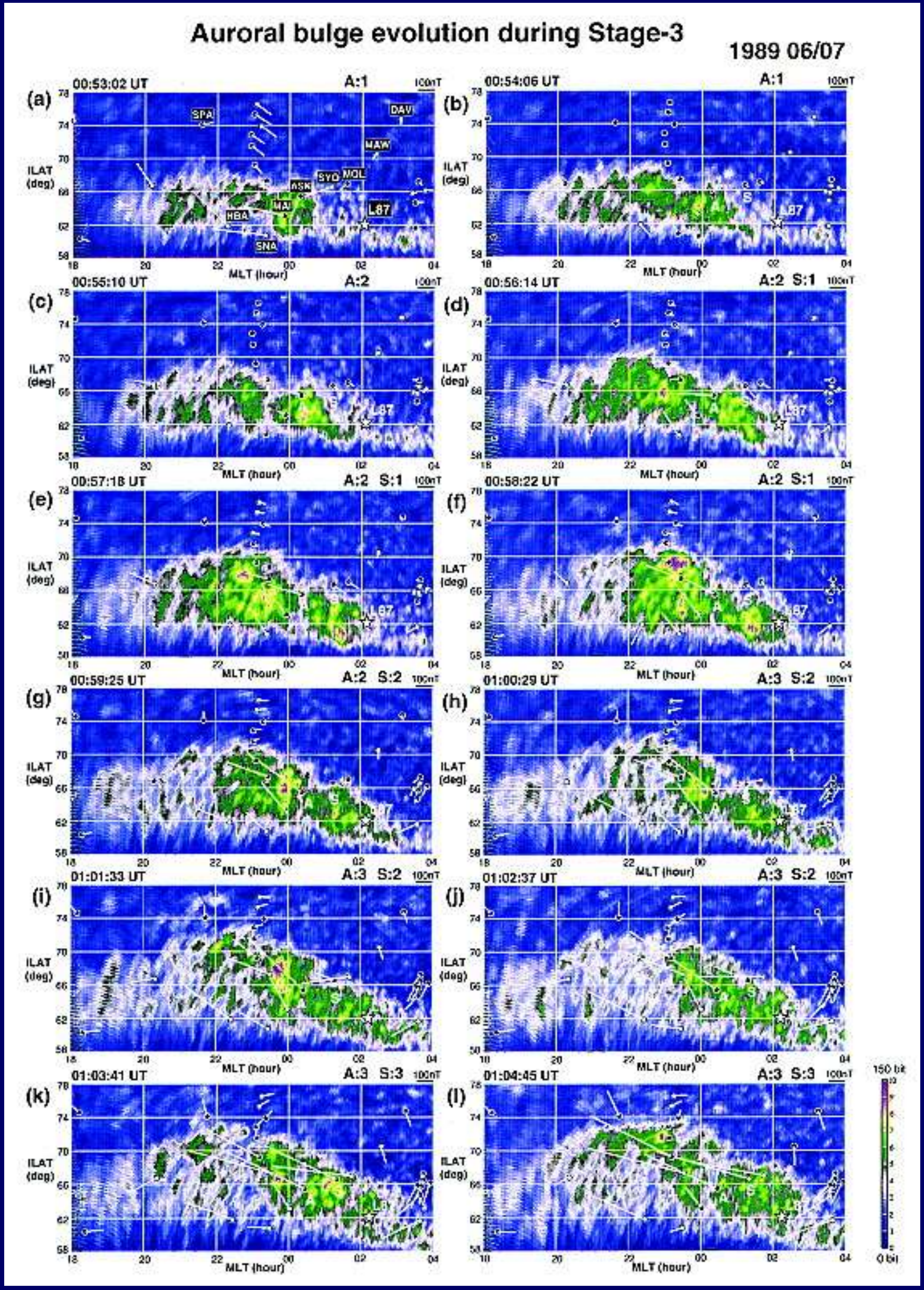

Classical Morphology に対する追加、修正

- Stepwise evolution during the expansion phase

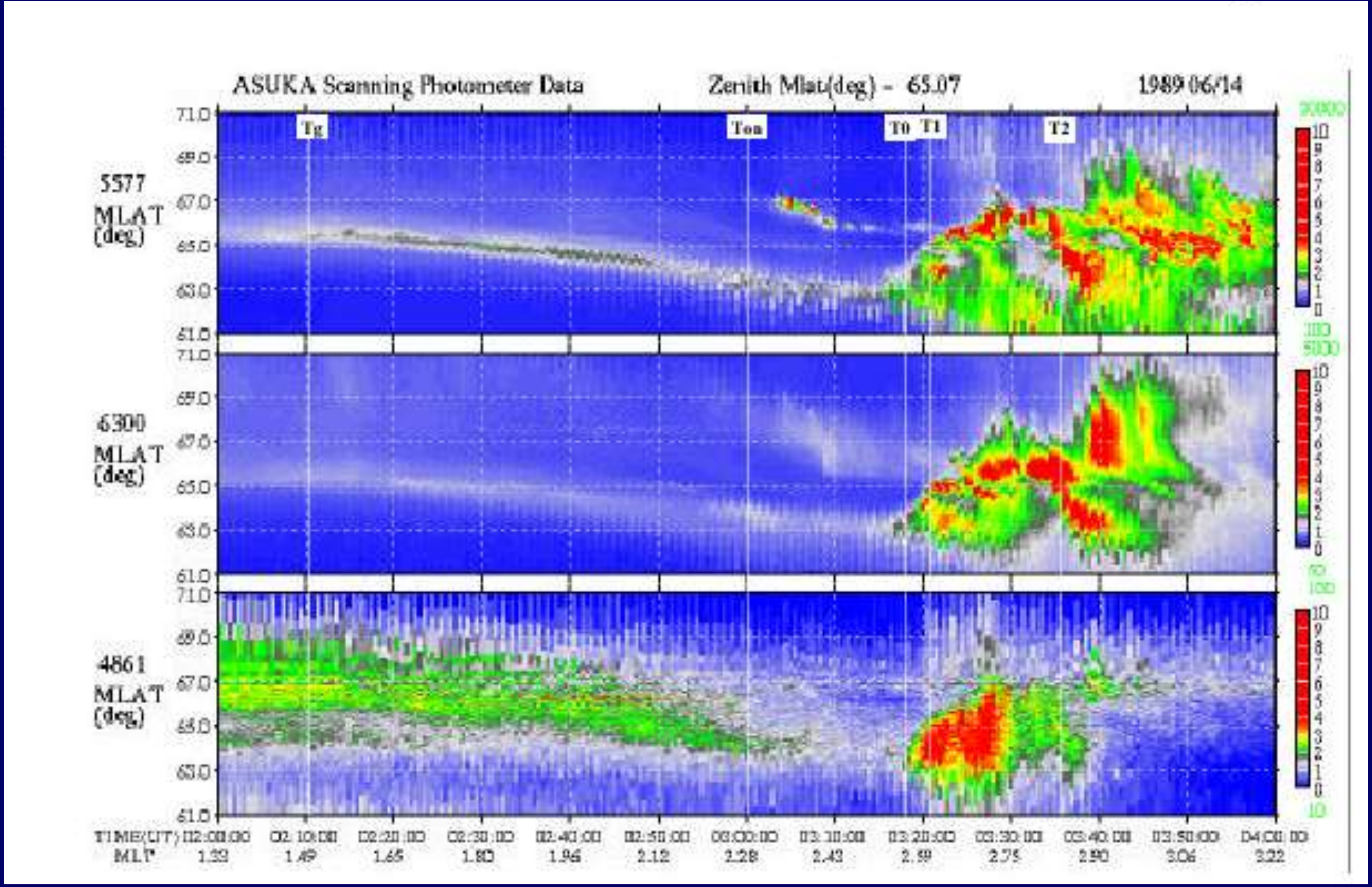

Classical Morphology に対する追加、修正

- Stepwise evolution during the expansion phase

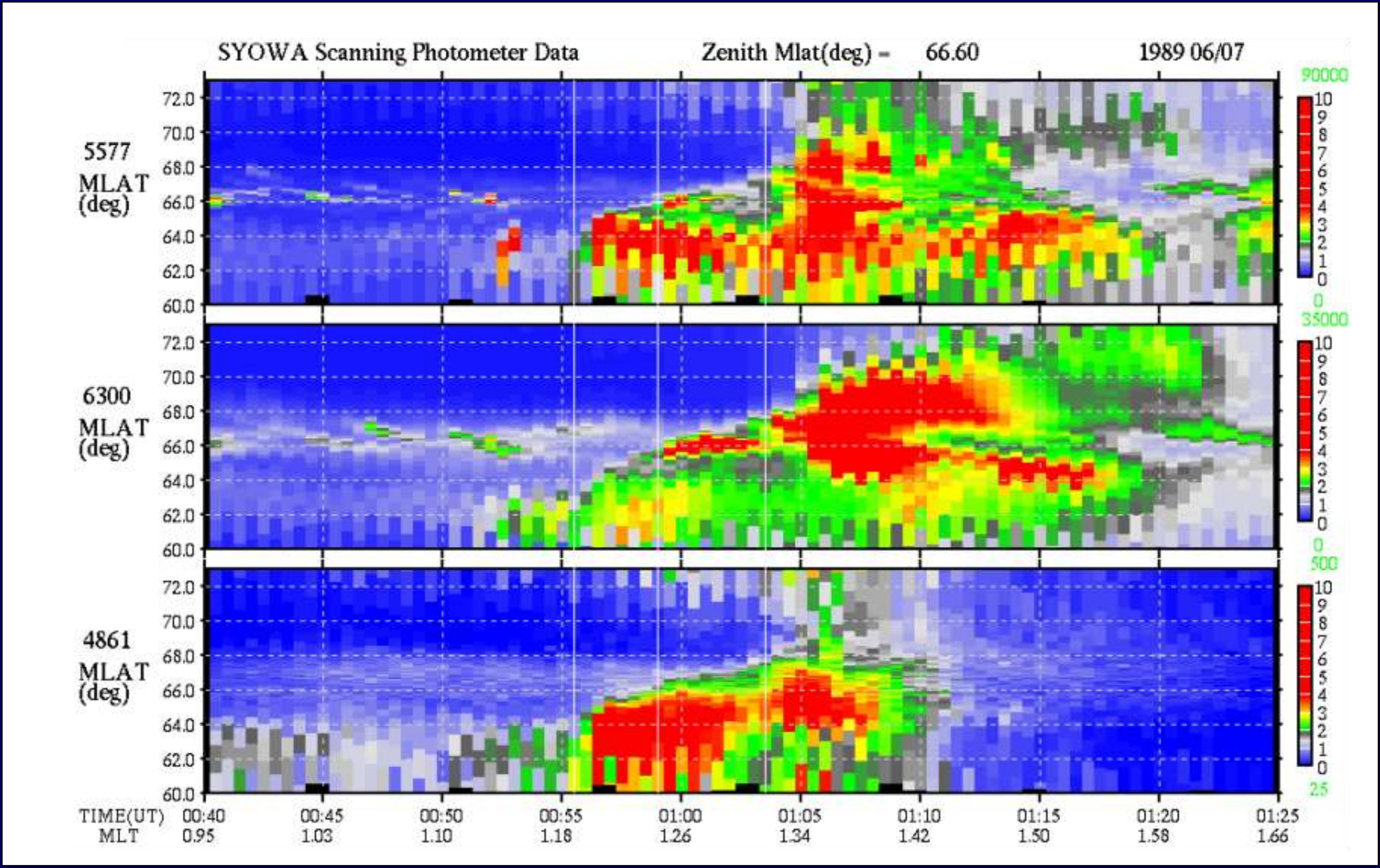

➢ Stepwise evolution during the expansion phase

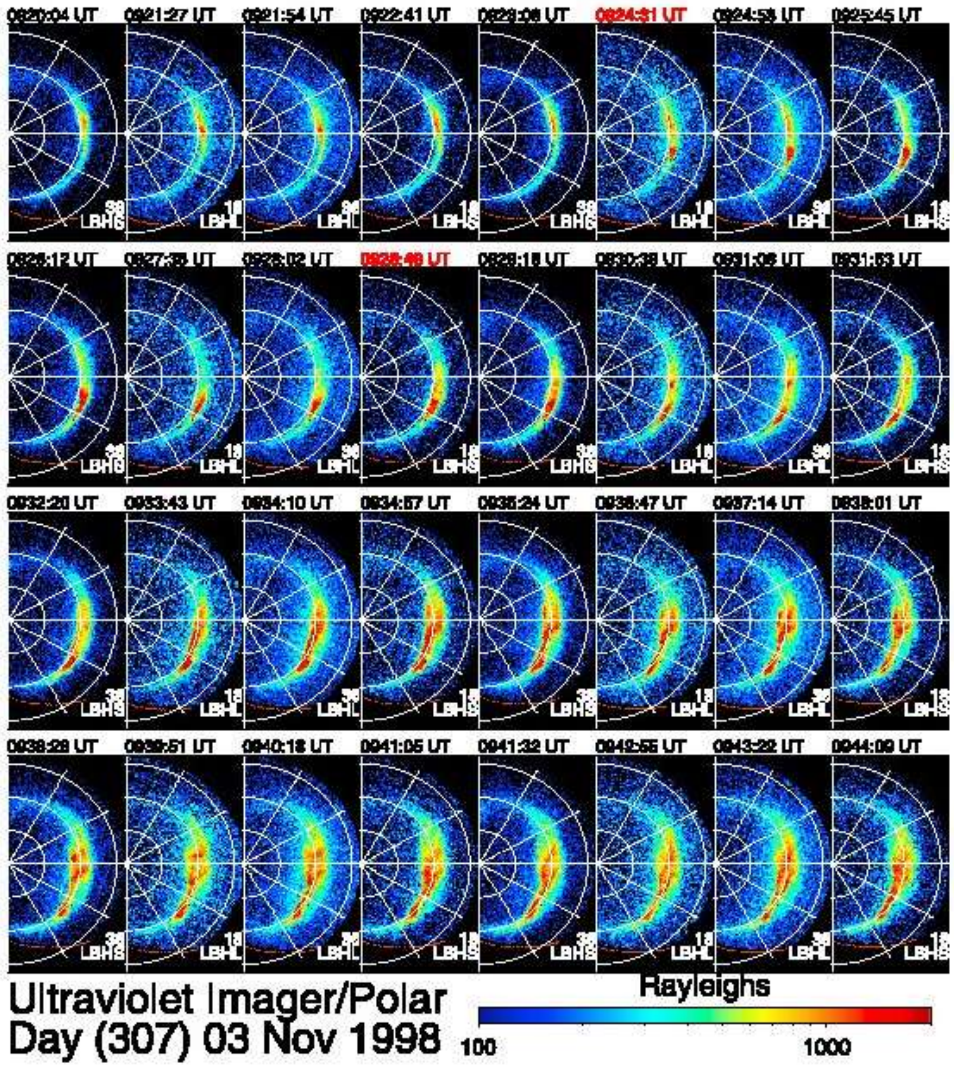

Figure 2. A sequence of nightside auroral images in the N_2 Lyman–Birge–Hopfield (LBH) bands with the exposure time of 18 and 36 s from Polar ultraviolet imager on 3 November 1998. The first aurora activation (snapshot labeled 0924:31 UT in red) and the second aurora activation (snapshot labeled 0928:49 UT in red) are shown.

Saito, et al. (2010)

N-S aurora

Nakamura et al. (1993)

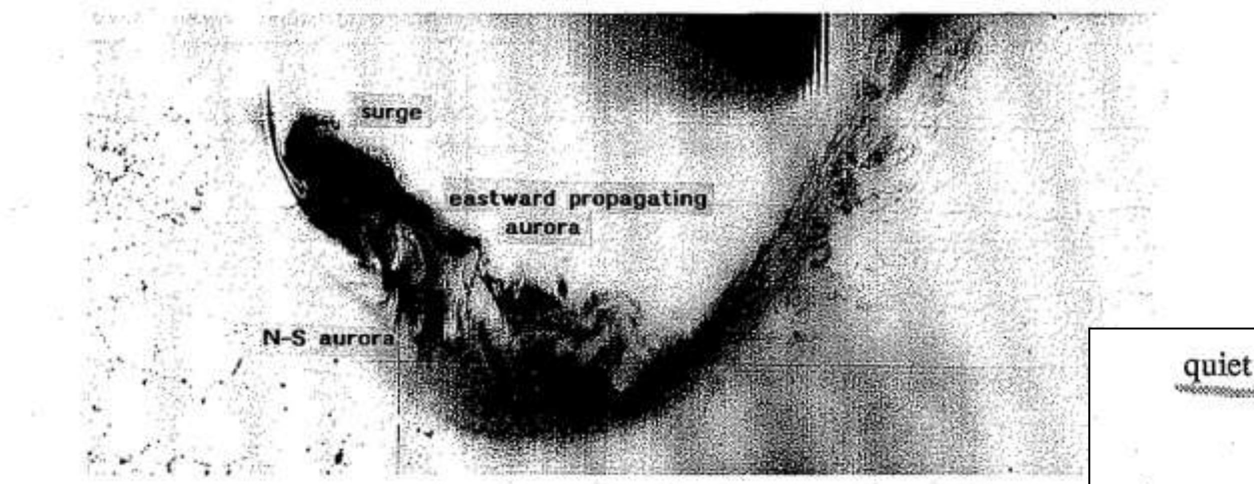

Fig. 2. DMSP auroral image of a bulge including characteristic auroral structures: the surge, the N-S aurora, a
propagating aurora.

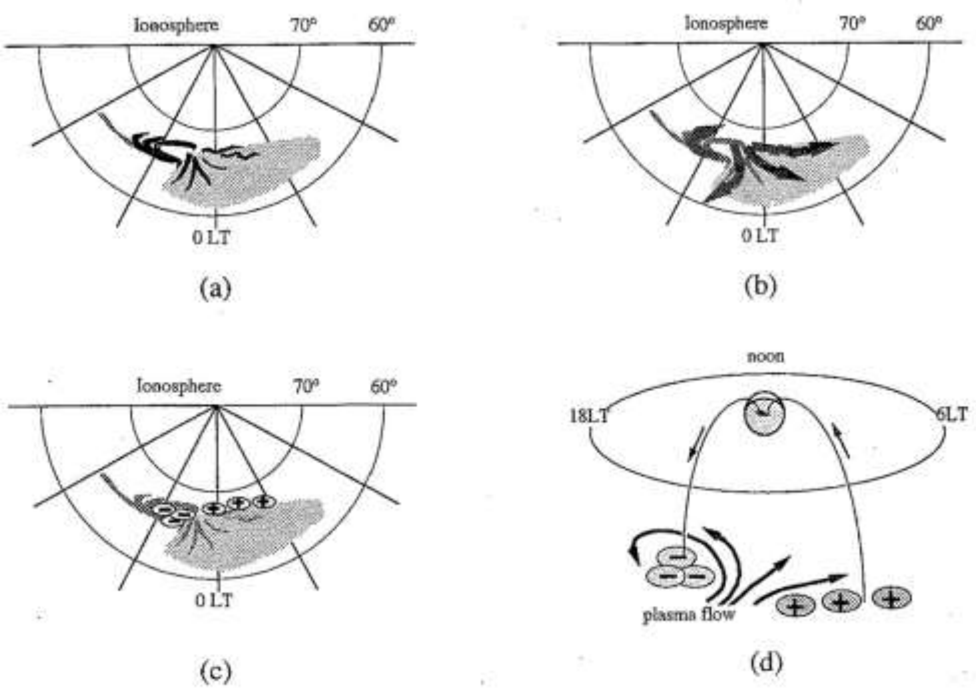

Fig. 11. (*a*) A schematic representation of the bulge at the maximum epoch. (*b*) The direction of the expansion of each aurora within the bulge. (*c*) The location of the expected space charges in the magnetosphere transferred onto the ionosphere, which could be expected from the evolution of the aurora. (*d*) The expected plasma flow in the magnetosphere associated with the auroral expansion.

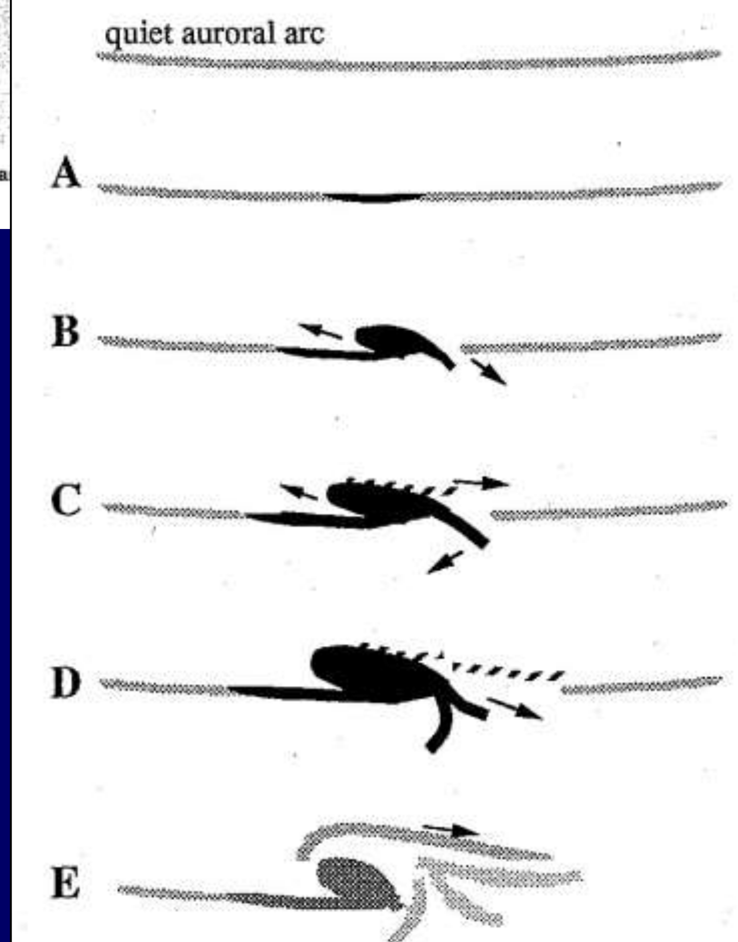

Fig. 5. A schematic representation of the development of a bulge. The arrows represent the direction of the development of the auroras.

Relationship between WTS and N-S aurora

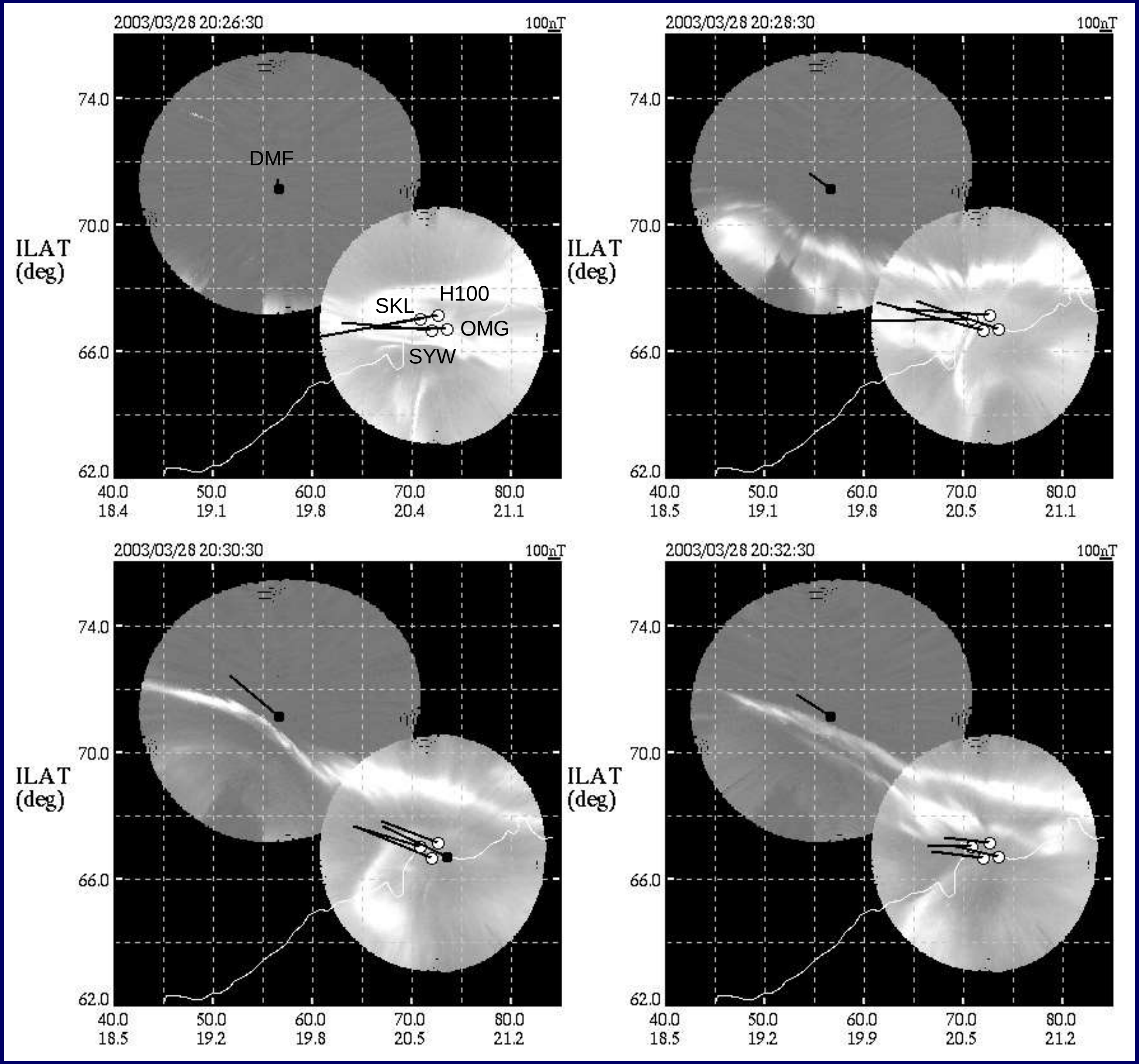

Kadokura et al. (2008)

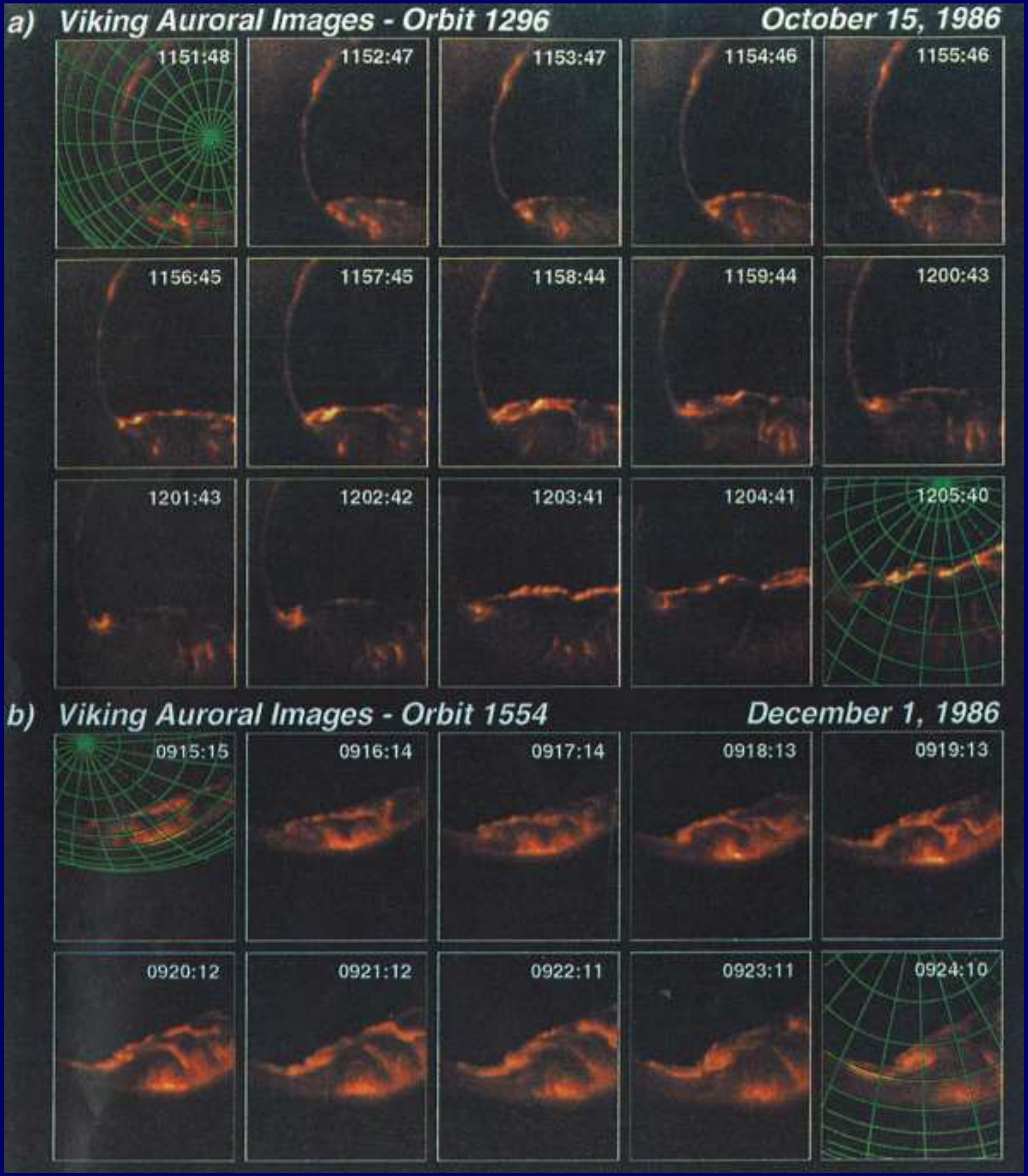

N-S aurora

Henderson et al. (1998)

Auroral Streamer

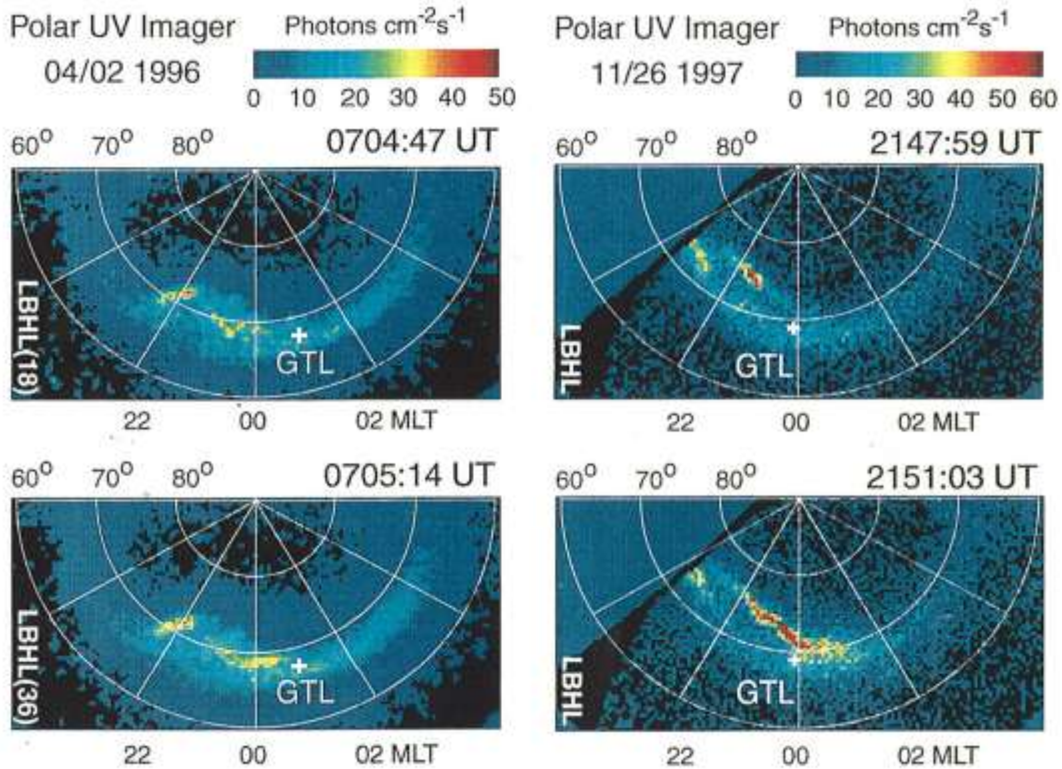

Plate 1. Selected UVI images on April 2, 1996, shown in geomagnetic coordinates. The foot point of Geotail is marked in the figure.

Plate 2. UVI images for November 26, 1997, event in the same format as Plate 1.

Nakamura et al. (2001)

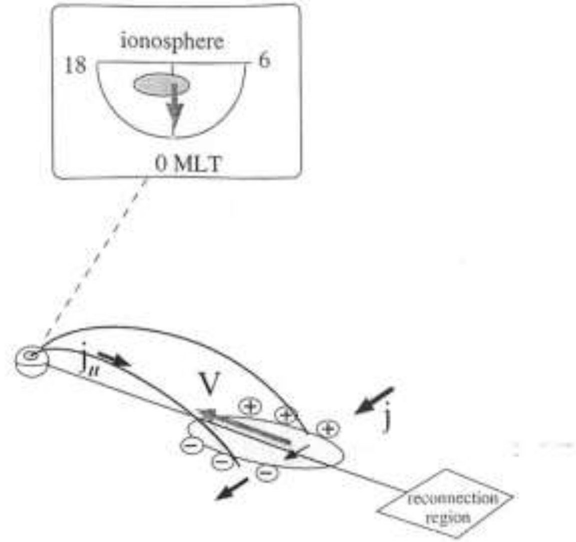

Figure 7. Illustration showing the relationship between aurora and plasma bubble in ionosphere and in magnetosphere. Expansion aurora is centered west of the flow burst.

Auroral Streamer

Sergeev et al. (2000)

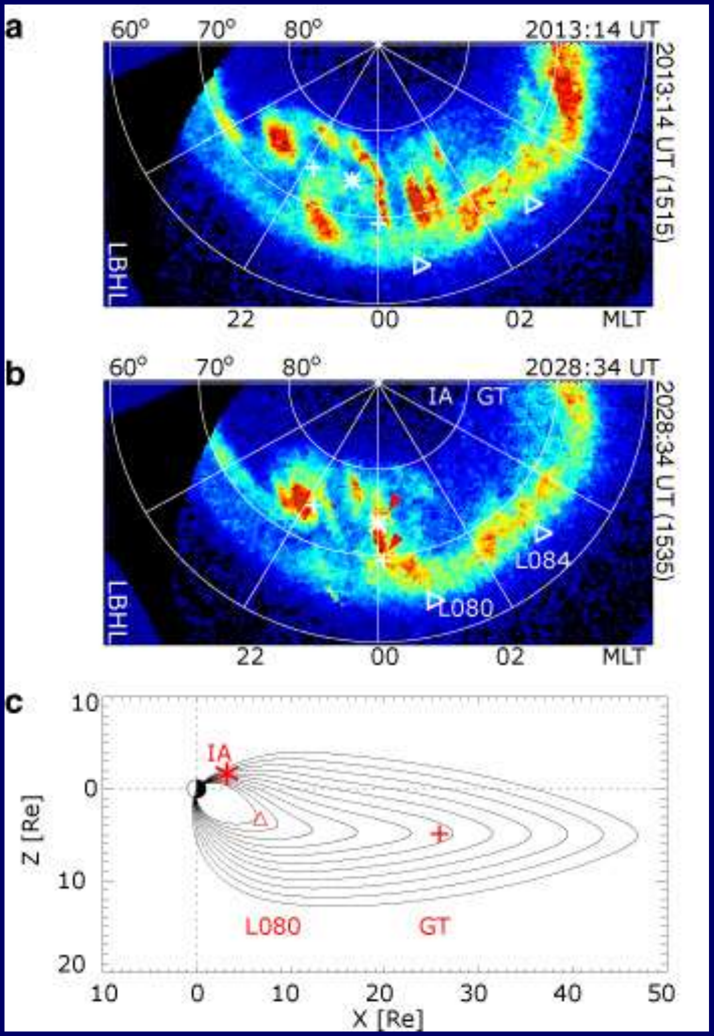

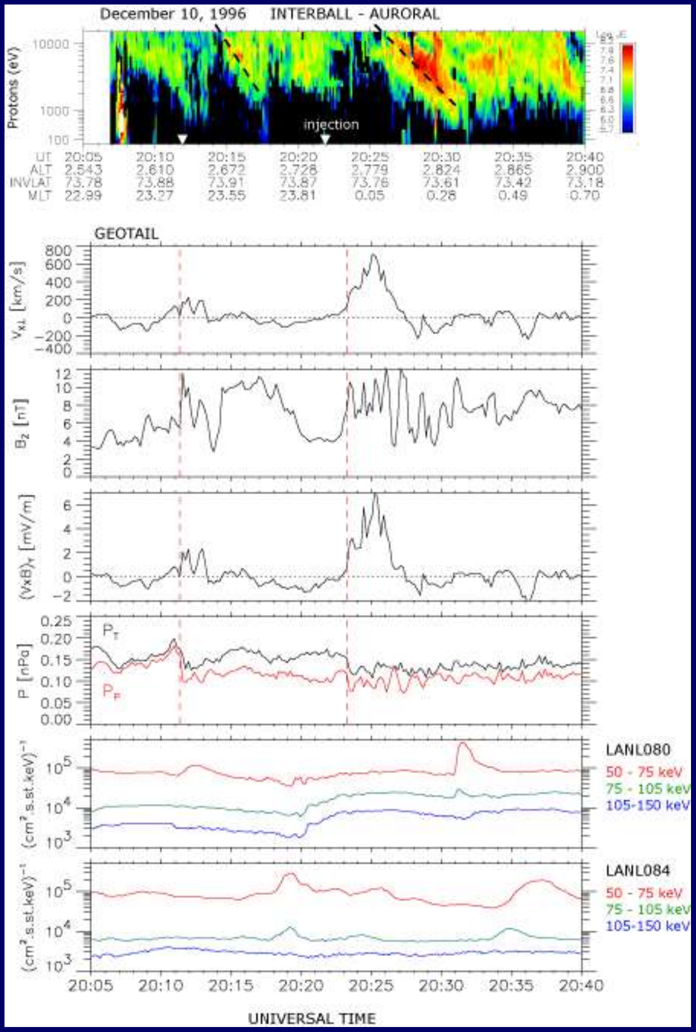

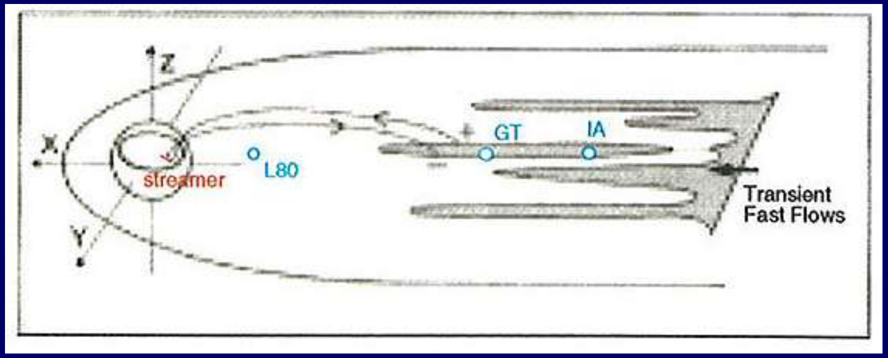

Plasma sheet projection

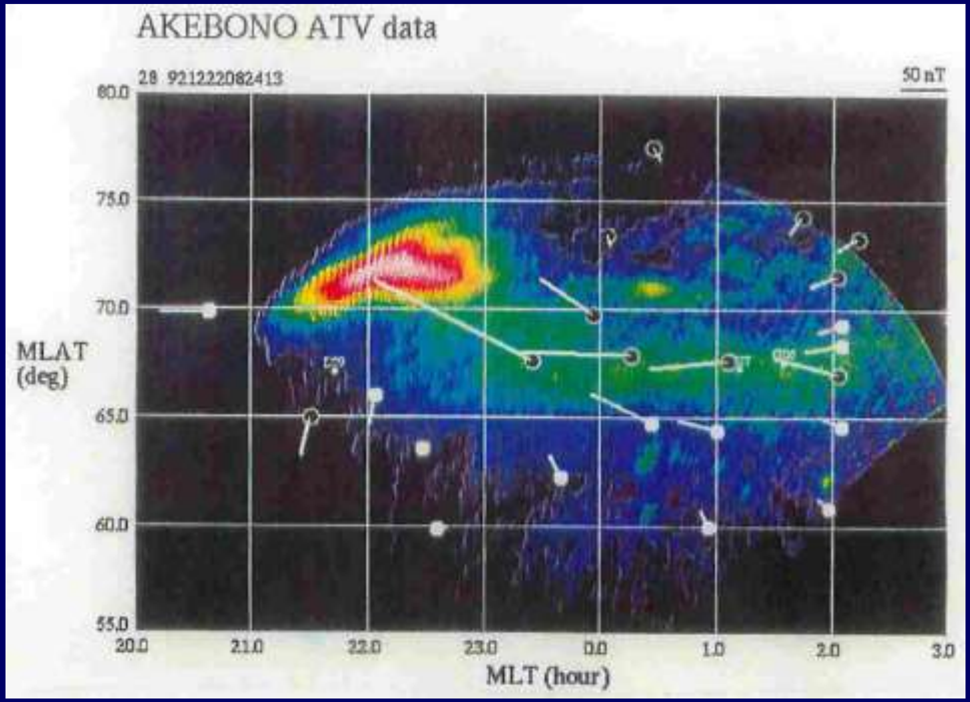

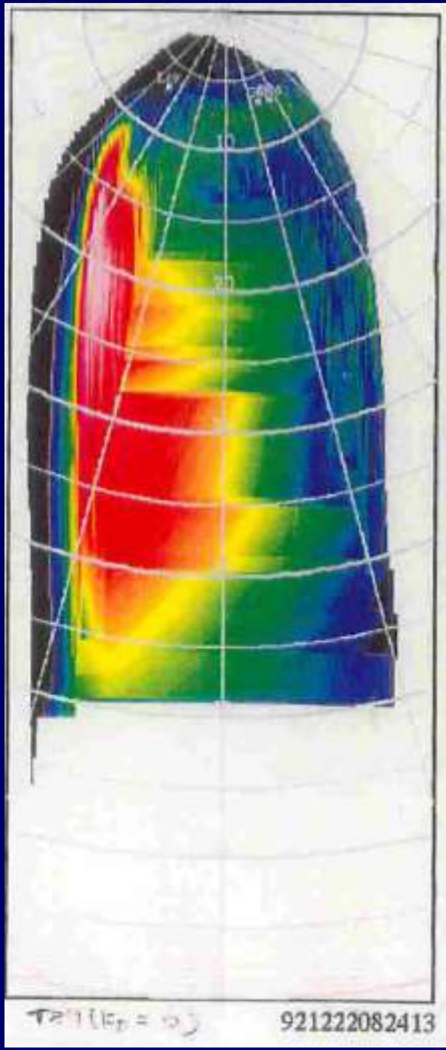

T89(Kp=0)

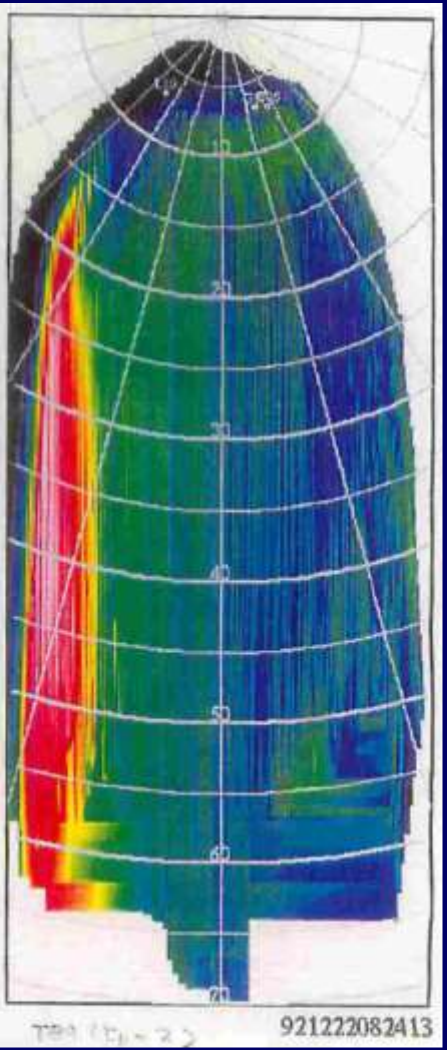

T89(Kp=2)

Aurora ≠ Intense upward Field-aligned current

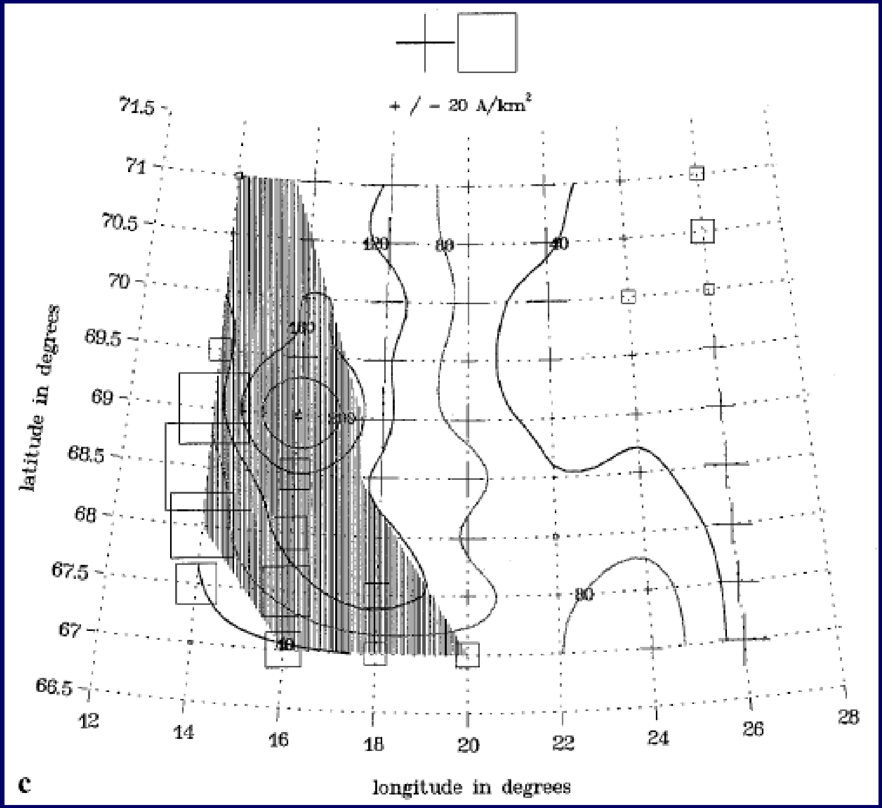

Field-aligned current

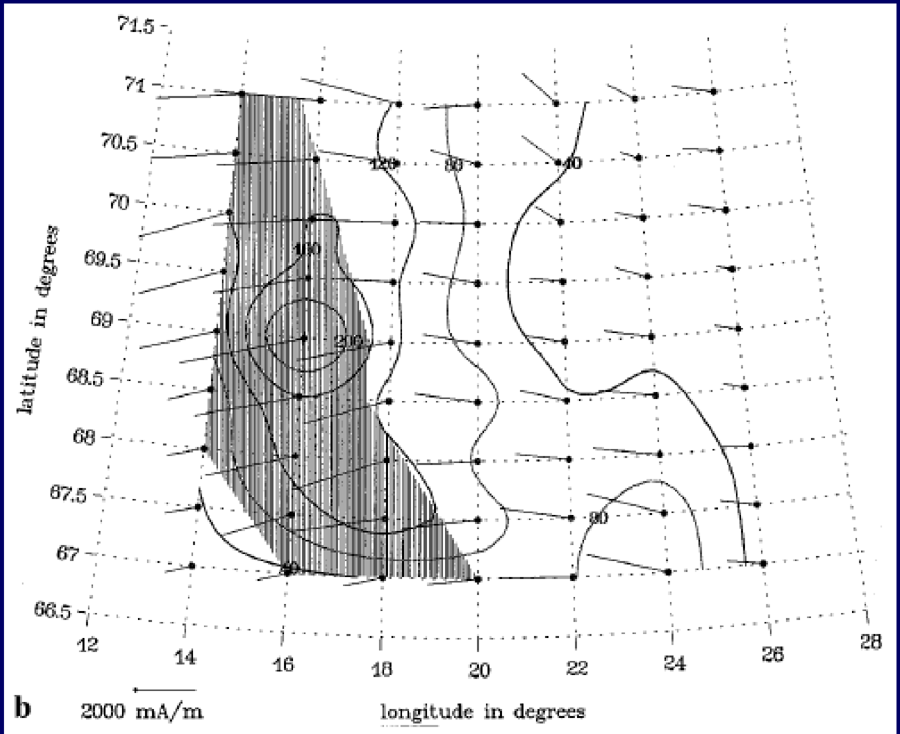

Ionospheric current

Contour: Hall conductance, Shaded area: discrete N-S aurora

O. Amm et al. (Ann. Geophys., 17, 1385, 1999)

Expansion Phase

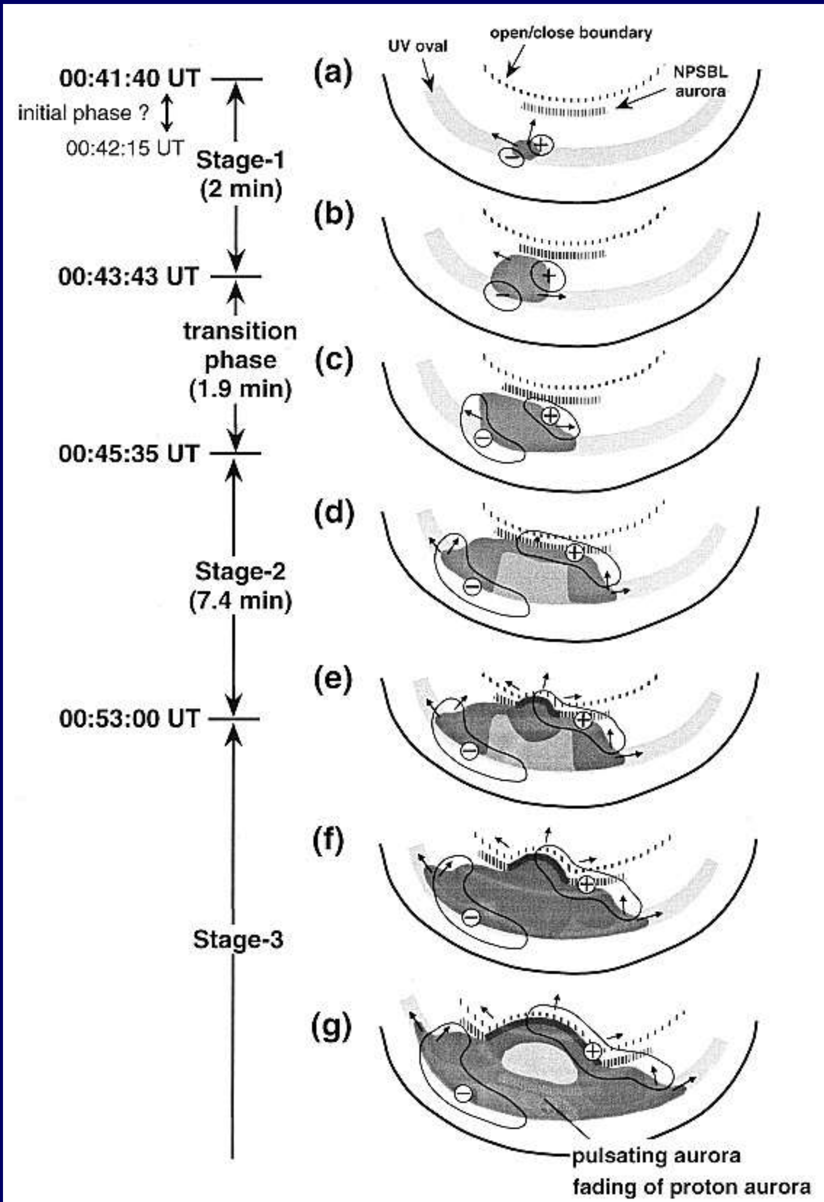

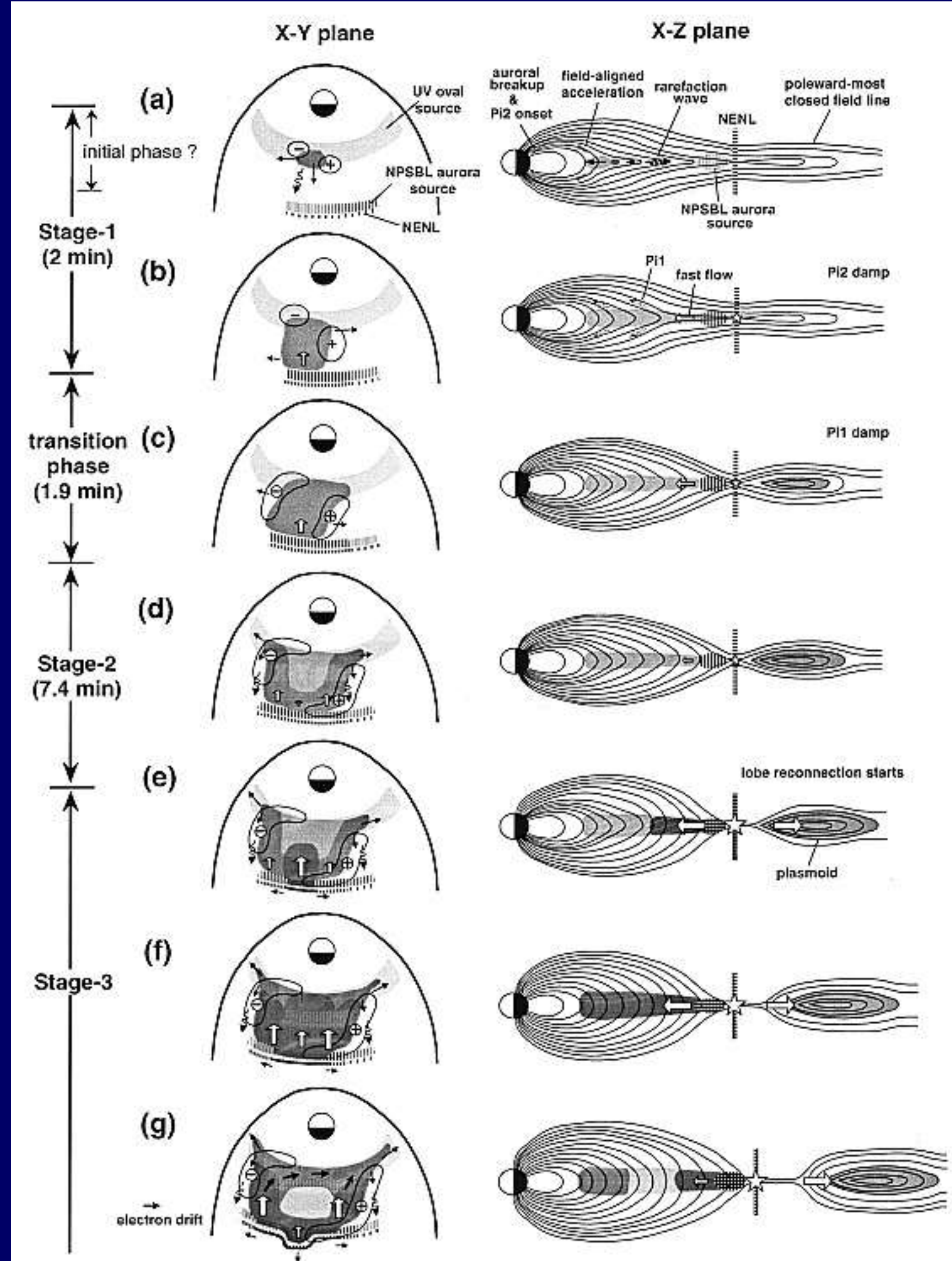

オーロラサブストーム　～何が説明されるべきか

① Source mechanism of the onset arc, and its relationship with the onset mechanism

② Onset mechanism

③ Premidnight preference of the onset region

④ Localization of the onset region

⑤ Explosiveness of the onset phenomena

⑥ Causal relationship between the various onset signatures:

NENL formation, CD, dipolarization, injection, Pi2, Pi1B, SCW, DP1 current system, and the auroral brightening

⑦ Causal relationship between the phenomena during the expansion phase and the recovery phase:

NENL activity, CD, dipolarization, injection, Pi2, Pi1, SCW, DP1 current system, and the auroral bulge evolution, N-S aurora, Pulsating aurora

オーロラサブストーム研究：今後５～10年の進め方

- 今後、解明すべき重要課題・研究の方向性
  - 磁気圏内現象・構造との対応付け（電離圏 - 磁気圏マッピング）
  - 磁気圏現象に電離圏が果たす役割（全球的な視点で）

- 必要な観測・シミュレーション
  - 地上オーロラ光学観測ネットワークの充実化（特に南半球）
  - 衛星からのオーロラ撮像
    - グローバル撮像：全体像の把握
    - 高時間・空間分解能観測
    - 両極の同時観測
  - 磁気圏グローバルシミュレーションモデルの発展とデータ同化

地上オーロラ光学観測ネットワークの充実化

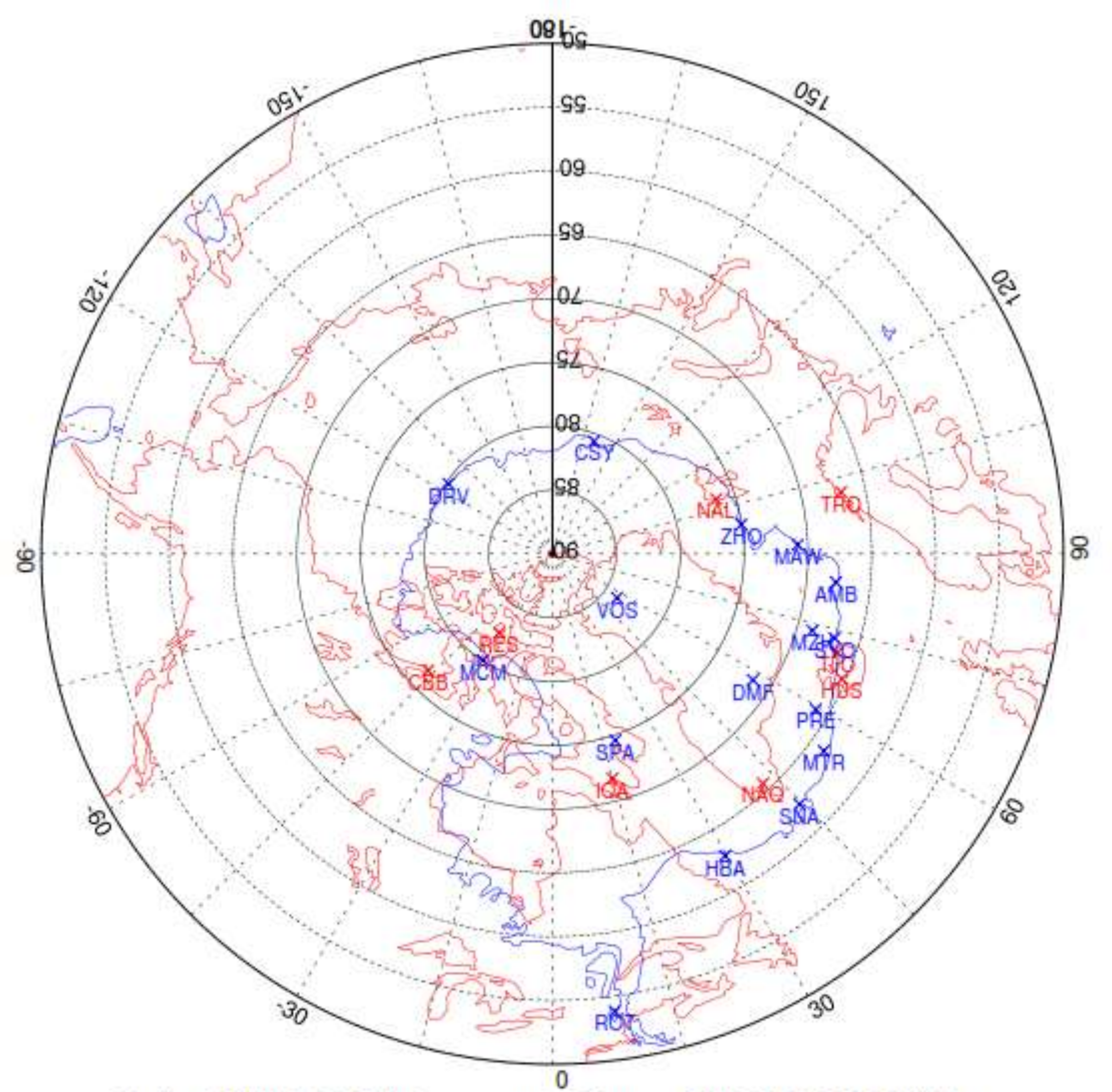

Station FOV(el>90.0) in Geomagnetic Map on 20130101-000000(UT)

地上オーロラ光学観測ネットワークの充実化